

SYNTHESIS OF 1,3-BUTADIENE LIGNDS, THEIR COORDINATION IN A METAL
ORGANIC FRAMEWORK, AND INVESTIGATION OF THEIR CYSTALLINE PROPERTIES

A thesis presented to the faculty of the Graduate School of Western Carolina University
in partial fulfillment of the requirements for the degree of Master of Science in Chemistry.

By

Andrew James Stutesman

Director: Dr. Brian Dinkelmeyer

Associate Professor of Chemistry

Department of Chemistry and Physics

Committee Members: Dr. William Kwochka, and Dr. Channa De Silva.

April 2017

ACKNOWLEDGEMENTS

I would like to dedicate this project to my parents Michael and Karen Stutesman. Without their constant support and love this would not have been possible. In addition, I would like to thank my grandparents Bob and Diane Wege who helped me acquire my bachelor's degree. I would like to thank Dr. Brian Dinkelmeyer for taking me under his wing and teaching me how to be a chemist. Finally, I would like to thank Dr. William Kwochka, Dr. Charles Marth, and Dr. Channa De Silva for their help as well as Wes Bintz and James Cook for keeping Western's chemistry departments operating. Special thanks to Dr. Robert Pike at the College of William and Mary in Williamsburg, VA and Dr. Michael Young at the University of Toledo for obtaining the XRD crystallographic data.

TABLE OF CONTENTS

LIST OF SCHEMES.....	vi
ABSTRACT.....	viii
CHAPTER 1 INTRODUCTION	1
1.1 PROJECT STATEMENT	1
1.2 BACKGROUND.....	1
CHAPTER 2 LIGAND SYNTHESIS	5
2.1 BIS(METHYLENE)HEXANEDIOIC ACID	5
2.2 FULGENIC ACID	5
2.3 2,3-DI(3-PYRIDYL)-1,3-BUTADIENE	9
CHAPTER 3 MOF SYNTHESIS	21
3.1 BACKGROUND/ INTRODUCTION	21
3.2 MOF SYNTHESIS.....	23
CHAPTER 4 EXPERIMENTALS	33
APPENDIX A.....	60
Gas chromatograph/mass spectrometer parameters.....	60
APPENDIX B	62
Crystallographic data for BMHA-Cu MOF	62
APPENDIX C	71
Crystallographic Data for Zinc Formic Acid crystal.....	71
APPENDIX D.....	75
Crystallographic Data for BMHA: Benzylamine Cocrystal	75
APPENDIX E	79
Crystallographic Data for Fulgenic Acid:2-Aminomethylnaphthylene Cocrystal.....	79
APPENDIX F.....	84
Crystallographic Data for Fulgenic Acid	84

LIST OF FIGURES

1.1	Carboxyl and pyridyl functionalities coordinating with metal clusters.....	3
1.2	Ligands of interest.....	3
1.3	Schematics of MOFs containing terephthalate and BMHA.....	4
2.1	Pyridyl series of ligands	9
2.2	Dimer products in various stages of oxidation.....	15
3.1	Zinc formate hydrate complex crystal structure.....	25
3.2	Crystals of Cu-BMHA MOF under magnification.....	26
3.3	Cross-conjugation in fulgenic acid and 1-dendralene.....	27
3.4	Conformation of BMHA and fulgenic acid in their respective crystal structures.....	28
3.5	Crystal structure of naphthylmethylamine and fulgenic acid.....	29
3.6	Crystal structure of benylamine and BMHA.....	30
3.7	Crystal structure of Cu-BMHA MOF (vertical view).....	31
3.8	Crystal structure of Cu-BMHA MOF (horizontal view).....	32
3.9	Crystal structure of Cu-BMHA MOF (BMHA conformation).....	32
4.1	¹ H-NMR diethyl-3,4-bis(methylene)hexanedioate.....	44
4.2	¹ H-NMR diethyl-3,4-bis(methylene)hexanedioate (zoomed in).....	44
4.3	¹³ C-NMR of diethyl-3,4-bis(methylene)hexanedioate.....	45
4.4	¹ H-NMR of bis(methylene)hexandioic acid (BMHA).....	45
4.5	¹³ C-NMR of bis(methylene)hexandioic acid (BMHA).....	46
4.6	¹ H-NMR of 2,3-dimethylmaleic acid, dimethyl ester.....	46
4.7	¹ H-NMR of 2,3-dimethylmaleic acid, dimethyl ester.....	46
4.8	¹³ C-NMR 2,3-dimethylmaleic acid, dimethyl ester.....	47
4.9	¹ H-NMR of diethyl-2,3-bis(bromomethyl)maleate.....	47
4.10	¹ H-NMR of diethyl-2,3-bis(bromomethyl)maleate (zoomed in).....	48
4.11	¹³ C-NMR of diethyl-2,3-bis(bromomethyl)maleate.....	48
4.12	¹ H-NMR of dimethyl fulginate.....	49
4.13	¹ H-NMR of dimethyl fulginate (zoomed in).....	49
4.14	¹³ C-NMR of dimethyl fulginate.....	50

4.15	¹ H-NMR of fulgenic acid.....	50
4.16	¹ H-NMR of fulgenic acid (zoomed in).....	51
4.17	¹³ C-NMR of fulgenic acid.....	51
4.18	¹ H-NMR of 4,4'-ethene-1,2-dipyridyl	52
4.19	¹³ C-NMR of 4,4'-ethene-1,2-dipyridyl.....	52
4.20	¹ H-NMR of 2,3-dipyridin-2-ylbutane-2,3-diol	53
4.21	¹ H-NMR of 2,3-dipyridin-2-ylbutane-2,3-diol (zoomed in).....	53
4.22	¹ H-NMR of 2,3-dipyridin-2-ylbutane-2,3-diol (showing isomeric ratio).....	53
4.23	Gas chromatogram of 2,3-dipyridin-2-ylbutane-2,3-diol (showing isomeric ratio).....	54
4.24	Mass spectrum of 2,3-dipyridin-2-ylbutane-2,3-diol (meso isomer).....	54
4.25	Mass spectrum of 2,3-dipyridin-2-ylbutane-2,3-diol (d and l isomers).....	55
4.26	¹ H-NMR of crude momobromo-4-vinylpridine.....	55
4.27	¹ H-NMR of crude momobromo-4-vinylpridine (zoomed in).....	55
4.28	Mass spectrum of aniline.....	56
4.29	Mass spectrum of 2-hydroxy-1,2-di(pyridine-3-yl)ethanone.....	56
4.30	Mass spectrum of N-phenyl-3-pyridinecarboxamide.....	56
4.31	Mass spectrum of N,N'-2-(phenylamino)-1,2-di(pyridine-3-yl)ethylidineaniline.....	57
4.32	Mass spectrum of N,N'-diphenyl-1,2-di(pyridin-3-yl)ethane-1,2-diamine.....	57
4.33	Mass spectrum of N,N'-diphenyl-1,2-di(pyridin-3-yl)ethane-1,2-diamine.....	57
4.34	¹ H-NMR of 1,3-di(3-pyridyl)1,3-butadiene.....	58
4.35	¹³ C-NMR of 1,3-di(3-pyridyl)1,3-butadiene.....	58
4.36	¹ H-NMR of fulgenic dimer.....	59

LIST OF SCHEMES

1	Synthesis of diethyl-3,4-bis(methylene)hexanedioate.....	5
2	Initial synthetic route for fulgenic acid.....	6
3	Synthesis of fulgenic anhydride.....	7
4	Synthesis of diethyl-2,3-bis(bromomethyl)maleate.....	8
5	Synthesis of fulgenic acid.....	8
6	Proposed synthetic route for 2,3-di(4-pyridyl)-1,3-butadiene.....	9
7	Synthesis of 4,4'-ethene-1,2-diyl dipyridyl.....	10
8	Proposed synthetic route for 2,3-di(4-pyridyl)-1,3-butadiene.....	10
9	Synthesis of 2,3-pyridin-2-ylbutane-2,3-diol.....	10
10	Preferred synthetic route for pyridine diols.....	11
11	Proposed synthesis for 2,3-di(2-pyridyl)-2,3-butene.....	12
12	Proposed olefin synthesis via thiocarbonate elimination.....	12
13	Proposed synthesis route for 2,3-di(4-pyridyl)-1,3-butadiene.....	13
14	Attempted salting of dibromo-4-vinylpyridine.....	14
15	Base catalyzed elimination of dibromo-4-vinylpyridine.....	14
16	Proposed synthetic route for 2,3-di(3-pyridyl)-1,3-butadiene.....	15
17	Theorized synthetic pathway for 1,2-di(3-pyridyl)ethane-1,2-dione.....	17
18	Synthesis of 2,3-di(3-pyridyl)-1,3-butadiene.....	18

LIST OF ABBREVIATIONS

BMHA.....	bis(methylene)hexanedioic acid
BPO.....	benzoyl peroxide
DEF.....	diethylformamide
DMF.....	dimethylformamide
DMSO.....	dimethylsulfoxide
FT/IR.....	Fourier transform/infrared
GC/MS.....	gas chromatograph/ mass spectrometer
LDA.....	lithium diisopropylamide
MOF.....	metal organic framework
NaH.....	sodium hydride
NBS.....	N-bromosuccinamide
NMR.....	nuclear magnetic resonance
TBC.....	tertbutyl catechol
t-BuOK.....	potassium tertbutoxide
2-PBD.....	2,3-di(2-pyridyl)-1,3-butadiene
3-PBD.....	2,3-di(3-pyridyl)-1,3-butadiene
4-PBD.....	2,3-di(4-pyridyl)-1,3-butadiene

ABSTRACT

SYNTHESIS OF 1,3-BUTADIENE LIGANDS, THEIR COORDINATION IN A METAL ORGANIC FRAMEWORK, AND INVESTIGATION OF THEIR CRYSTALLINE PROPERTIES

Andrew James Stutesman M.S.

Western Carolina University, April 2017

Director: Dr. Brian Dinkelmeyer

This project focuses on the synthesis of novel dienes containing dicarboxylic acid and dipyridyl groups and their use in constructing metal organic frameworks (MOFs) and coordination polymers. Dicarboxylate and dipyridyl ligands are commonly used when forming these supramolecular structures. Many examples of MOFs exist the literature where the bridging ligands are terephthalic acid, muconic acid, and 4,4'-bis-pyridyl-1,2-ethyene. The ligands used in this study are analogous to the previously mentioned ligands and should form similar MOF architectures and coordination polymers. These diene ligands could theoretically give us the ability to modify the pores contained within the metal organic frameworks. If successful, this could enable the size of the pore to be altered and is also a means to add different functional groups inside the pores. These MOFs could potentially be tailored for use in specific applications ranging from gas storage to semiconductors.

CHAPTER 1 INTRODUCTION

1.1 PROJECT STATEMENT

The goal of this project was to form metal organic frameworks (MOFs) containing ligands with a 1,3-butadiene functionality. There were two distinct phases in the project. Phase one was the synthesis of di-topic ligands containing the 1,3-butadiene functional group. These ligands are separated into two categories, those containing dicarboxylate functionalities and those containing dipyridyl functionalities. The hope is the ligands synthesized in this study will behave similarly to terephthalic acid, muconic acid, and 4,4'-bis-pyridyl-1,2-ethylene and coordinate with metals to form three dimensional structures.^{1,2,3} The second phase was to synthesize metal organic frameworks and/or coordination polymers using the previously produced ligands. Finally, the proposed metal organic framework had its structure determined with the use of single crystal x-ray diffraction.

1.2 BACKGROUND

A coordination polymer is a polymer in which organic ligands are linked together by metal centers or metal clusters. These networks can be in the form of one, two, or three dimensional structures. Metal organic frameworks or MOFs are defined by IUPAC as “a coordination network with organic ligands containing potential voids”.⁴ These voids, also called pores, have a variety of possible applications. One of the potential uses is gas storage.⁵ The pores formed in MOFs can have gasses dissolved inside the crystal structure. These gasses can be held inside the crystal structure until they are needed. One real world use would be hydrogen fuel cells. A major problem of hydrogen is the danger of having pressurized tanks in moving vehicles.⁶ If the hydrogen is sequestered inside a solid material such as the voids of a MOF, the danger would be greatly minimized.

The high porosity of metal organic frameworks may also make them useful for gas purification. Currently many nitrogen selective synthetic zeolites are on the market for use as solid sorbents. Additionally, there are oxygen selective carbon molecular sieves. These products are used in air separation processes to produce oxygen or nitrogen respectively. In the late 1970s, studies began to investigate the possible use of metal-complex materials. These studies included sorption studies for oxygen, carbon monoxide, and carbon dioxide. The main advantage of the metal-complex materials are their high selectivity toward specific gasses. Other possible uses for these materials include gas sensors, catalysts, and semiconductors.^{7,8}

Commonly used metal ligand interactions employed when forming MOFs include metal-carboxylate coordination and metal-pyridine coordination demonstrated in figure 1.1. There are many examples of MOFs formed using terephthalic acid, muconic acid, and 4,4'-bis-pyridyl-1,2-ethylene.^{1,2,3} These commonly used ligands have a few characteristics in common. They are rigid and have two coordination sites per molecule. We made ligands that are analogous to these carboxylate and pyridine ligands but also contain a butadiene functional group imbedded in the structure (figure 1.2). These compounds have additional applications in polymer chemistry and as substrates for Diels Alder reactions.⁹

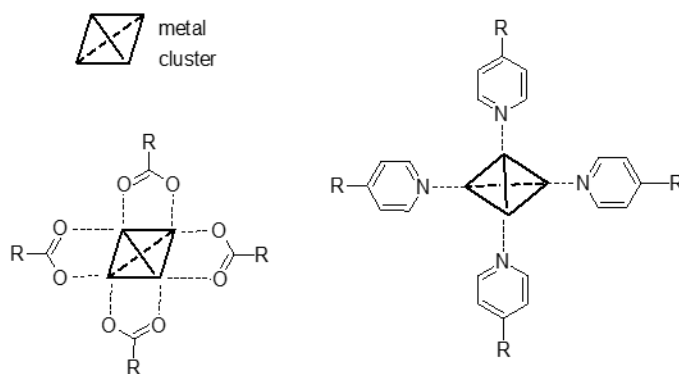


Figure 1.1 Carboxyl and Pyridyl Functionalities coordinating with metal clusters

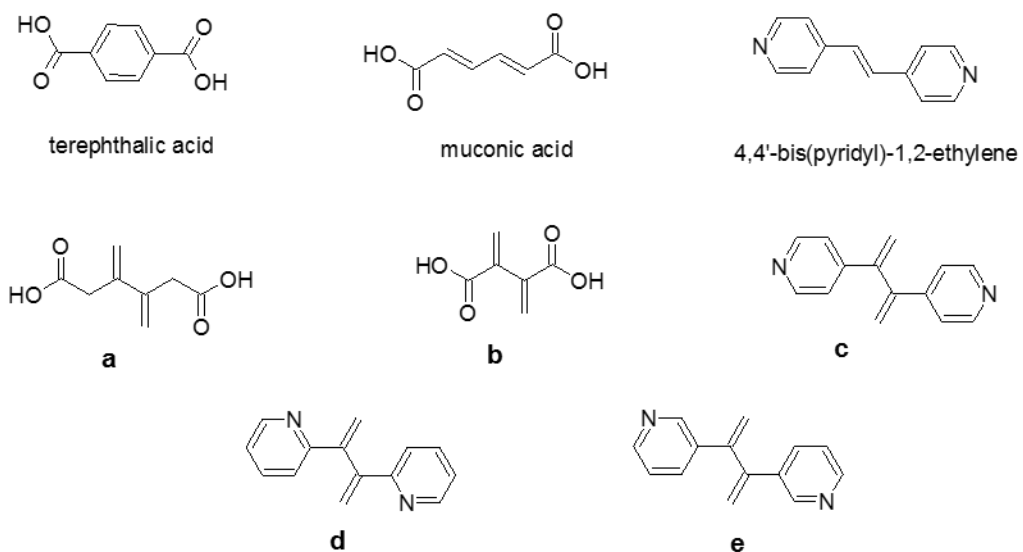


Figure 1.2 The syntheses of ligands a-e were attempted. These ligands should be analogous to terephthalic acid, muconic acid, and 4,4'-bis(pyridyl)-1,2-ethylene. a. BMHA, b. Fulgenic Acid, c. 4-PBD, d. 2-PBD, e. 3-PBD

The butadiene functionality was chosen due to its reactivity. The dienes imbedded in the structure of these MOFs can act as a synthetic handle and allow for chemical manipulation of the pores contained within the structure. (Figure 1.3) This could enable the size of the pore to be altered and is also a means to add different functional groups inside the pores.¹⁰ If this is possible these MOFs could be tailored for use in specific applications.

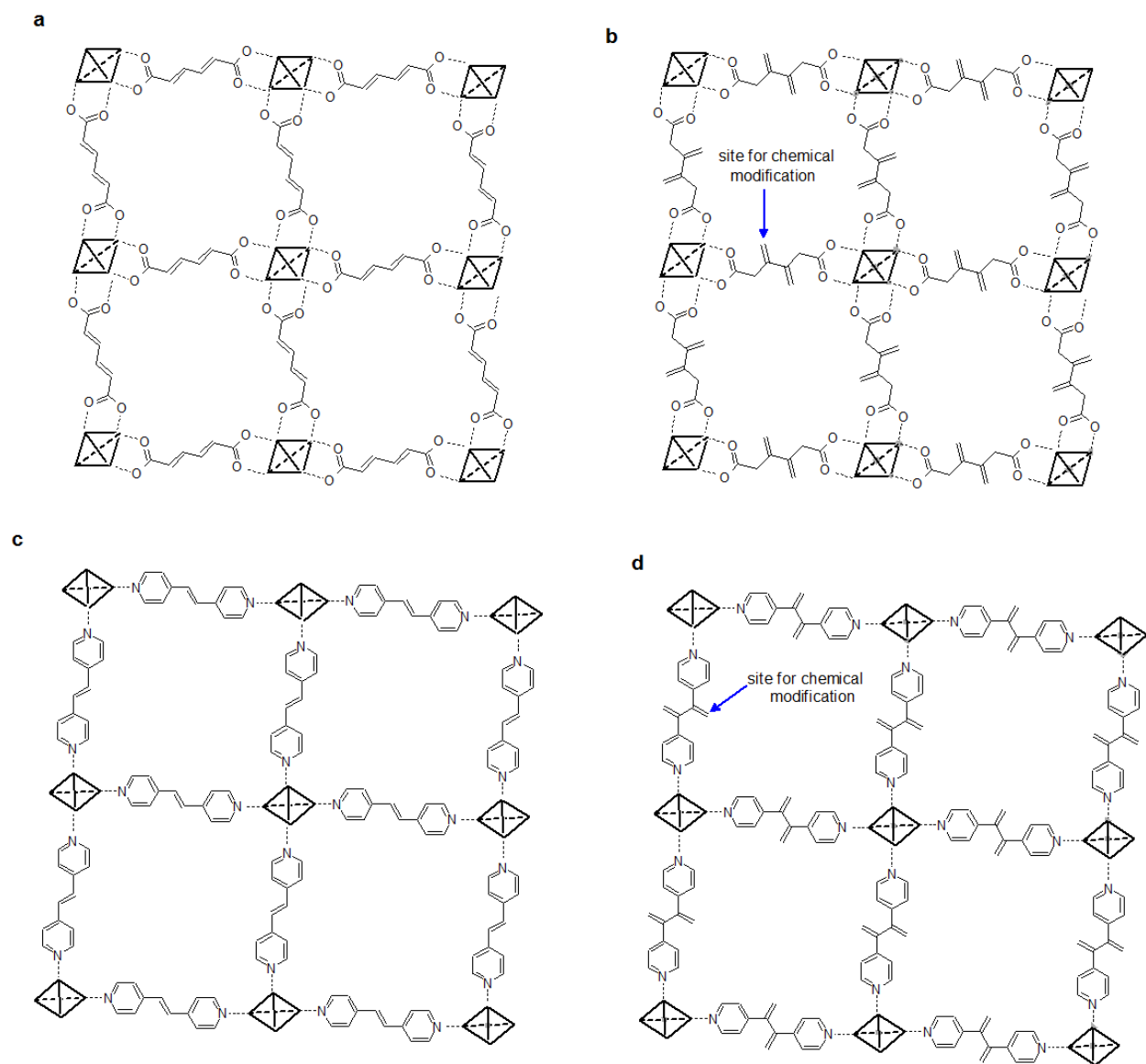
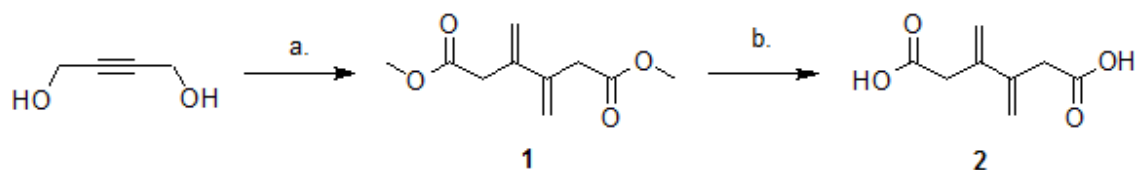


Figure 1.3 Schematics of MOFs containing a. muconic acid, b. 3,4-bis(methylene)hexanedioic acid, c. 4,4'-bis(pyridyl)-1,2-ethylene, and d. 2,3-di(4-pyridyl)-2,3-butadiene showing the chemical modification sites.

CHAPTER 2 LIGAND SYNTHESIS

2.1 BIS(METHYLENE)HEXANEDIOIC ACID

The synthesis of diethyl-3,4-bis(methylene)hexanedioate (**1**) was the first ligand attempted. (scheme 1) The synthesis uses 2-butyne-1,4-diol in the presence of excess triethyl orthoacetate. An acid catalyst is used and the reaction mixture is exposed to microwave radiation. A modified kitchen microwave was used to irradiate the reaction mixture at reflux for one hour. First, esterification happens and the orthoesters are formed. These undergo elimination to afford the allyl orthoester. This molecule then undergoes a double oxy-Cope rearrangement to form dimethyl-3,4-bis(methylene)hexanedioate (**2**) constituting a 60% yield.^{11,12}



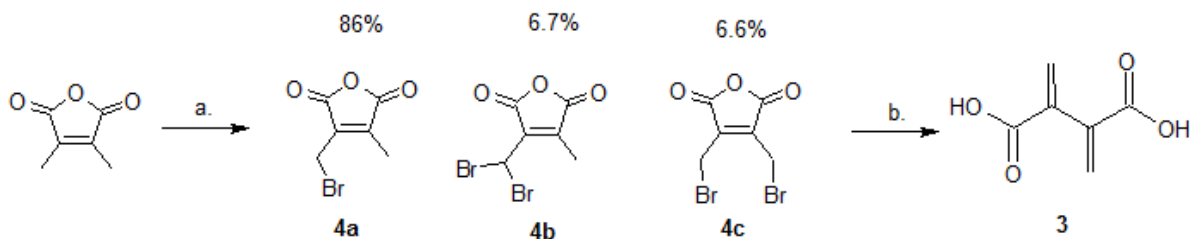
Scheme 1 Synthesis of diethyl 3,4-bis(methylene)hexanedioate. a) triethylorthoacetate, catalytic propionic acid, DMF, microwave irradiation. b) 95% ethanol, NaOH, aqueous acid work-up.

The final step involves a simple base catalyzed hydrolysis of diethyl 3,4-bis(methylene)hexanedioate (**1**) that produced 3,4-bis(methylene)hexanedioic acid (**2**) with a 59% yield.^{12,13}

2.2 FULGENIC ACID

Our first attempt at synthesizing fulgenic acid (**3**) involved a base induced E2' elimination of the allylic bromo atom of 3-(bromomethyl)-4-methylmaleic anhydride.¹⁴ It was a two-step synthesis using dimethylmaleic anhydride as a starting point. The first step was bromination of dimethyl maleic anhydride by N-bromosuccinamide. This step produced three

separate products as seen in scheme 2. Using GC/MS and $^1\text{H-NMR}$, it was determined that the ratio of products was 86% product **4a**, 6.7% product **4b**, and 6.6% product **4c**. The products were then separated using a kugelrohr apparatus. This process was time consuming and destroyed much of the material, but the monobrominated product was able to be isolated. The final step was the 1,4-elimination ($\text{E2}'$) of the mono-brominated anhydride (**4a**). (scheme 2) This step was performed multiple times varying the type of base. The bases tried were KOH, t-BuOK, LDA and NaH. In all cases, a small amount of fulgenic acid (**3**) was detected in the NMR along with a large amount of polymerized material.

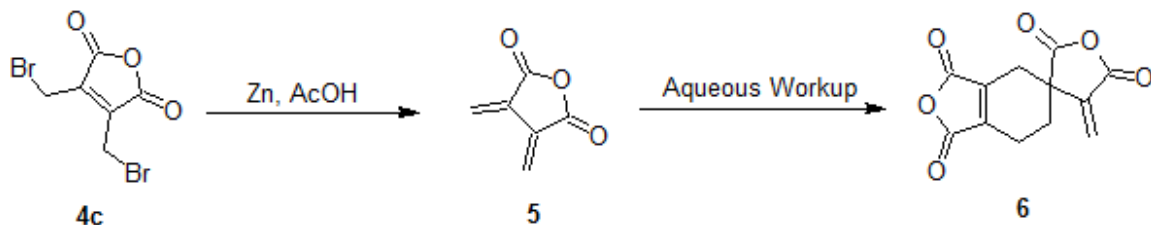


Scheme 2 Initial attempt at synthesizing fulgenic acid a) NBS, CCl_4 , BPO. (**4a**) was purified by Kugelrohr. b) Base induced $\text{E2}'$, NaH, LDA, KOH or t-BuOK.

Many attempts at purification of the crude product were tried including recrystallization and column chromatography. In the paper “A Facile Synthesis of Fulgenic Acid via Base Induced 1,4-Dehydrobromination of (Bromomethyl)methylmaleic Anhydride” a solvent system composed of a 6:4 ratio of petroleum ether to ethyl acetate was used for chromatography. This system was selected and it was found that neither the product nor polymerized impurities moved on the column. Various other solvent systems were tried but no separation was achieved. This method was abandoned as a practical synthetic route.

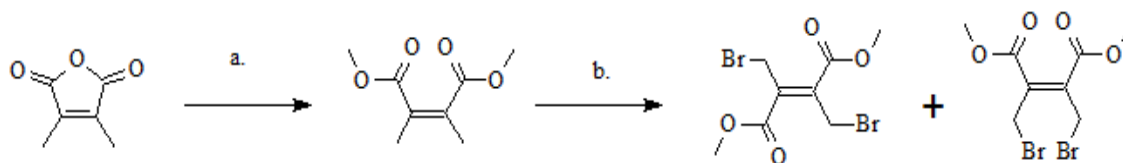
During the purification of the crude 3-(bromomethyl)-4-methylmaleic anhydride (**4a**) a small amount of the dibrominated anhydride (**4c**) was also purified in the distillation process. It

was thought that this compound could be directly treated with zinc metal and acid to undergo a reductive elimination and produce fulgenic acid (**3**) directly. When the reaction was carried out the product was a white sparkly powder. It seemed like a success but the $^1\text{H-NMR}$ told a different story. With the help of GC/MS it was determined that fulgenic anhydride (**5**) had indeed been produced. The problem was all the product had dimerized. The white powder was the Diels Alder adduct (**6**) of fulgenic anhydride (**5**) shown in scheme 3. Fulgenic dimer was obtained with a yield of 4.8%. Spectral data for fulgenic dimer (**6**) can be found at the end of the experimental section. (figure 4.36)



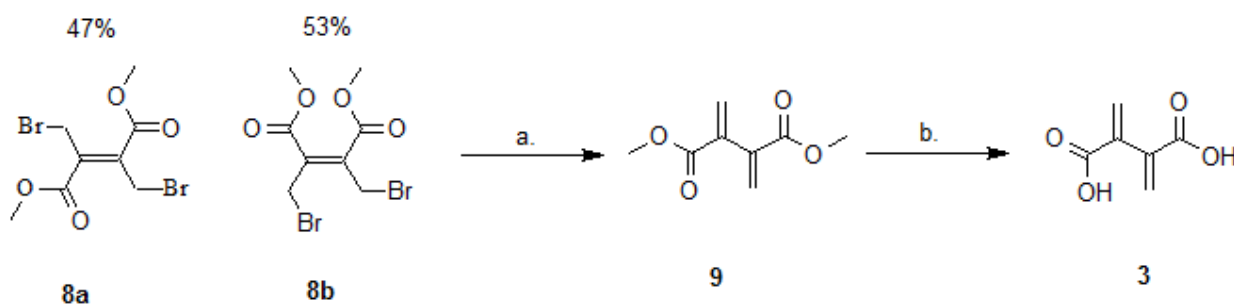
Scheme 3 Formation of fulgenic anhydride (**5**) and fulgenic dimer (**6**)

Due to the failure of the initial method it was thought that derivatization of the starting material to the according dimethyl ester, may decrease the amount of polymerization upon elimination. Dimethyl maleic anhydride was refluxed in methanol with an acid catalyst. (scheme 4) Water was removed via 3Å molecular sieves in a Dean Stark trap to push the equilibrium to the products side. Yield was 80%, but much of the unreacted starting material can be recovered. The resulting di-ester (**7**) was then subjected to the same N-bromosuccinamide bromination conditions with the expectation of getting a mixture of various brominated products. It was discovered by GC/MS and $^1\text{H-NMR}$ that rather than a mixture of products there was a 47:53 ratio of two isomers of dibrominated product, (**8a**) and (**8b**) constituting an 84% yield. (Scheme 4)



Scheme 4 Synthesis of Fulgenic Acid Steps 1 and 2 a) CH_3OH , acid catalyst, Dean-Stark trap, 3 Å sieves. b) NBS, CCl_4 , BPO.

The mixture of resulting isomers were reacted with Zn and catalytic acetic acid. A Zn atom displaces a bromine; then both isomers undergo a 1,4-elimination reaction to create the butadiene functionality. This reaction results in a 92% yield of dimethyl fulginate (**9**).¹⁵ (scheme 5) The final step is a simple base catalyzed hydrolysis of dimethyl fulginate (**9**). To minimize the polymerization upon hydrolysis a small amount of 4-tertbutylcatechol is added as a radical scavenger.¹⁶ The entire final hydrolysis step is performed using 3M NaOH solution at 0°C with vigorous stirring. The resulting sodium fulginate solution was added dropwise to chilled aqueous acid to reform the free fulgenic acid. A detailed procedure can be found in the experimental section. Yield of fulgenic acid (**3**) was 42% based on dimethyl fulginate (**9**). The total yield over 4 steps is 26% based on the commercially available dimethylmaleic anhydride starting material.



Scheme 5 Synthesis of Fulgenic Acid Steps 3 and 4 a) Zn powder, catalytic acetic acid. b) NaOH, TBC.

2.3 2,3-DI(3-PYRIDYL)-1,3-BUTADIENE

The pyridyl series is another group of ligands that are of interest in this study. There are three isomers. The only difference is the connection point of the pyridine ring. Attempts were made to synthesize all three isomers. The pyridyl ligands of interest can be seen in figure 2.1. Just like the carboxylate ligands, these too contain the internal 1,3-butadiene functionality.

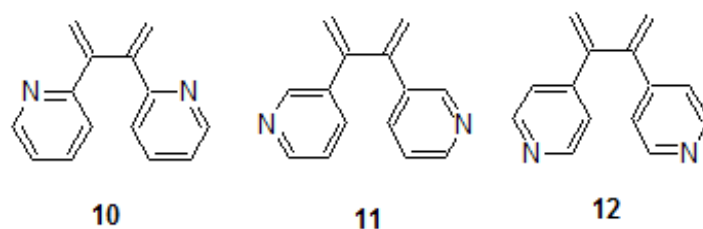
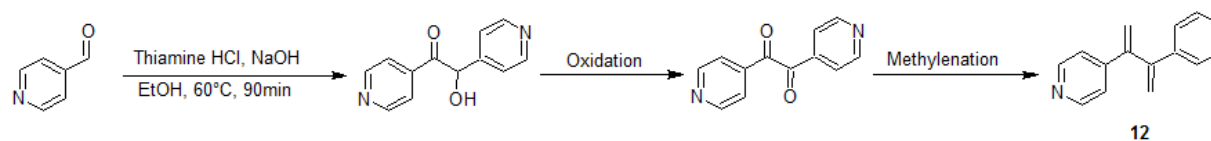


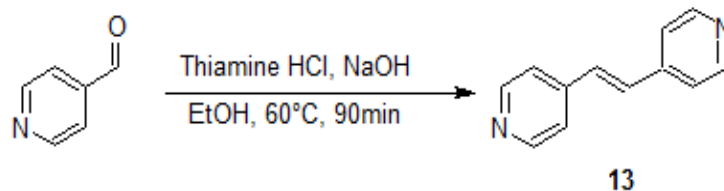
Figure 2.1 Pyridyl series of ligands showed left to right: 2,3-di(2-pyridyl)-1,3-butadiene, 2,3-di(3-pyridyl)-1,3-butadiene, and 2,3-di(4-pyridyl)-1,3-butadiene.

The first attempt at the synthesis of the 4-pyridyl isomer (**12**) involved an acyloin condensation of 4-pyridine carboxaldehyde catalyzed by thiamine HCl. It was hoped that this reaction would produce the corresponding acyloin moiety. This product could then be gently oxidized to a 1,2-diketone. The diketone could then simply be treated with a methylenation reagent such as a Wittig or Tebbe reagent. (scheme 6)



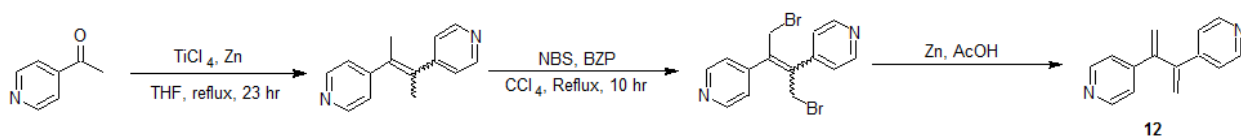
Scheme 6 Proposed Synthetic Route for 2,3-di(4-pyridyl)-1,3-butadiene (**12**)

Unfortunately during the acyloin condensation step an elimination reaction occurred and the major product of the reaction was 4,4'-ethene-1,2-diyl dipyridine (**13**) pictured in scheme 7. This method was abandoned as a valid synthetic route.



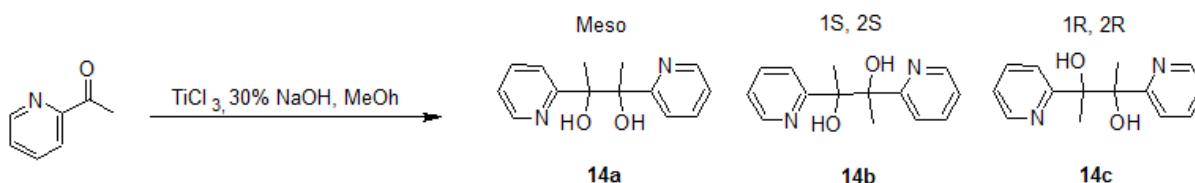
Scheme 7 Major Product was 4,4'-ethene-1,2-dipyridine (**13**)

After the failure of the first method, a different route was attempted. This synthesis involved the use of titanium tetrachloride and Zn metal to couple 4-acetylpyridine. It was hoped that the reaction would go by the McMurray coupling mechanism and afford 4,4'-but-2-ene-2,3-dipyridine. This proposed synthetic route is visible in scheme 8. This procedure did not produce any detectable product and was abandoned.



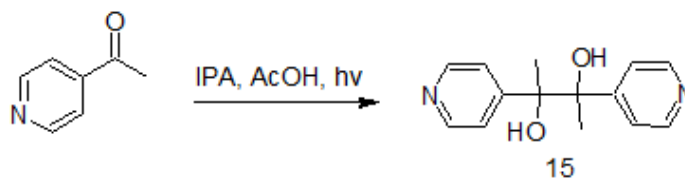
Scheme 8 Proposed Synthetic Route for 2,3-di(4-pyridyl)-1,3-butadiene

A symmetrical titanium catalyzed coupling reaction was attempted to synthesize the 2-pyridyl isomer (**10**). This method instead uses TiCl_3 under basic conditions and 2-acetylpyridine as the substrate.¹⁷ Rather than creating the desired olefin the major product of the attempted reaction was a mixture of d (**14a**), l (**14b**), and meso (**14c**) isomers of 2,3-pyridin-2-ylbutane-2,3-diol. (scheme 9) The spectral data is available at the end of the experimental section.



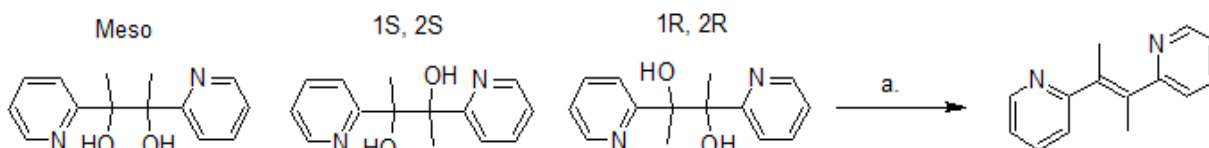
Scheme 9 Coupling of acetylpyridine with TiCl_3 , Meso (**14a**), l (**14b**), and d (**14c**) isomers of 2,3-pyridin-2-ylbutane-2,3-diol

The diol compounds produced in preceding reaction were investigated as starting points for the synthesis of the pyridyl ligand series (**10**), (**11**), and (**12**). Previously work completed by Catherine Garrison gave us a simpler synthetic routes to the 2, 3, and 4 pyridyl diols. The method she developed involved simply dissolving the corresponding acetylpyridine isomer in isopropanol, adding catalytic acetic acid, and placing the flask in a UV light box. After a few days the crystals can simply be filtered out and washed.¹⁸ (scheme 10) This is the preferred method of preparing these diol compounds.



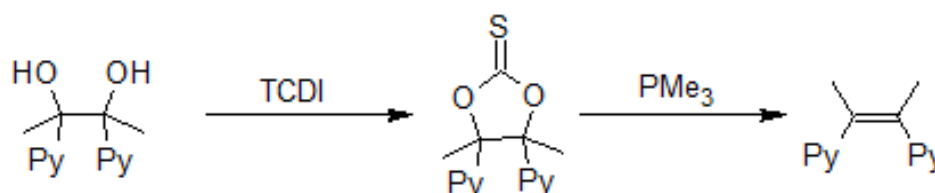
Scheme 10 preferred synthetic route for synthesis of pyridyl diols

It was theorized that perhaps these diols can be converted to their corresponding olefin by a simple acid catalyzed pinacol deoxygenation.¹⁹ The product could then be used to synthesize the dipyriddy butadiene using the synthetic route outlined in scheme 8. The appropriate diol, 2,3-pyridin-2-ylbutane-2,3-diol (**14**), was mixed with ethyl orthoformate and a small amount of benzoic acid. This mixture was heated for one hour at 100°C at which point additional benzoic acid was added. The resulting mixture was heated for an additional two hours at 175°C. Not only did this method not produce any product it also destroyed all of the starting material (scheme 11).



Scheme 11 Elimination attempt on 2,3-pyridin-2-ylbutane-2,3-diol (**14**) a. ethylorthoformate, benzoic acid, 175°C, 2 hours

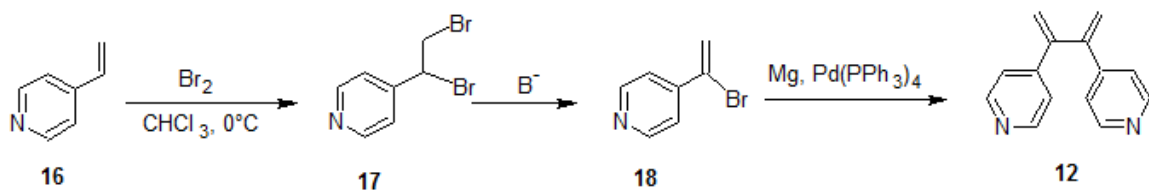
After the elimination attempt failed another method to facilitate elimination was devised. The diol compounds can first be converted to their corresponding thiocarbonate compounds. This was historically done by treating the diol with phosgene.²⁰ Due to the toxicity of phosgene other reagents are preferred. This method involved the use of thiocarbonyldiimidazole. The resulting thiocarbonate can then be converted to the olefin by refluxing in trimethylphosphite. (Scheme 12) This reaction favors the cis conformer.²¹ Thiocarbonyldiimidazole was obtained and it was refluxed in toluene with the diol. This was done for each isomer and in all cases thiocarbonate product was undetectable in the reaction mixture.



Scheme 12 Proposed olefin synthesis via thiocarbonate elimination

After the abandonment of the thiocarbonate route a new synthetic pathway was designed. Rather than the aldehyde or acetyl starting point, this new method uses 4-vinylpyridine (**16**) as the initial substrate. The 4-vinylpyridine was first brominated with liquid bromine in chloroform to produce dibromo-4-vinylpyridine (**17**).²² Next a base catalyzed elimination reaction will be utilized to produce monobromo-4-vinylpyridine (**18**). The final step is a coupling reaction using

Mg powder and palladium triphenylphosphine that should directly produce the desired olefin (12).²³ (Scheme 13)

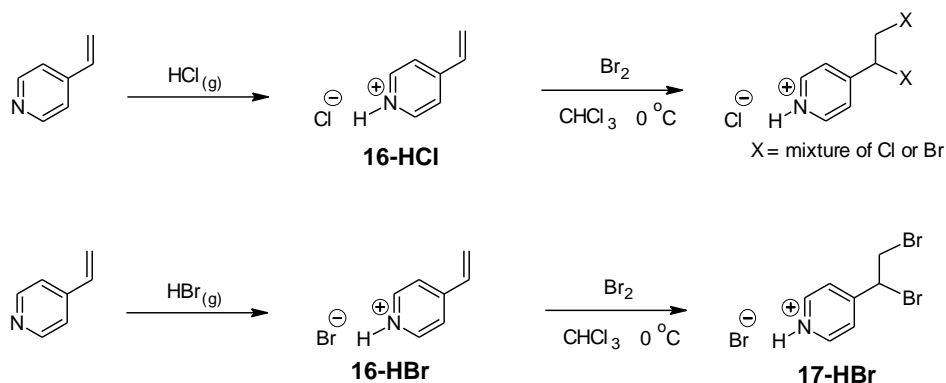


Scheme 13 Proposed synthetic route for 2,3-di(4-pyridyl)-1,3-butadiene (12).

Dibromo-4-vinylpyridine (17) has very poor solubility in its freebase form. The product immediately precipitates out of solution. This reaction proceeds with nearly quantitative yield. Characterization of the resulting yellow powder was hindered by its insolubility in chloroform, acetone, methanol, water, and DMSO. Deuterated pyridine was even tried to get a ¹H-NMR with no results.

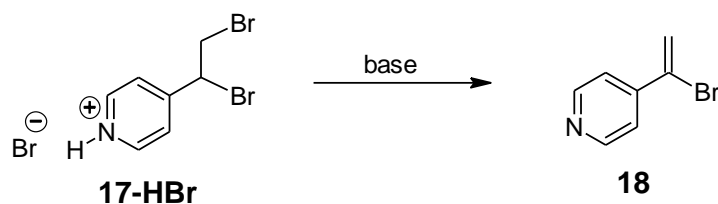
After the discovery of the insolubility of dibromo-4-vinylpyridine, an attempt was made to convert the 4-vinylpyridine (16) starting material to its corresponding HCl salt (16-HCl) before bromination. The 4-vinylpyridine (16) was dissolved in hexanes and anhydrous HCl gas was bubbled through the hexanes. The HCl salt (16-HCl) was then brominated in the same manner in which its freebase had been brominated previously. The resulting product was collected and it was discovered by GC/MS to be a mixture of various brominated and chlorinated products. It seems the chloride ion takes place in the reaction. In order to eliminate the possibility of substrate chlorination, 4-vinylpyridine HBr (16-HBr) was investigated. In this case, the 4-vinylpyridine freebase (16) was treated with anhydrous HBr gas. The resulting HBr salt was then again brominated to produce dibromo-4-vinylpyridine HBr (17-HBr). Satisfied with the purity,

yield, and solubility of the product, efforts were began to design an elimination reaction to produce the mono-brominated 4-vinylpyridine (**18**).



Scheme 14 The H-Br salt of **17** was accomplished to improve its solubility. The reaction of the HCl salt **16-HCl** created a mixture of dihalogenated products.

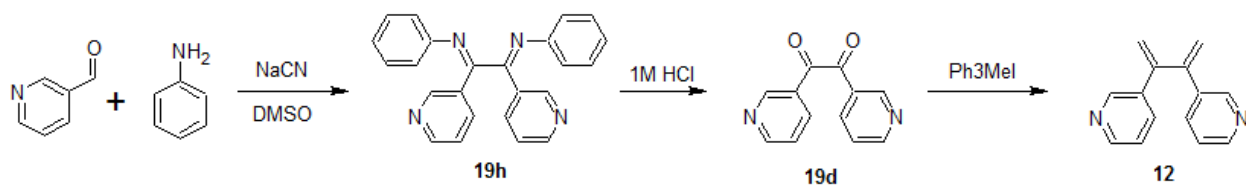
The next step is the base catalyzed elimination of the dibromo-4-vinylpyridine HBr (**17-HBr**). This step was attempted with various bases including K_2CO_3 , triethylamine, and NaOH .^{24,25} Monobrominated product (**18**) was detected in $^1\text{H-NMR}$ and GC/MS. However the monobrominated product is highly reactive and yields in all cases was $>1\%$. Due to the instability of the intermediate product, this was abandoned as a valid synthetic route.



Scheme 15 Elimination under basic conditions produced the desired compound **18**. The instability of **18** prevented further progress along this synthetic pathway.

The final synthetic route tried for the pyridyl series of ligands, (**10**), (**11**), and (**12**), is featured in scheme 14. It began with a coupling reaction where 3-pyridinecarboxaldehyde (**19b**)

was reacted with aniline (**19a**) in the presence of sodium cyanide in dimethyl sulfoxide. First the imine is formed, then it dimerizes to produce the desired diimine (**19h**). This was adapted from a paper entitled “The Dimerization of Anils of Pyridine Aldehydes Catalyzed by Cyanide” This paper claims that the procedure directly produces the desired diimine product (**19h**). It was found that the reaction produces a mixture of dimers in varying states of oxidation seen in figure 2.2.



Scheme 16 Proposed synthetic route for 2,3-di(3-pyridyl)-1,3-butadiene (**12**)

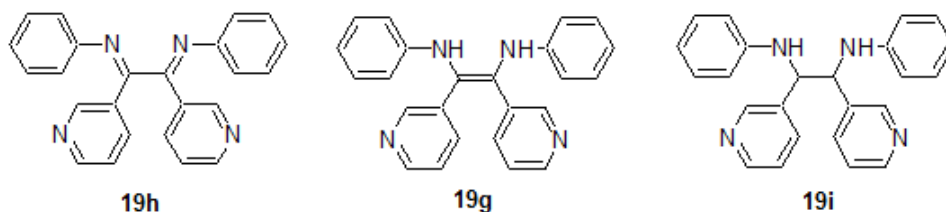


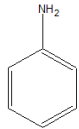
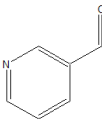
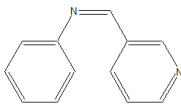
Figure 2.2 dimer products in various stages of oxidation

The next step in this synthetic route is the hydrolysis of the diimine (**19h**) to produce the diketone (**19d**) as a product. The procedure that was followed was very time consuming. The hydrolysis step is a slow evaporation of aqueous HCl acid that takes weeks to complete. If one works up the reaction without the slow evaporation step no product can be recovered.

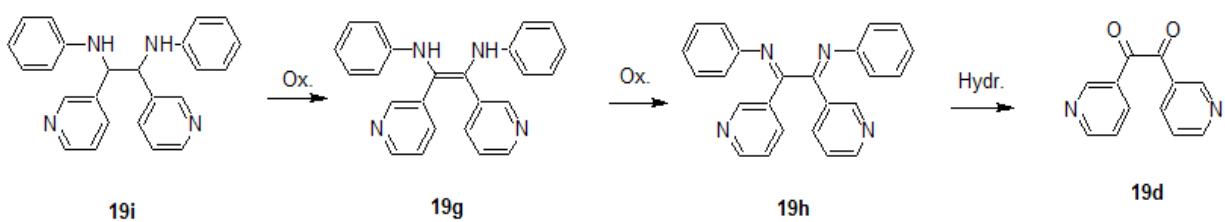
A ten day study was begun to determine why the slow evaporation was necessary for the formation of diketone product (**19d**). The “diimine” product a mixture of (**19g**), (**19h**), and (**19i**) was mixed with 1M HCl and immediately produced a dark red solution. An aliquot was taken

each day for ten days and tested with GC/MS. A total of nine different compounds were found in the reaction mixture. These can be found in Table 1. It was theorized that compound (**19h**) is the reactive species that is converted to compound (**19d**), the desired diketone product. However the reaction produces a mixture of (**19c**), (**19d**), (**19e**), (**19f**), (**19g**), (**19h**), and (**19i**). While (**19c**) and (**19f**) are useless side products, compounds (**19h**) and (**19i**) may be oxidized to (**19h**) which can then be hydrolyzed to the desired diketone (**19d**). (scheme 15) This is the reason the evaporation step is necessary, it takes time for (**19i**) and (**19g**) to be oxidized to (**19h**). It is theorized that this oxidation is the result of air coming in contact with the compounds. Only after the diimine (**19h**) is produced can hydrolysis occur and (**19d**), the diketone, be formed. With this knowledge, efforts were made to speed up the production of the diimine (**19h**) from **19g** and **19i**.

Table 1 Species identified through GC/MS in ten day Aniline/3-PCA study

I	Compound Name	Structure	Formula weight (g/mol)	Retention Time (min)
19a	Aniline		93.13	5.304
19b	3-pyridinecarboxaldehyde		107.11	5.542
19c	<i>N</i> -[(<i>Z</i>)-pyridin-3-ylmethylidene] aniline		182.22	12.492

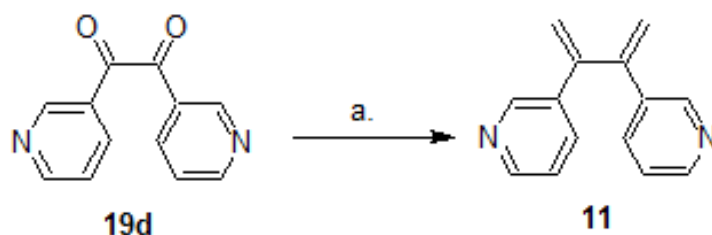
19d	1,2-di(pyridin-3-yl)ethane-1,2-dione		212.20	13.490
19e	2-hydroxy-1,2-di(pyridin-3-yl) ethanone		214.22	13.915
19f	N-phenyl-3-pyridinecarboxamide		197.23	14.277
19h	N,N'[-1,2-di(pyridin-3-yl)ethane-1,2-diylidene]dianiline		362.43	16.954
19g	of N,N'[-1,2-di(pyridin-3-yl)ethene-1,2-diylidene]dianiline		364.44	17.068
19i	of N,N'[-1,2-di(pyridin-3-yl)ethane-1,2-diylidene]dianiline		365.47	17.640



Scheme 17 Theorized synthetic route for 1,2-di(pyridin-3-yl)ethane-1,2-dione (**19d**)

In order to speed up the oxidation of (**19g**) and (**19i**) to (**19h**) the crude product was dissolved in acetone and air was bubbled through the solution for 30 minutes. The oxidized solution was then acidified with 1M aqueous HCl. The result was precipitation of 1,2-diphenylethane-1,2-dione HCl (**19d**). This white powder was then converted to its freebase using aqueous K₂CO₃. Yield was 38% of a yellow crystalline solid. Satisfied with the improvements made to the diketone (**19d**) synthesis, work was begun on methylenation of (**19d**) to produce 2,3-di(3-pyridyl)-1,3-butadiene (**11**), one of the five ligands of interest in this study.

A simple methyl Wittig reagent was tested first to accomplish methylenation of (**19d**). The ylide was produced in situ using triphenylphosphonium iodide and lithium diisopropylamide, which was produced in situ from n-butyl lithium and diisopropylamine.²⁶ (scheme 16) It was thought that this step would be easy to perform and produce (**11**) in high yield. Unfortunately, upon addition of aqueous acid during the workup the reaction mixture immediately turned black. The desired butadiene (**11**) was detected by GC/MS but the product was contaminated with various polymerized side products. Due to the impurity of the product a reliable yield could not be calculated.



Scheme 18 Synthesis of 2,3-di(3-pyridyl)-1,3-butadiene (**11**) a. methyltriphenylphosphonium iodide, n-butyl lithium, diisopropylamine, tetrahydrofuran

The base used to create the methylphosphonium ylide was varied to try and minimize the production of unwanted side products. Both potassium t-butoxide and potassium bis(trimethylsilyl)amide were tested and in both cases the results were very similar to those of

lithium diisopropylamide. At this point it was determined that changing the methylenation reagent from the phosphonium ylide to a Tebbe complex may result in higher yields. Tebbe's reagent is often used on sterically hindered substrates where Wittig reagents do not perform as well.²⁷ The Tebbe reagent worked very similarly to all methylenations previously attempted resulting in a mixture of polymerized side products with (**11**) being detectable only through GC/MS analysis.

After the similar results of all previous methylenation tests and the darkening in color upon addition of aqueous acid, an attempt was made to prevent 2,3-di(3-pyridyl)-1,3-butadiene (**11**) from being protonated during the workup. A means of quenching the reaction mixture that avoids water and acid in particular was desired. Acetone was chosen to quench the reaction mixture as it will react with the remaining ylide producing isobutylene, a gas at room temperature. Once the reaction was quenched, the crude product was analyzed by GC/MS and was found to contain, in addition to the desired product (**11**), triphenylphosphine, triphenylphosphine oxide, and free diisopropylamine. The crude product was run through a plug of silica gel in effort to remove the impurities. Acetone:chloroform, (1:9), was used to elute the triphenylphosphine and some of the triphenylphosphine oxide. The solvent system was changed to acetone:dichloromethane (1:1) to increase the polarity of the solvent system and elute the desired product (**11**). The product eluted from the silica plug was found to still contain triphenylphosphine oxide and diisopropylamine. The elution solvents were removed affording a brown oil. This oil containing crude (**11**) was dissolved in dichloromethane and washed with concentrated sodium bicarbonate solution to remove the diisopropyl amine. The crude product was then subjected to column chromatography using Acetone:chloroform, (3:7) as the mobile phase. The butadiene (**11**) was eluted in fractions 8-11 while the triphenylphosphonium oxide

eluted in the earlier fractions being completely absent in fraction 8. The fractions containing the product were pooled and solvents removed. The product was a light amber oil being composed of 92% 2,3-di(3-pyridyl)-1,3-butadiene (**11**). Two minor contaminants were noted however at this time they have yet to be fully characterized. The yield was quite poor at 8%, however, this particular procedure was only performed once. It is believed that the acetone quenching step and the avoidance of any protic hydrogens species during the workup is a breakthrough in the synthesis of this particular compound (**11**), and that subsequent work will be able to achieve higher yields.

CHAPTER 3 MOF SYNTHESIS

3.1 BACKGROUND/ INTRODUCTION

The formation of MOFs is generally accomplished by crystallization of a metal salt mixed with an organic ligand linker. These two constituents are mixed in a specific molar ratio that will be present in the desired framework. Typically slow crystallization is desired to produce large crystals suitable for crystal structure determination using x-ray diffraction.

There are many techniques in the literature for forming these MOFs. The most common technique utilized in these publications is solvothermal synthesis. All of these methods entail heating solutions containing metal salts and multi-topic ligands in sealed vessels often at high pressures and temperatures. MOF architecture, pore dimensions and crystal size are dependent on solvent type, metal salt type, reaction temperature, reaction pressure, reaction time and the presence of trace additives. By adjusting these parameters it is possible to control structure variables such as size, shape, and crystallinity of metal oxide nanostructures.^{28,29} The most commonly used solvents used in the solvothermal synthesis of carboxylate-metal MOFs are dimethylformamide (DMF) and diethylformamide (DEF). These solvents slowly decompose under the reaction conditions to form dimethylamine and diethylamine respectively. The slow build-up of these weak bases in the reaction mixture control the rate of crystallization as they deprotonate carboxylic acid ligands allowing them to ligate to the metal centers.

Hydrothermal synthesis is identical with solvothermal synthesis except it uses aqueous solvent. Due to the danger of heating sealed vessels of water, these reactions must be carried out in special autoclaves. These autoclaves are made of thick steel that can withstand the pressure of

the water. These methods were primarily designed to grow large single crystals suitable for structural determination.

Other methods that are much easier and cheaper to perform are also available. These methods often produce MOFs with smaller pores or coordination polymers which do not have any open spaces. These methods do not require the use of any specialized equipment such as autoclaves and rely on either solvent diffusion or slow evaporation to accomplish slow crystallization.

Arguably the simplest method is to dissolve both the metal salt and the organic ligand together in a solution and then allow that solution to evaporate. Often when the ligand and metal salt are mixed an immediate precipitation of co-crystalline material will occur. This precipitate is often crystalline however the crystals are normally of poorer quality. In order to slow down this rapid precipitation slow diffusion methods are employed. There are two types, liquid/liquid diffusion and liquid/vapor diffusion. In liquid/liquid synthesis the organic ligand is dissolved in one solvent and the metal salt is dissolved in another. The denser of the solutions should be placed in the bottom of a thin tube. The less dense solution is then carefully floated on top of the other solution and the tube is sealed. This set up allows for slow co-crystallization at the solvent interface as ligand and metal components slowly diffuse together. The solvents chosen for this method are typically miscible but some methods use immiscible solvents to slow down the crystallization rate further.

The final synthetic technique explored in this study is liquid/vapor diffusion. This method is particularly useful for forming MOFs that have carboxylate metal interactions within the structure. In order for carboxylate metal coordination to occur the carboxy group must be deprotonated. By using a base, the equilibrium can be shifted in favor of the deprotonated

species and increase the rate of crystallization. In this method the dicarboxylate ligand is dissolved with a metal salt. This solution is placed inside a vial then sealed in an airtight chamber of some sort. Inside this chamber is placed a solution of triethylamine. This will guarantee that the vapor inside the chamber is saturated with triethylamine gas. Over time this gas will diffuse into the ligand/salt solution and slowly deprotonate the carboxy groups. As this happens the hope is slow coordination and crystallization of organic ligands and metal atoms will occur.

The major downside of the slow evaporation and diffusion techniques is time. These techniques can take months to produce any results. The solvothermal and hydrothermal are much faster but as stated before require the use of specialized and expensive equipment that is not available at all research institutions.

3.2 MOF SYNTHESIS

The first method attempted for the formation of MOFs relied on the principle of vapor diffusion. Both BMHA (**2**) and fulgenic acid (**3**) were each dissolved in ethanol. Additionally, various nitrate salts were also dissolved in ethanol. These salts included $\text{Cr}(\text{NO}_3)_3$, $\text{Cu}(\text{NO}_3)_2$, $\text{Co}(\text{NO}_3)_2$, $\text{Zn}(\text{NO}_3)_2$, $\text{Ni}(\text{NO}_3)_2$, AgNO_3 , and $\text{Cd}(\text{NO}_3)_2$. The ligands and salts were mixed in a 1:2 ligand to metal ratio. A total of 14 different samples were prepared in 20mL scintillation vials each containing only one metal and one ligand. These vials were then placed inside a modified dessicator. The dessicator contained no dessicant but rather a small amount of ethanol and triethylamine solution. Once the vessel was sealed the triethylamine vapor slowly diffused into the solutions contained within the vials and deprotonated the carboxylic acid to facilitate coordination with a metal atom. After two weeks each of the vials contained a precipitate. After microscopic examination of the variously colored powders, it was determined that the powders were amorphous and this technique was abandoned.

Due to the amorphous nature of the previously produced powders, solvothermal synthesis seemed like a logical next step to produce crystallographic quality crystals. A literature procedure that produced x-ray crystallographic quality crystals of terephthalic acid-Zn MOFs was modified for our use. Both BMHA and fulgenic acid were mixed with diethylformamide and $\text{Zn}(\text{NO}_3)_2$ in vials. These vials were sealed and heated in an oven at 100°C for 24 hours. The vials were removed from the oven and left in a vibration free environment. This method relies on the slow decomposition of DEF to form diethylamine. The slow production of diethylamine ensured a slow crystallization process necessary for obtaining x-ray quality crystals. For many months no crystals developed in the vials. The experiment was thought to have failed. After approximately six months it was noted that large clear crystals had formed inside some of the vials. These crystals were sent off for crystal structure analysis. The results from the crystal structure showed that the crystal did not contain any of the desired butadiene ligands (**2**) or (**3**). The crystals were of a previously described Zn, formic acid, and water complex seen in figure 3.1.

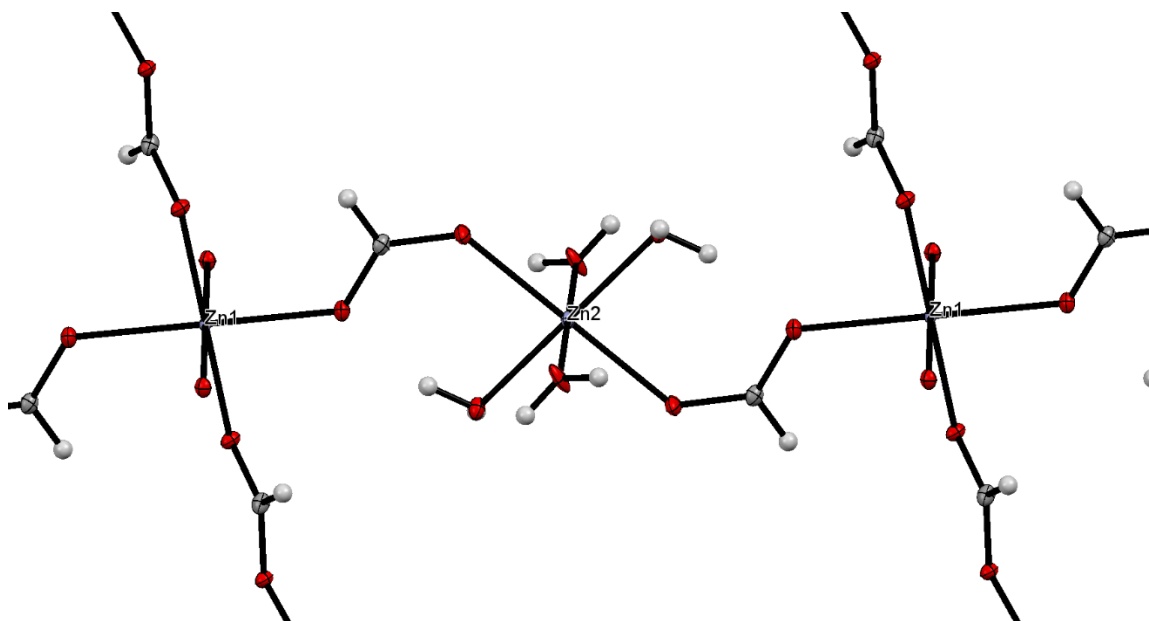


Figure 3.1 Zinc formate hydrate complex

The final method used to synthesize MOFs involved the use of slow liquid/liquid diffusion of an aqueous metal acetate salt solution and an ethanolic organic ligand solution. Both BMHA and Fulgenic acid were dissolved in ethanol to make 0.100M solutions. The metal solutions were made using acetate salts and deionized water and prepared in 0.200M solutions. Thin glass tubes about 20cm long with an outer diameter of 0.5cm were cut to be used as the crystallization chambers. One end was fitted with a plastic NMR cap and keeping the tubes vertical (cap down) the various metal solutions were loaded in the bottom the tubes. The ethanol solution containing the organic ligand was then gently pipetted down the side of the tube so as to form a layer on top of the aqueous metal solution. Each tube only contained one metal species and one ligand. These tubes were capped and left in a vibration free environment. After only one night solid material was visible at the solvent interface of some of the tubes. These were left undisturbed for 2 weeks at which point the crystals were removed from the tubes and analyzed

under magnification. It was determined that only the combination of BMHA and $\text{Cu}(\text{OAc})_2$ had produced crystals of sufficient quality for single crystal XRD analysis. (figure 3.2)

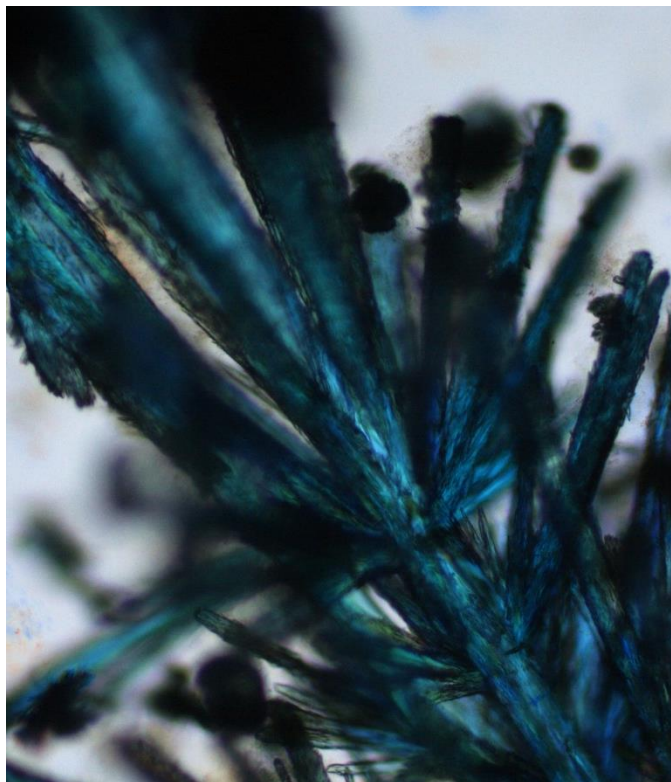


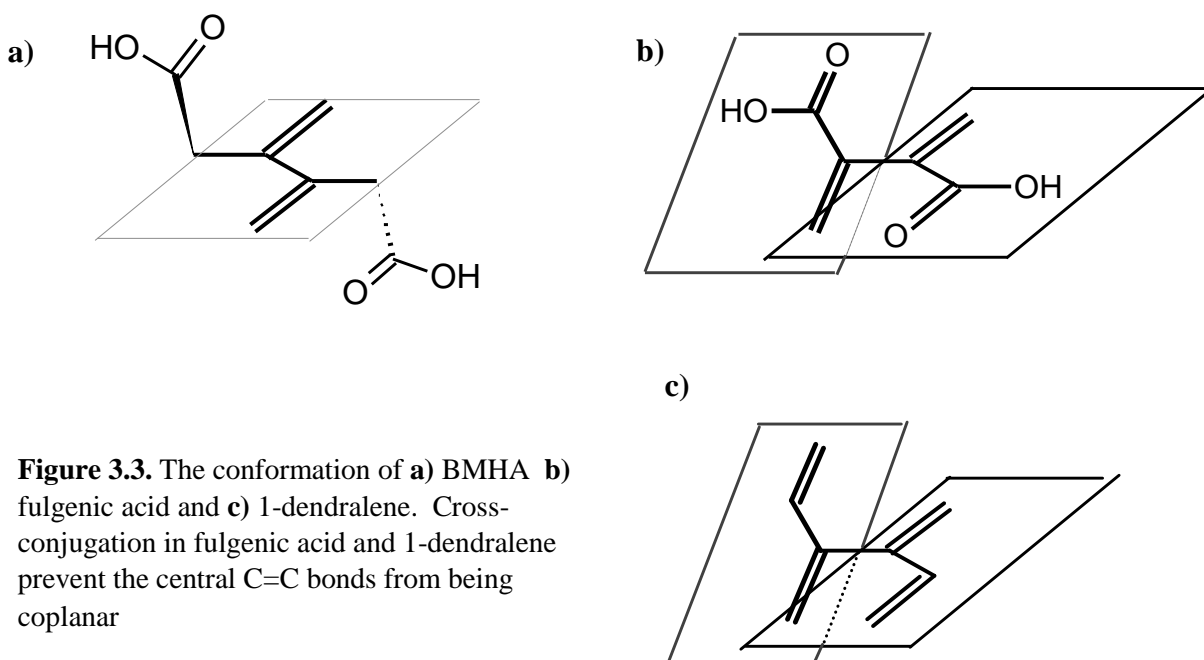
Figure 3.2 Crystals of Cu-BMHA MOF

3.3 CRYSTAL CHARACTERIZATION

Fulgenic acid was recrystallized from ethyl acetate. Fulgenic acid formed monoclinic crystals of space group $C-2/c$ with four fulgenic molecules in the unit cell. Its unit cell angle parameters are $\alpha = 90.0000^\circ$, $\beta = 102.2985^\circ$, $\gamma = 90.0000^\circ$ with the sides of the cell measuring $a = 10.26935 \text{ \AA}$, $b = 5.49754 \text{ \AA}$, $c = 11.18398 \text{ \AA}$. (figure 3.4) A sample of fulgenic acid was placed in a Rayonet photochemical reactor and exposed to UV light measuring 254nm for 18hrs. Unlike crystalline BMHA¹², fulgenic acid crystals did not undergo any solid-state reactions when

exposed to UV radiation or when heated. The crystal packing and distance between reactive centers was not suitable for a solid state reaction.

Interestingly, the conformation of the methylene units in fulgenic acid differ significantly from that found in BMHA. In BMHA both C=C bonds are coplanar and conjugated. Fulgenic acid, on the other hand, is a cross-conjugated system. Cross conjugation refers to pi systems in which some of the pi bonds branch off and are not arranged consecutively. In these systems, it is energetically unfavorable for all of the pi bonds to remain conjugated in a single plane. In fulgenic acid C=C bonds can either be conjugated with one another or to the C=O of the carboxylic acid. The fulgenic acid crystal structure shows that C=C is coplanar with the carboxylic acid instead of the neighboring methylene. This conformation is similar to that of the lowest energy conformation of 1-dendralene.³⁰ The C=C-C=O units are nearly coplanar and the dihedral angle between the two C=C units is 57.46° (Figures 3.3 and 3.4).



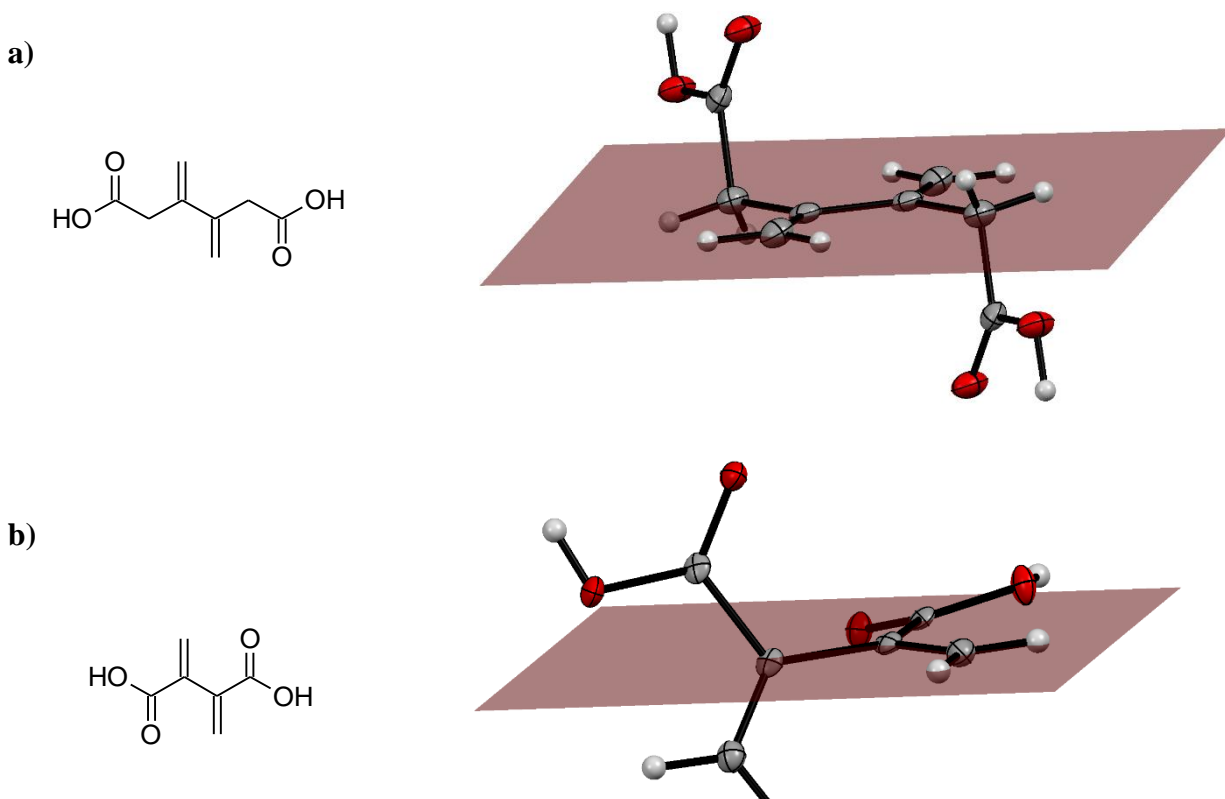


Figure 3.4 The conformation of **a)** BMHA (**2**), and **b)** fulgenic acid (**3**) in their respective crystal structures.

The next structure obtained was of a crystal that was formed when a 1:2 ratio of fulgenic acid and 1-naphthylmethylamine was dissolved in ethanol allowed to evaporate at room temperature. The crystal contained a 1:1 ratio of the two components rather than the 1:2 ratio expected. The unit cell contained four molecules of fulgenic acid and four molecules of 1-naphthylmethylamine. The crystals were monoclinic with unit cell dimensions $a = 10.7662(4) \text{ \AA}$, $b = 13.0275(4) \text{ \AA}$, $c = 8.3714(3)$ and angles measuring $\alpha = 90^\circ$, $\beta = 100.195(2)^\circ$, $\gamma = 90^\circ$. Most importantly, the methylene groups on fulgenic acid are conjugated rather than cross conjugated

as seen in the fulgenic acid crystal structure. This is evidenced by the planar geometry of methylene groups in figure 3.5. It seems when fulgenic acid is deprotonated that it adopts this conformation. This is very desirable for this project as the fulgenic acid will be deprotonated before coordination can occur and the conjugated nature of the alkenes should allow for greater reactivity inside the pores.

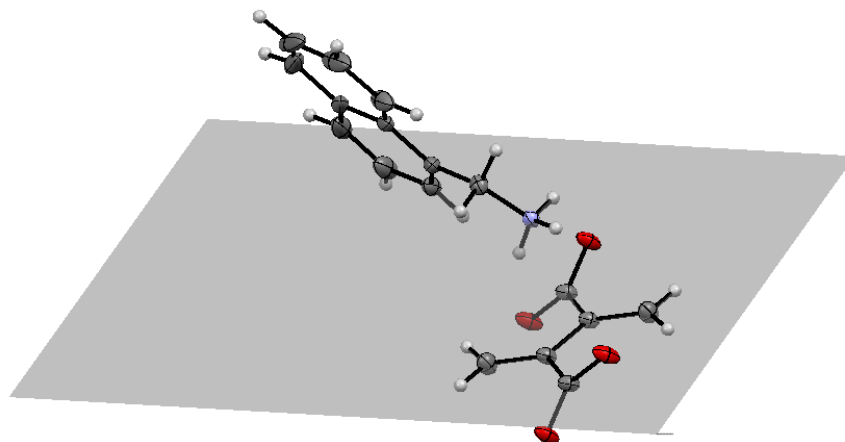


Figure 3.5 Crystal structure of naphthylmethylamine and fulgenic acid. The planar nature of deprotonated fulgenic acid is visible (bottom right)

An additional crystal of BMHA and benzylamine was grown. This one was formed in the same way as the fulgenic acid and naphthylmethylamine crystal. Both BMHA and benzylamine were dissolved in ethanol and allowed to evaporate at room temperature. Again the unit cell contained a 1:1 ration of BMHA to benzylamine and contained four molecules of each compound. The crystals were again monoclinic and the unit cell measured $a = 10.524(6)\text{\AA}$, $b = 8.435(4)\text{\AA}$, $c = 11.826(6)\text{\AA}$ with angles measuring $\alpha = 90^\circ$, $\beta = 102.145(14)^\circ$, $\gamma = 90^\circ$. This crystal structure again confirmed conjugation of the butadiene functionality of BMHA. (figure 3.6)

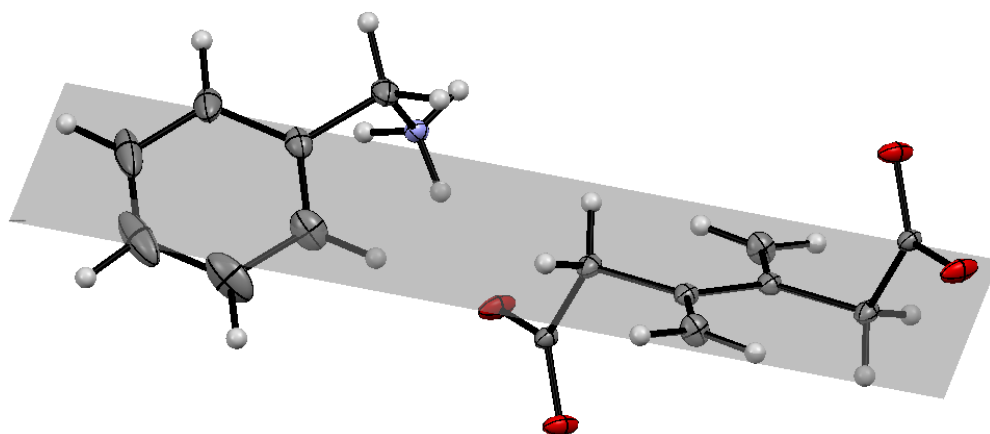


Figure 3.6 Crystal structure of benzylamine and BMHA (2) confirming conjugation of the butadiene

During the project, only one metal organic framework of sufficient crystalline quality was produced. This crystal was formed by simple, slow, liquid/liquid diffusion of aqueous copper acetate and ethanolic BMHA. The blue crystals (figure 3.2), were triclinic of space group P-1 and the unit cell parameters are as follows: $a = 9.9660(3)\text{\AA}$, $b = 11.9416(3)\text{\AA}$, $c = 12.8417(4)\text{\AA}$; $\alpha = 95.522(2)^\circ$, $\beta = 112.718(2)^\circ$, $\gamma = 112.190(2)^\circ$. The overall structure consists of copper oxide ladders that are linked together by the terminal carboxylates on BMHA. (figures 3.7 and 3.8) Rather than each carboxylate being bidentate, the carboxylate groups bridge the copper atoms within a single ladder structure. Additionally, the geometry around the copper centers varies from octahedral to square pyramidal. For each octahedral copper atom there are two square pyramidal copper atoms in the ladder. The presence of voids was confirmed when water molecules were found amidst the Cu-BMHA coordination polymer. Each unit cell contained four water molecules trapped within the voids. The volume of a water molecule is approximately 29.9\AA^3 , therefore the voids contained within the unit cell must be at least 119.6\AA^3

in volume. This accounts for 7.8% of the entire unit cell. (figure 3.8) As with all other crystal structures of BMHA obtained in this study, the butadiene group was planar indicating the desired conjugation of the methylene groups. (figure 3.9)

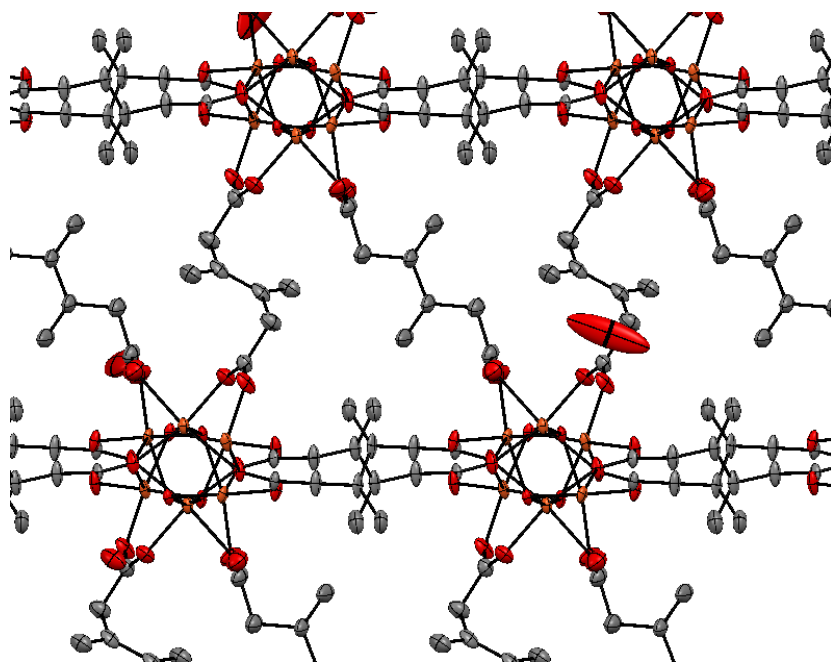


Figure 3.7 Crystal structure of Cu-BMHA looking down the copper oxide ladders and showing voids between the BMHA molecules

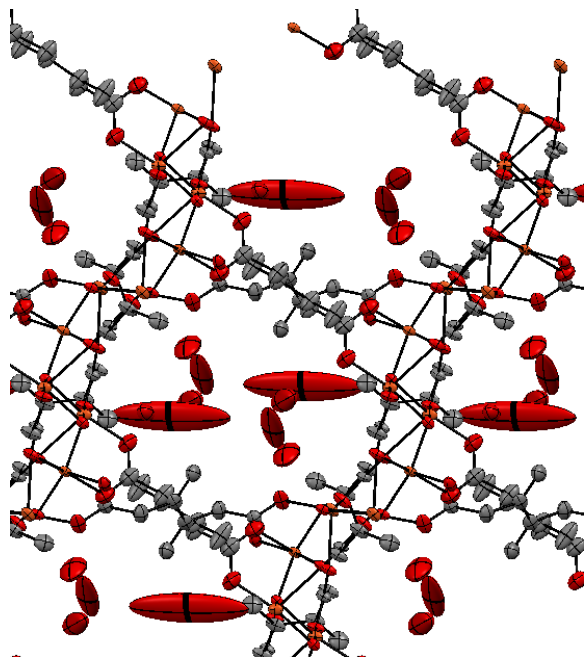


Figure 3.8 Crystal structure of Cu-BMHA showing copper oxide ladders (side view) and water molecules (large red ellipsoids) trapped within the voids.

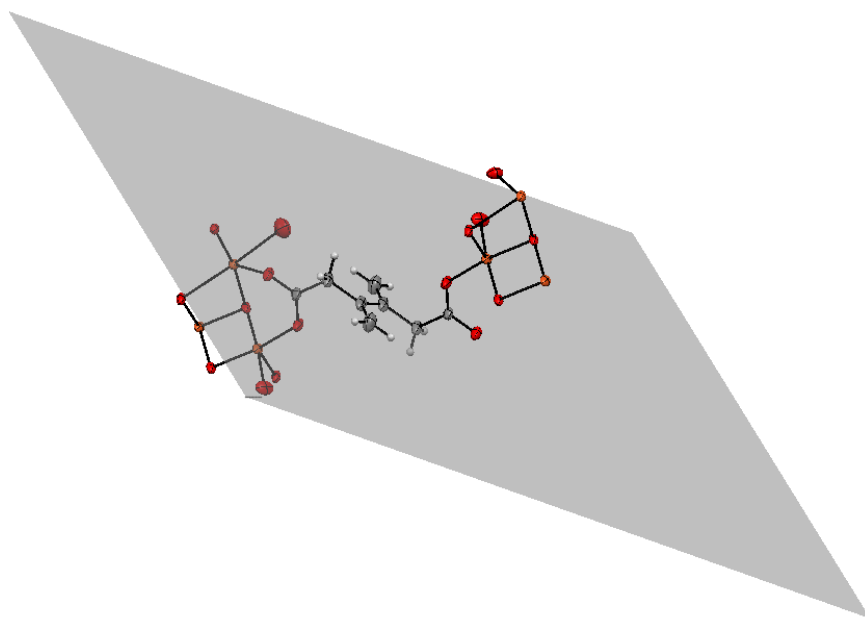


Figure 3.9 Crystal structure of Cu-BMHA MOF showing the planar butadiene group between the copper oxide ladders

CHAPTER 4 EXPERIMENTALS

General Experimental All reagents were purchased from Sigma Aldrich or Acros Organics and used without further purification unless otherwise stated. NMR spectra were obtained using a JEOL 300 MHz Eclipse NMR. Gas chromatograms and mass spectra were obtained using an Agilent Technologies 7890 A GC System with a 7693 Autosampler and an Agilent J&W GC Column-HP-5MS (30 m × 0.25 mm × 0.25 μm), coupled with a 5975 C Inert XL EI/CI MSD (with Triple Axis Detector). FT-IR spectra were obtained using a Perkin Elmer Spectrum One.

Crystal data for fulgenic acid, zinc formate hydrate and Cu-BMHA were collected using graphite-monochromated Mo K α X-radiation ($\lambda = 0.71073 \text{ \AA}$) on a Siemens R3 four-circle diffractometer using the $\theta - 2\theta$ technique over a 2θ range of $3 - 55^\circ$. The data were corrected for Lorentz and polarization effects and absorption using SADABS. The structures were solved by direct methods. Least squares refinement on F^2 was used for all reflections. Structure solution, refinement and the calculation of derived results were performed using the SHELXTL package of software. The non-hydrogen atoms were refined anisotropically. In all cases, hydrogen atoms were located then placed in theoretical positions.

Crystal data for fulgenic acid/naphthylamine, and BMHA/benzylamine were collected at 140 K with a Bruker platform diffractometer equipped with a Smart6000 CCD detector. Data were integrated using SAINT 6.45. Correction for absorption, decay, and inhomogeneity of the X-ray beam were applied using SADABS and or TWINABS. Structures were solved using direct methods. Hydrogen atoms were located and refined isotropically. In all cases the non-hydrogen atoms were refined with anisotropic atomic displacement parameters, and calculations were performed using SHELXTL 6.12

Diethyl-3,4-bis(methylene)hexanedioate (1). To an oven dried 1000mL round bottom flask was added 2-butyne-1,4-diol (9.6398g, 111.97mmol, 1eq), and recently distilled triethylorthoacetate (104 mL, 92.04g, 567.34mmol, 5eq), 100mL of dry dimethylformamide, and a stir bar. A reflux condenser was fitted to the reaction vessel and the top the condenser was fitted with a drying tube. The entire apparatus was purged with argon. The reaction vessel was placed inside an improvised microwave reactor. The water to the condenser was turned on and 1mL of propionic acid was added through the top of the condenser. With the drying tube in place, the reaction mixture was refluxed in the microwave with stirring for 1.5 hours. Careful control of the microwave power is necessary to prevent the condenser from boiling over. The apparatus is allowed to come to room temperature at which point the reaction mixture was transferred to a 2L separatory funnel. The solution was diluted with ethyl acetate and then washed with 3 x 300mL of 0.5M HCl followed by 3 x 300mL of concentrated NaCl solution. Organic layer was dried over anhydrous MgSO₄, filtered, and the volatiles were removed under reduced pressure. Product was obtained as 12.3691g of diethyl-3,4-bis(methylene)hexanedioate, a 48% yield. ¹H-NMR 300MHz (CDCl₃): δ 1.21 (t, 6H); 3.26 (s, 4H); 4.10 (q, 4H); 5.13 (s, 2H); 5.25 (s, 2H). ¹³C-NMR 300MHz (CDCl₃): δ 14.1, 40.4, 60.7, 117.1, 139.5, 171.2. FT/IR (ATR) 2984 (CH₃), 1731 (C=O), 1602 (C=C), 1027 (C-O) cm⁻¹.

3,4-bis(methylene)hexanedioic acid (2). To a 250mL round bottom flask was added (58mL) of 1M NaOH solution, (78mL) of ethanol, (6.0500g, 30.5mmol, 1eq) of diethyl-3,4-bis(methylene)hexanedioate (1), and a stir bar. Reaction mixture was stirred at room temperature for 2 hours. The reaction flask was then placed in an ice water bath and allowed to come to 0°C. At this point the reaction mixture was transferred to a 400mL beaker and diluted with (40mL)

deionized water. The reaction mixture was then brought down to a pH of 3 with concentrated HCl solution. The now acidic reaction mixture was transferred to a separatory funnel and extracted with 3 x 75mL of ethyl acetate. The organic layers were reserved, combined, and then washed with 3 x 75mL of concentrated NaCl solution. The organic layer was then dried over MgSO₄, gravity filtered, and the solvent was removed via rotary evaporator. Product was recovered 1.5235g of a white crystalline solid a 29% yield. ¹H-NMR 300MHz (DMSO-d₆): δ 3.20 (s, 6H); 5.12 (s, 2H); 5.72 (s, 2H); 12.22 (s, 2H). ¹³C-NMR 300MHz (CDCl₃): δ 40.0, 116.6, 140.1, 172.5. FT/IR (ATR): 2920 (OH), 1683 (C=O), 1603 (C=C) cm⁻¹.

2,3-dimethylmaleic acid, dimethyl ester (9). To a 500mL round bottom flask was added dimethylmaleic anhydride (10.9729g, 63.7298mmol, 1eq), 150mL of methanol, 2mL of concentrated sulfuric acid, and a stir bar. A Dean Stark trap is filled with 3A molecular sieves and primed with methanol. The reaction mixture was refluxed with stirring for 48 hours. The reaction mixture was then allowed to cool and transferred to a 400mL beaker. Using 10% sodium bicarbonate solution the mixture was brought to a pH of 8. Reaction mixture was then transferred to a 1000mL separatory funnel and 100mL of diethyl ether was added. No phase separation was observed so 100mL of deionized water was added. After swirling the biphasic mixture the ether layer was reserved. The aqueous layer was then extracted with an additional 2 x 100mL of diethyl ether. Organic layers were pooled and washed with 2 x 100mL of concentrated NaCl solution. Aqueous layer was reserved for recovery of unreacted starting material. Organic layer was then dried over MgSO₄, gravity filtered, and the solvent was removed via rotary evaporator. Product was obtained as 12.0168g of a slightly yellow mobile fluid, 80% yield. ¹H-NMR 300MHz (CDCl₃): δ 1.93 (s, 6H); 3.74 (s, 6H). ¹³C-NMR 300MHz (CDCl₃): δ 15.6, 52.2, 133.4, 169.4. FT/IR (ATR): 2954 (CH₃), 1717 (C=O), 1648 (C=C), 1264 (C-O) cm⁻¹.

Dimethyl-2,3-bis(bromomethyl)maleate (8a), (8b). To a 250mL round bottom flask containing a stir bar was added 2,3-dimethylmaleic acid, dimethyl ester (1eq, 3.7913g, 10.40mmol), 60mL of carbon tetrachloride, and N-bromosuccinamide (2.05eq, 3.7913g, 21.30mmol). Benzoyl peroxide, 60mg, was added and the reaction flask was fitted with a reflux condenser. The reaction mixture was refluxed for 5 hours at which time an additional 60mg on benzoyl peroxide was added. Mixture was refluxed for 5 more hours then allowed to come to room temperature. The resulting slurry was vacuum filtered. The filter cake was washed with 2 x 10mL of carbon tetrachloride. The organic layers are combined and washed with 2 x 30mL of deionized water followed by 2 x 20mL of concentrated NaCl solution. The organic layer was then dried over anhydrous magnesium sulfate, gravity filtered, and solvent was then removed via a rotary evaporator. Product was obtained as a pale yellow oil, dimethyl-2,3-bis(bromomethyl)maleate that turned to a darker amber color within a few days. Product weighed 1.3575g constituting an 84% yield. ¹H-NMR 300MHz (CDCl₃): δ E-isomer: 3.83 (s, 3H); 4.33 (s, 2H); Z-isomer: 3.90 (s, 3H); 4.49 (s, 2H). ¹³C-NMR 300MHz (CDCl₃): δ E-isomer: 26.9, 53.2, 137.2, 166.1; Z-isomer: 24.1, 53.2, 137.1, 165.7. FT/IR (ATR): 2952 (CH₃), 1721 (C=O), 1634 (C=C), 1265 (C-O) cm⁻¹.

Dimethyl Fulginate (9). Dimethyl-2,3-bis(bromomethyl)maleate (2.2678g, 8.86mmol, 1eq) was dissolved in 22mL of dichloromethane and transferred to a 100 mL round bottom flask containing a stir bar. The flask was placed on a stir plate and powdered zinc metal (1.1660g, 17.8342mmol, 2.01eq) was added. With stirring 1mL of glacial acetic acid was added dropwise. The exothermic reaction is enough to boil the solvent so care should be taken at this step to prevent thermal runaway. The reaction mixture was stirred for 4 hours after which the dark slurry was vacuum filtered. It is advisable not to use a frit for this filtration as it will likely clog. A fast flow filter paper is recommended. The filter cake was extracted with 2 x 5mL of

dichloromethane. The filtered reaction mixture and cake rinses were transferred to separatory funnel and washed with 3 x 30mL of deionized water followed by 2 x 30 mL of concentrated NaCl solution. The organic layer was reserved, dried over anhydrous MgSO₄, gravity filtered, and concentrated under reduced pressure affording 1.3575g of light yellow oil, 92% yield.

Product was used without further purification. ¹H-NMR 300MHz (CDCl₃): δ 3.76 (s, 6H); 5.81 (d, J=1.38Hz, 2H); 6.28 (d, J=1.38, 2H). ¹³C-NMR 300MHz (CDCl₃): δ 52.1, 127.9, 166.1.

FT/IR (ATR): 2955 (CH₃), 1718 (C=O), 1619 (C=C) cm⁻¹.

Fulgenic acid (3). To a 200 mL round bottom flask was added dimethyl fulginate (10.9841g, 64.5708mmol, 1eq) and of 4-tertbutylcatechol (0.1210g, 0.7280mmol, 0.01eq). The flask was gently heated with a heat gun and swirled until all of the 4-tertbutylcatechol is dissolved. A stir bar was added and the reaction vessel was fitted with a 100mL pressure equalizing addition funnel containing 40mL of a 3M NaOH solution. The NaOH solution was added dropwise with vigorous stirring. The reaction mixture was left to stir overnight. The following day 22mL of aqueous 6M H₂SO₄ was placed in a 200mL beaker and chilled on an ice bath. A stir bar was added to the beaker. With vigorous stirring the reaction mixture was added dropwise over a period of 40 minutes to the H₂SO₄. A powdery tan precipitate was collected via vacuum filtration. An oily residue containing product remained stuck to the stir bar and pipet. Diethyl ether, 10mL, was added to the oil dissolving it and leaving behind some tan powder. This powder was vacuum filtered and added to the product netting a total of 3.4975g of fulgenic acid. The aqueous filtrate was transferred to a separatory funnel and extracted with 2 x 20mL of diethyl ether. The ether layers were pooled then washed with 2 x 20mL of concentrated NaCl solution, dried over anhydrous MgSO₄, and gravity filtered. The ether was removed under reduced pressure in a rotary evaporator and the crude product was placed in a -30° C freezer

overnight. To the crude product was added 7mL of hexanes. The mixture was gently heated with a heat gun. At this point two layers have formed; the bottom being the crude product and the top being the hexanes. Acetone (approximately 8mL) was added dropwise while swirling until a white precipitate separates from the oil. The flask is placed in the freezer overnight and the precipitate is filtered off the next day netting an additional 0.3615g of product bringing the total yield to 3.8590g of fulgenic acid, a 42% yield based on dimethyl fulginate. ¹H-NMR 300MHz (acetone-d₆): δ 5.88 (d, J=1.65 Hz, 2H); 6.22 (d, J=1.65, 2H). ¹³C-NMR 300MHz (acetone-d₆): δ 126.7, 139.8, 166.2, 205.5. FT/IR (ATR): 2885, 2573, 1669 (C=O), 1610 (C=C), 1279 (C-O) cm⁻¹.

Dibromo-4-vinylpyridine (7) To a 250mL round bottom flask containing a stir bar, was added (1.3365g) of 4-vinylpyridine and 150mL of chloroform. The flask was sealed with a septum and purged with argon. The reaction flask was then placed on an ice water bath and allowed to chill to 0°C. The argon was turned off but the needle was left in the septum to equalize pressure inside the reaction vessel. At this point (1mL) of liquid bromine was added dropwise to the 4-vinylpyridine solution with vigorous stirring. After addition of the bromine the reaction mixture was stirred for 15min on the ice bath, then removed from the ice bath and stirred for an additional 15min. The chloroform was removed under reduced pressure. To the dry reaction mixture was added (20mL) of chloroform and (50mL) of deionized water. The slurry was swirled then vacuum filtered. The resulting filter cake was washed with 3 x 20mL of acetone. Product was obtained as a light yellow amorphous powder weighing 2.2914g. Yield is near quantitative. FT/IR (ATR): 845, 1180, 1468, 1638, 3042cm⁻¹.

Monobromo-4-vinylpyridine (8) To a 50mL round bottomed flask was added Dibromo-4-vinylpyridine (0.3095g, 1.1681mmol, 1eq). To the flask was added a stir bar and 10mL of dry

tetrahydrofuran. With vigorous stirring anhydrous K_2CO_3 , (0.32289g, 2.3363mmol, 2eq) was added. The reaction mixture was stirred overnight. The following day, 10mL of deionized water was added to the reaction flask and the volatiles were removed via rotary evaporator. The aqueous layer was extracted with 3 x 30mL of diethyl ether. Organic layers were pooled and washed with 30mL of concentrated NaCl solution, dried over $MgSO_4$, filtered and ether was removed under reduced pressure. Product was acquired as a dark brown oil containing impurities. Yield is less than 1%. 1H -NMR 300MHz ($CDCl_3$) δ 6.01 (d, 1H); 6.40 (d, 1H); 7.54 (d, 2H); 8.63 (d, 2H).

N,N'-diphenyl-1,2-di(3-pyridyl)ethene-1,2-diamine (19g) To a 100mL round bottom flask was added a stir bar and 5.3839g of 3-pyridinecarboxaldehyde. To an addition funnel was added 4.9581g of aniline. The aniline was added dropwise to the aldehyde with vigorous stirring. After completion of addition the reaction mixture was heated to 110 °C for 1 hour on a sand bath with stirring. The mixture was then allowed to come to room temperature. Dimethyl sulfoxide, 20mL, was added followed by 1.0404g of NaCN. The reaction mixture was then stirred overnight at room temperature. The following day 200mL of ice water was added to a 1000mL tall-form beaker. The crude product was poured into the ice water causing an immediate precipitation of a gummy yellow powder. The yellow slurry was stirred and then vacuum filtered after all the ice had melted. The bright yellow filter cake was rinsed with 3 x 20mL of deionized water. The crude product was then transferred to a 300mL round bottom flask and 100mL of acetone was added. The solution was refluxed for 0.5 hours after which the acetone was removed via rotary evaporator. After removal of the acetone, 25mL of diethyl ether was added and swirled. The yellow product was collect via vacuum filtration. Yield was 8.2778g of N,N'-diphenyl-1,2-di(3-pyridyl)ethane-1,2-diamine (**19g**) a 90% of theoretical. 1H -NMR 300MHz ($CDCl_3$): δ 5.67 (s,

2H); 6.56 (d, 4H); 6.77 (t, 2H); 7.09 (t, 4H); 7.19 (m, 2H); 7.83 (m, 2H); 8.42 (d, 2H); 8.80 (s, 2H). ¹³C-NMR 300MHz (CDCl₃): δ. FT/IR (ATR):

1,2-diphenylethane-1,2-dione (19d) To a two neck 500mL round bottom flask was added 8.2778g of N,N'-diphenyl-1,2-di(3-pyridyl)ethane-1,2-diamine (**19g**) and 250mL of acetone. The solution was heated gently with a heat gun to help dissolve the solids. A fritted bubbler was employed to pump air through the solution for 1 hour. During this time the volume of the reaction mixture had been reduced to 100mL. After removal of the airline 100mL of a 2M HCl solution was added to the reaction flask resulting in a dark red solution. Concentrated HCl was added dropwise until a pH of 1 was achieved. During acidification a fine off white precipitate began to form. The mixture was placed in a refrigerator for 0.5 hours. The precipitate was then collected by vacuum filtration and transferred to a beaker containing 20mL of dichloromethane. The solution was neutralized with concentrated KCO₃ solution and 20mL of deionized water was added. The reaction mixture was extracted with 3 x 20mL of dichloromethane. Organic layer was dried over MgSO₄, filtered, and the volatiles were removed under reduced pressure. Product was obtained as 1.8486g of a yellow crystalline solid, a 38% yield. ¹H-NMR 300MHz (CDCl₃): δ 7.49 (m, 2H); 8.30 (m, 2H); 8.85 (m, 2H); 9.17 (m, 2H). ¹³C-NMR 300MHz (CDCl₃): δ 124.0, 128.4, 137.1, 151.6, 155.2, 191.1. FT/IR (ATR): 3072 (Ar-H), 1669 (C=O), 1583 (C=N) cm⁻¹.

2,3-di(3-pyridyl)-1,3-butadiene (11) To a flame dried, argon purged, 50mL round bottom flask fitted with a septum and stir bar, dry diisopropylamine, (0.4007g, 3.960mmol, 3.29eq) was injected through the septum followed by 15mL of dry tetrahydrofuran. The reaction flask was placed on a CO₂/acetone bath. The reaction flask was allowed to equilibrate at which point 1.4mL of a 2.25M n-butyl lithium (0.2019g, 3.150mmol, 2.58eq) solution in hexanes was injected through the septum. The mixture was then stirred 10 minutes at -78°C. After the

formation of the lithium diisopropylamide, the septum was removed to add (1.3627g, 3.3544mmol, 2.94eq) of methyl triphenylphosphonium iodide. The yellow color of the methyl ylide was observed. The septum was quickly replaced and the flask was again purged with argon. After purging, the flask was placed on an ice/water bath and stirred for one hour to ensure complete formation of the ylide. After an hour had elapsed the flask was transferred back to the CO₂/acetone bath and allowed to equilibrate. To a three dram vial was added (0.2558g, 1.205mmol, 1eq) of 1,2-di(pyridin-3-yl)ethane-1,2-dione (**19d**). The substrate was dissolved in 5mL of dry tetrahydrofuran. After the reaction flask had equilibrated to -78°C, the substrate solution was added dropwise over a period of 30 minutes with vigorous stirring. After addition of the substrate an additional 1mL of tetrahydrofuran was used to rinse the sides of the reaction vessel. The reaction mixture was stirred for one hour at -78°C at which point the reaction was then allowed to come to room temperature with stirring. The solution turned a brownish color at this point likely due to some polymerization of product. The septum was removed and 3mL of acetone was added slowly to quench the remaining ylide. Off gassing of isobutylene was observed at this step. The precipitate, likely consisting of LiI and triphenylphosphine oxide, was removed via vacuum filtration. A sample of the crude reaction mixture was taken for GC/MS analysis. The crude product was found to contain the desired product, 2,3-di(3-pyridyl)-1,3-butadiene, triphenyl phosphine, triphenylphosphine oxide, and a small amount of free diisopropylamine. The solution was placed on a rotary evaporator and the acetone was removed to lower the polarity of the solution to encourage the precipitation of triphenylphosphine oxide. The ethereal solution was placed in the freezer overnight. The following day the precipitate was gravity filtered and discarded. The filter cake was rinsed with approximately 5mL of dry tetrahydrofuran. The following day a small amount of the sample was taken and all remaining

solvents were removed under reduced pressure at 40°C. When the NMR sample tube was made with CDCl₃ it was noted that a precipitate formed in the tube. The sample was filtered to remove precipitate and 2,3-di(3-pyridyl)-1,3-butadiene (**11**) was confirmed to be present in the sample. The majority of residual solvent was removed by rotary evaporator at which point chloroform was added to the brown oil until a precipitate was observed. This dark brown precipitate was believed to be polymerized product and was removed from the product via vacuum filtration. The now yellow solution containing the product was left open in an evaporating dish for 48 hours to allow complete evaporation of the chloroform. Silica gel, 32-63µm, 40g was weighed out for a plug. Acetone:chloroform (1:9) was chosen as the mobile phase. The crude product was dissolved in 2mL of elution solvent and loaded onto the top of the plug. 192mLs of solvent were run through the plug in effort to elute triphenylphosphine and its oxide. The solvent system was then changed to acetone:dichloromethane (1:1). Five 75mL fractions were taken and tested by GC/MS. Fractions 3-5 were pooled and the majority of the solvent was removed under reduced pressure. The golden solution was dried over anhydrous MgSO₄, gravity filtered, then the solvent was removed under reduced pressure at 40°C. The resulting brown liquid was then placed on a vacuum line to remove any remaining solvents. After tests revealed the presence of triphenylphosphine oxide and diisopropylamine in the product. The crude product was dissolved in 20mL of dichloromethane and washed with 3 x 5mL of concentrated sodium bicarbonate solution to remove diisopropylamine. The organic solution was again dried over MgSO₄, gravity filtered and the solvent was removed. The remaining triphenylphosphine oxide was removed via column chromatography. The solvent system selected was 3:7 acetone:chloroform. Triphenylphosphine oxide was eluted in the 5th and 6th fraction while the product (**11**) eluted in fractions 8 through 11. The fractions containing the product were pooled and the solvent was

removed under reduced pressure at 40°C. Then 20mL of dichloromethane was added to dissolve the product. It was then dried over MgSO₄, gravity filtered, then solvent was removed under reduced pressure at 40°C. The product was then placed in a high vacuum environment to ensure the removal of all residual solvent. Product was obtained as a clear light amber oil weighing 0.0222g. The final product was found by GC/MS analysis to be 92% pure, being contaminated by two yet to be identified contaminants. Yield was 8.0% of theoretical. ¹H-NMR 300MHz (CDCl₃): δ 5.41 (d, J= 0.54Hz, 2H); 5.59 (d, J= 0.54 Hz, 2H); 7.18 (dd, 2H); 7.60 (m, 2H); 8.45 (dd, J= 4.95 Hz, J= 1.65 Hz, 2H); 8.59 (d, J= 2.48Hz, 2H). ¹³C-NMR 300MHz (CDCl₃): δ 118.9, 123.2, 135.0, 135.3, 146.2, 148.9, 149.1. FT/IR (ATR): 745 (C-H out of plane bend), 1412 (C=N-C), 1615 (C=C), 3030 (Ar-H) cm⁻¹.

Cu-BMHA MOF Thin glass tubes about 20cm long with an outer diameter of 0.5cm were cut to be used as the crystallization chambers. One end was fitted with a plastic NMR cap and keeping the tubes vertical (cap down) the tube was half filled with 0.100M aqueous Cu(OAc)₂. Then an ethanolic solution of BMHA (0.200M) was pipetted down the side of the tube so as to float on top of the aqueous copper (II) solution. The top of the tube was sealed with another NMR cap and left in a vibration free environment for two weeks. After two weeks crystals of sufficient size and quality had formed at the solvent interface. These crystals were carefully removed from the tube and washed with a few milliliters of ethanol. The crystals were dried and then sent for XRD crystal analysis.

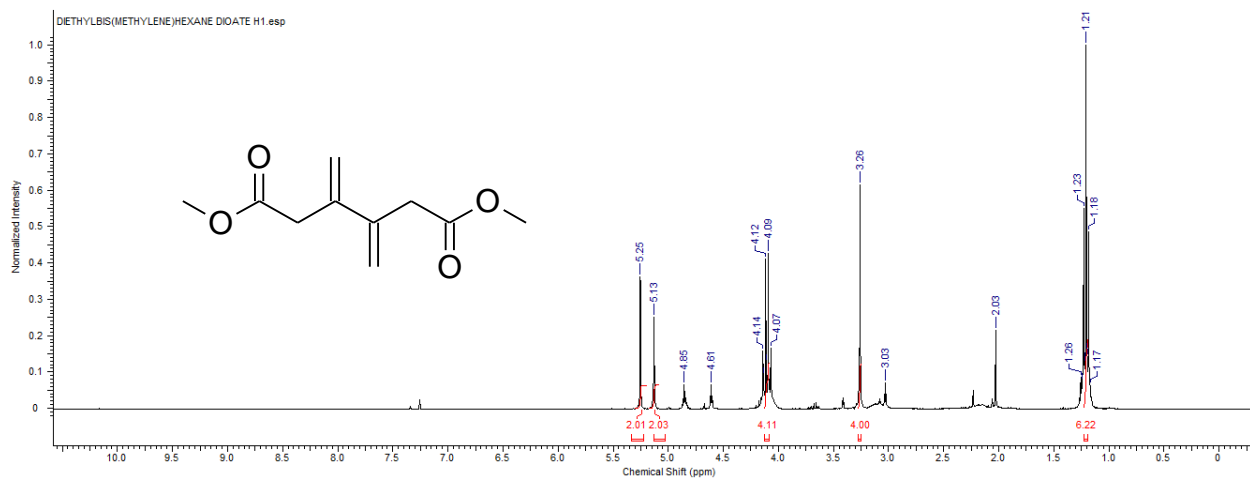


Figure 4.1 $^1\text{H-NMR}$ diethyl-3,4-bis(methylene)hexanedioate

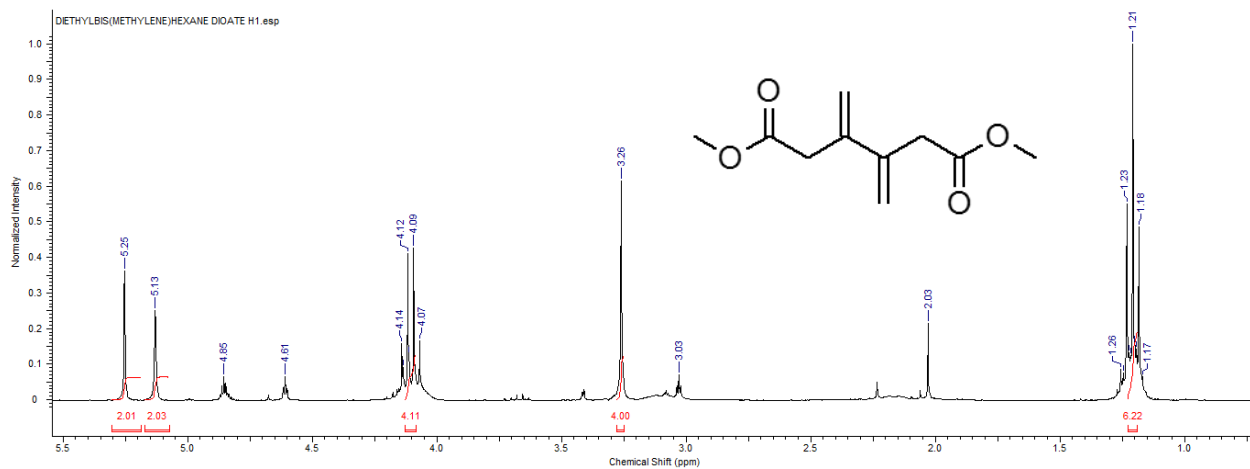


Figure 4.2 $^1\text{H-NMR}$ diethyl-3,4-bis(methylene)hexanedioate zoomed in

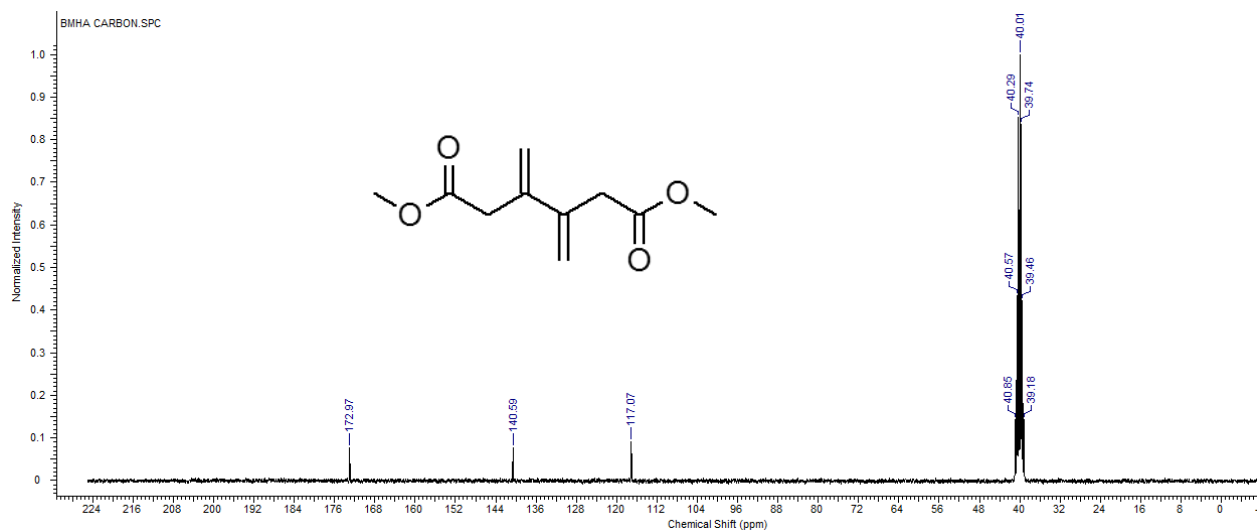


Figure 4.3 ^{13}C -NMR of diethyl-3,4-bis(methylene)hexanedioate

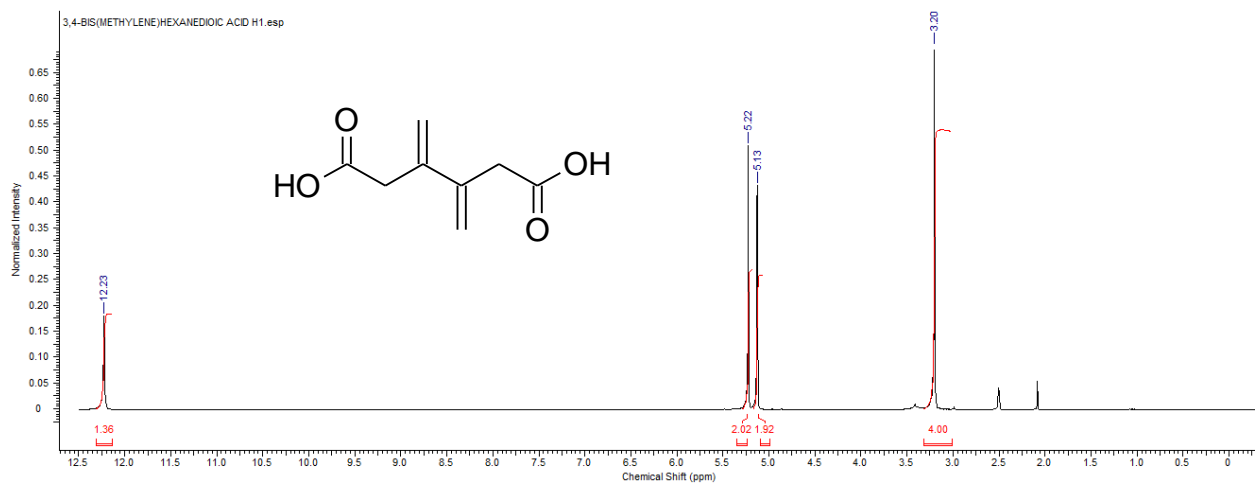


Figure 4.4 ^1H -NMR of bis(methylene)hexanedioic acid

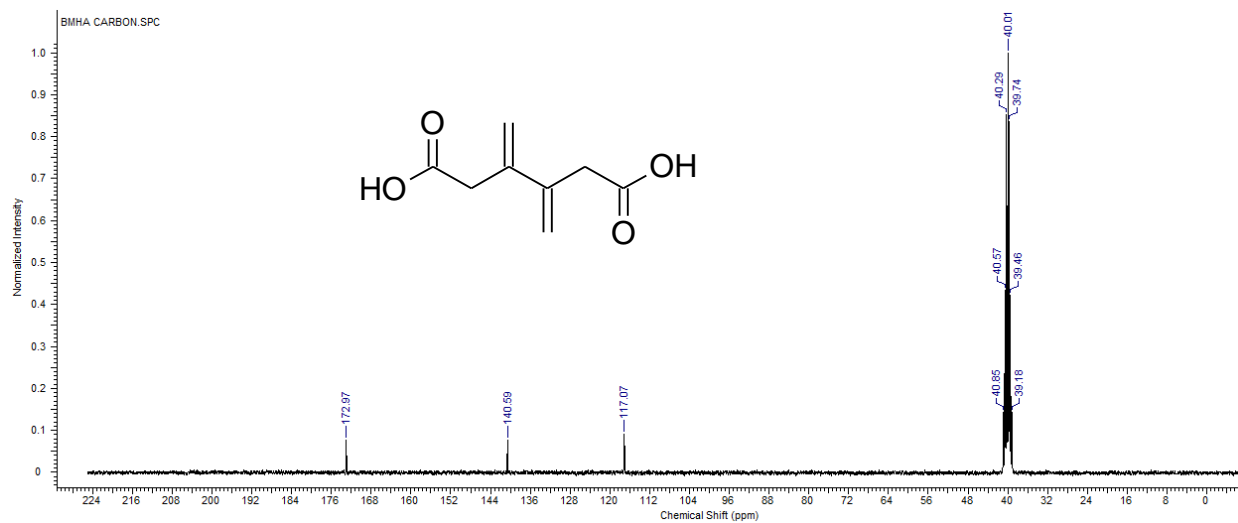


Figure 4.5 ^{13}C -NMR of bis(methylene)hexanedioic acid

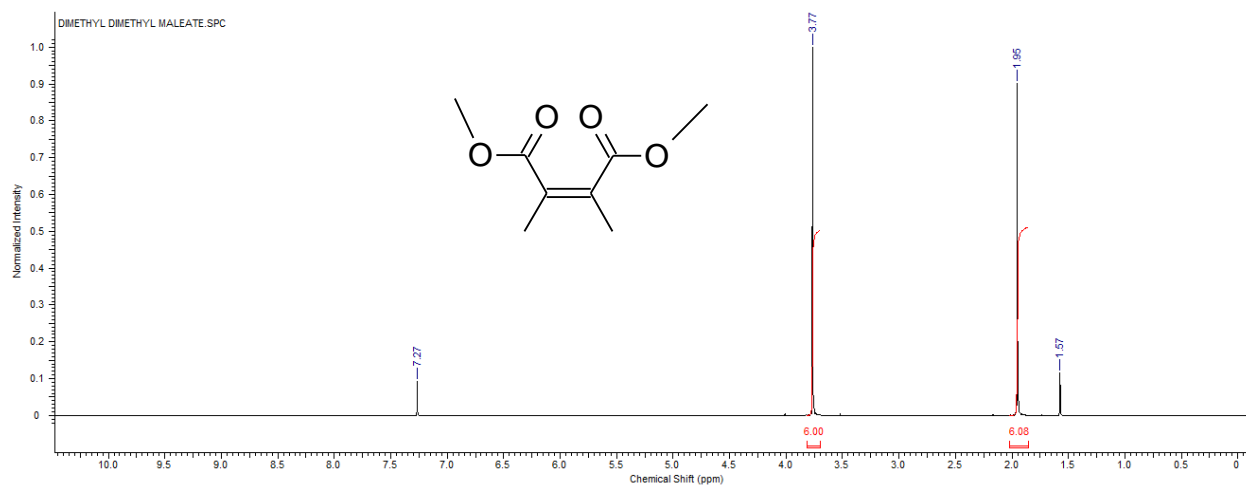


Figure 4.6 ^1H -NMR of 2,3-dimethylmaleic acid, dimethyl ester

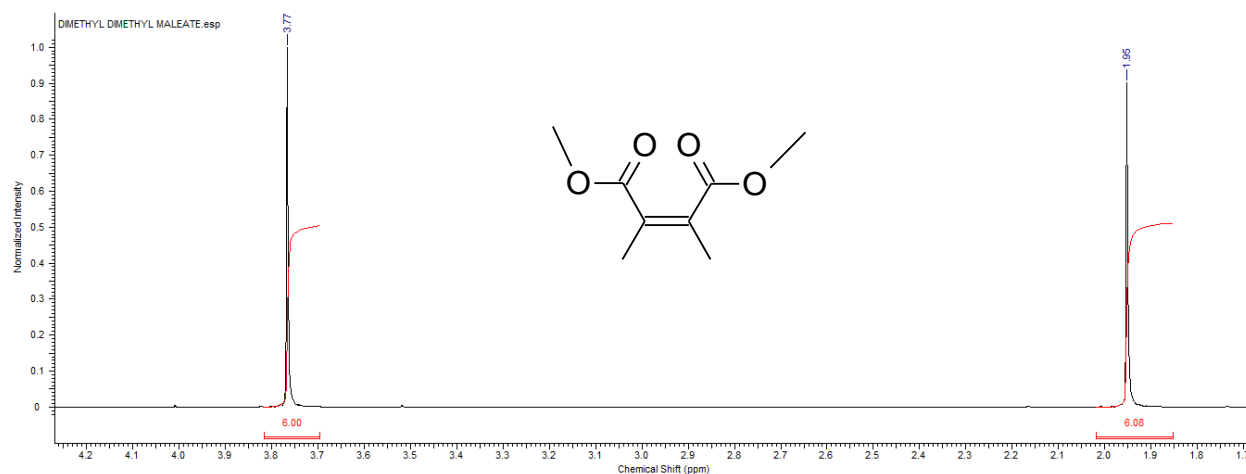


Figure 4.7 ^1H -NMR of 2,3-dimethylmaleic acid, dimethyl ester zoomed in

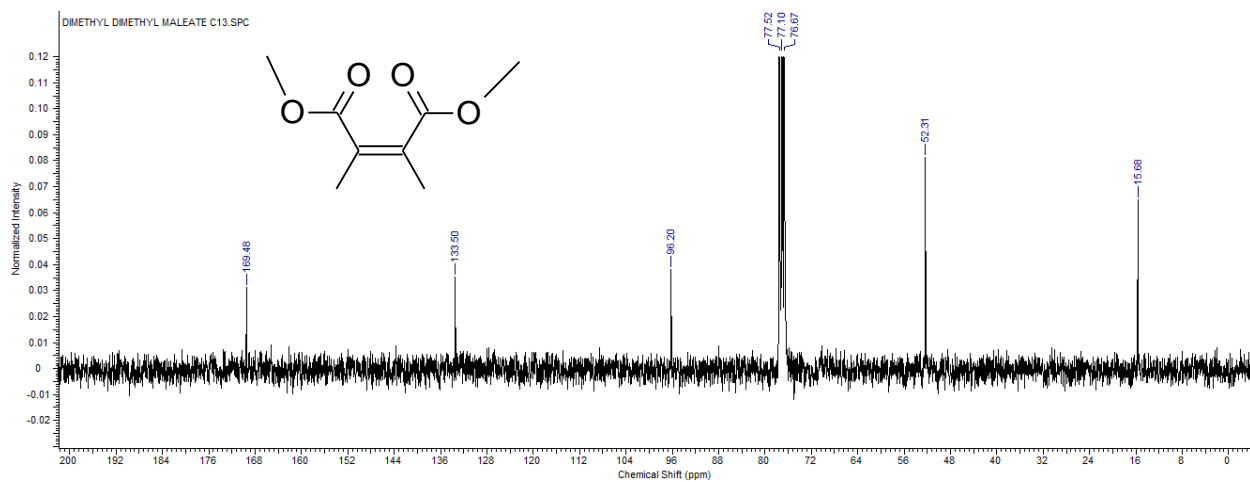


Figure 4.8 ^{13}C -NMR of Z 2,3-dimethylmaleic acid, dimethyl ester

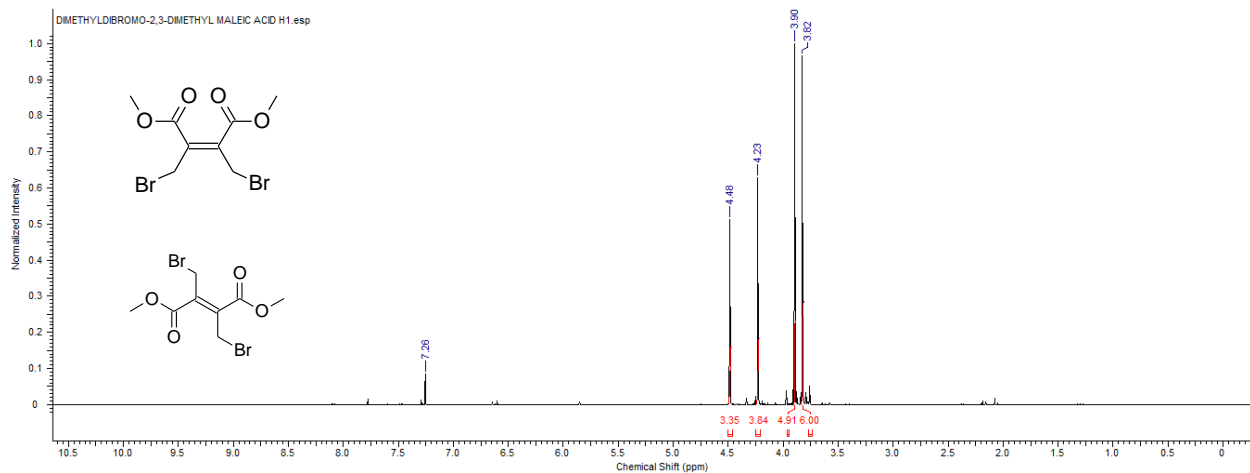


Figure 4.9 ^1H -NMR of E and Z dimethyl-2,3-bis(bromomethyl)maleate

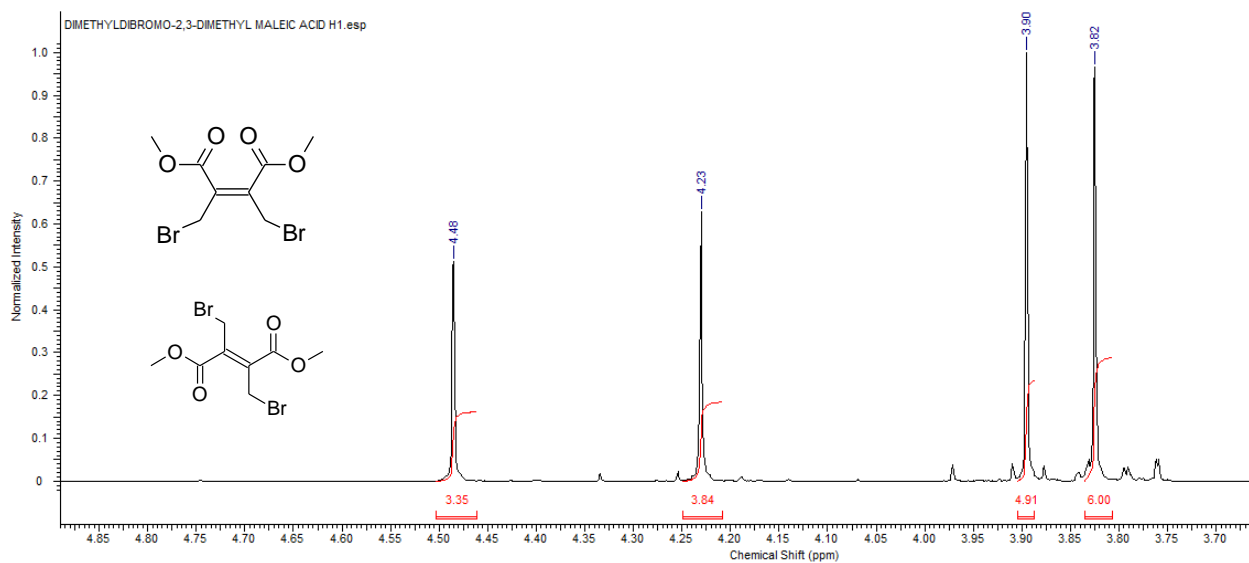


Figure 4.10 ^1H -NMR of E and Z dimethyl-2,3-bis(bromomethyl)maleate zoomed in

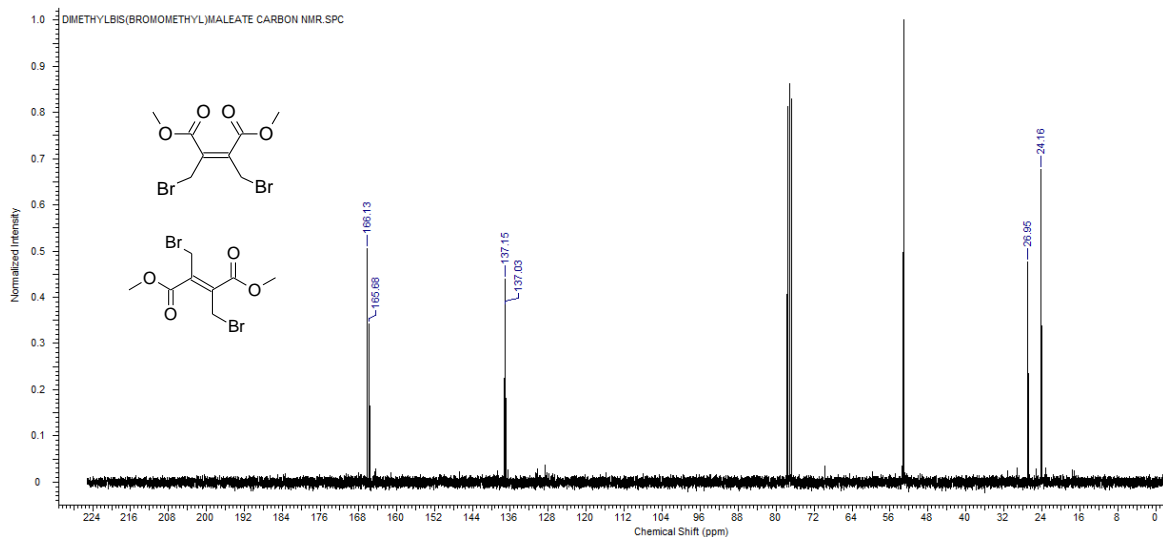


Figure 4.11 ^{13}C -NMR of E and Z dimethyl-2,3-bis(bromomethyl)maleate

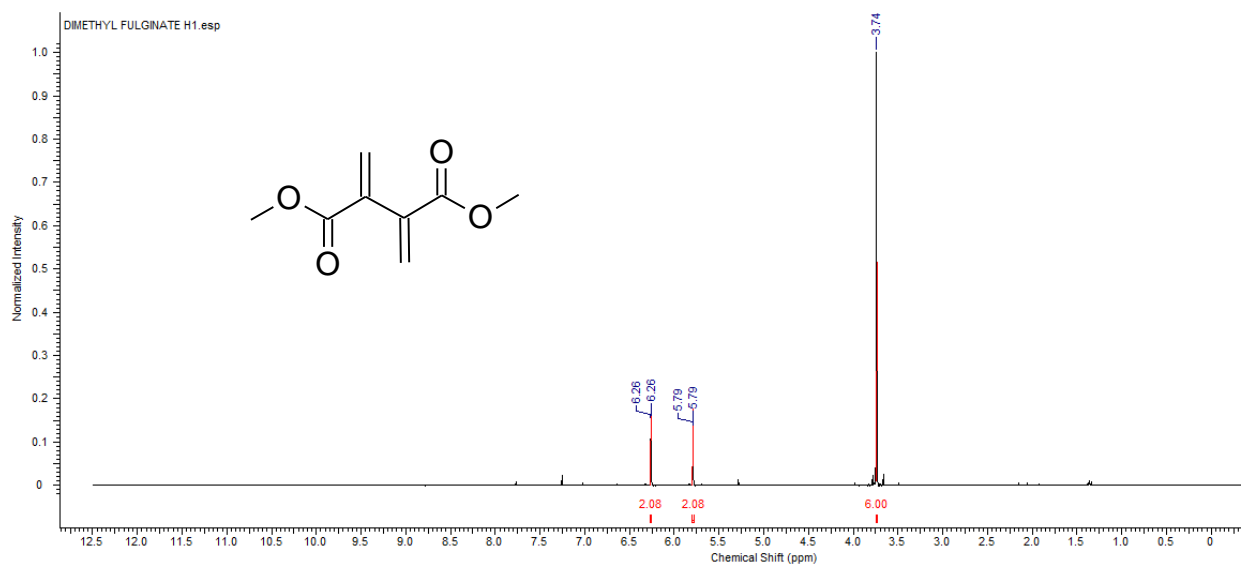


Figure 4.12 $^1\text{H-NMR}$ of dimethyl fulginate

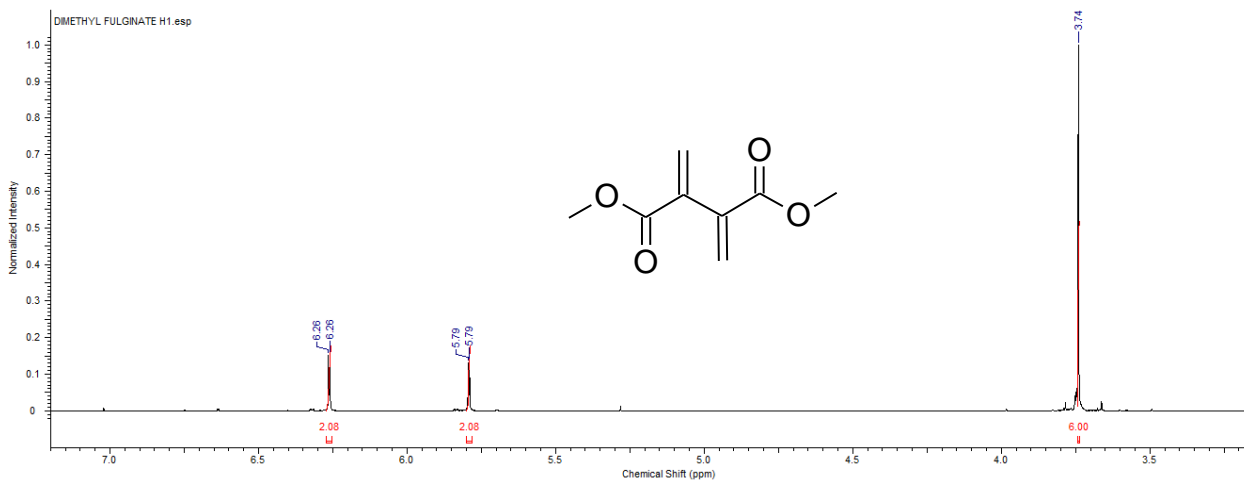


Figure 4.13 $^1\text{H-NMR}$ of dimethyl fulginate zoomed in

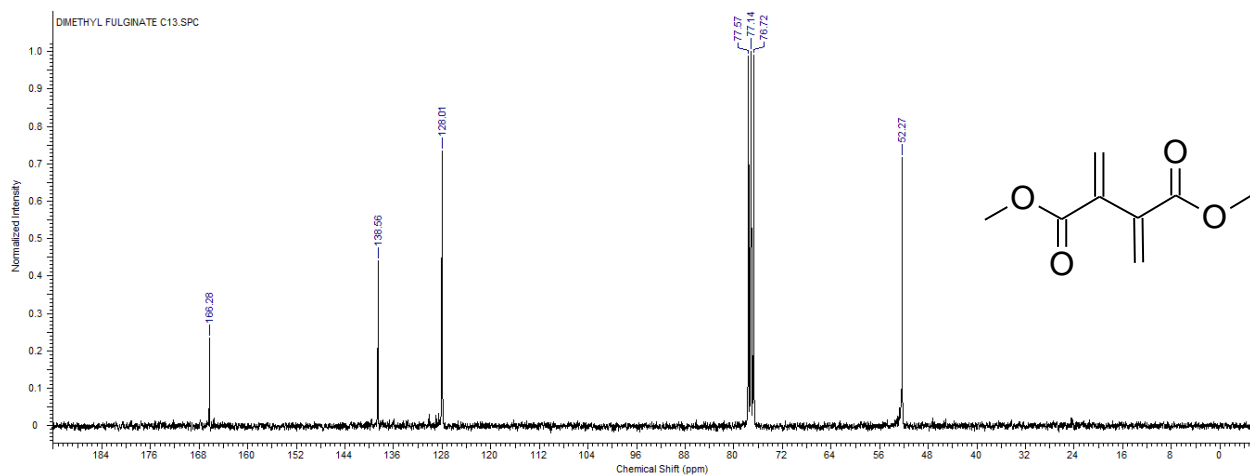


Figure 4.14 ^{13}C -NMR of dimethyl fulginate

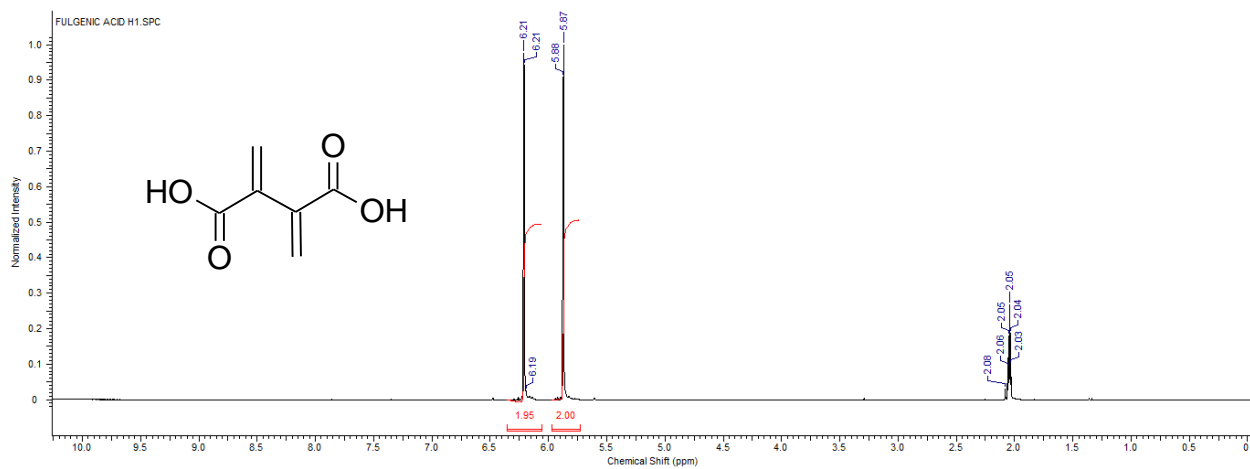


Figure 4.15 ^1H -NMR of fulgenic acid

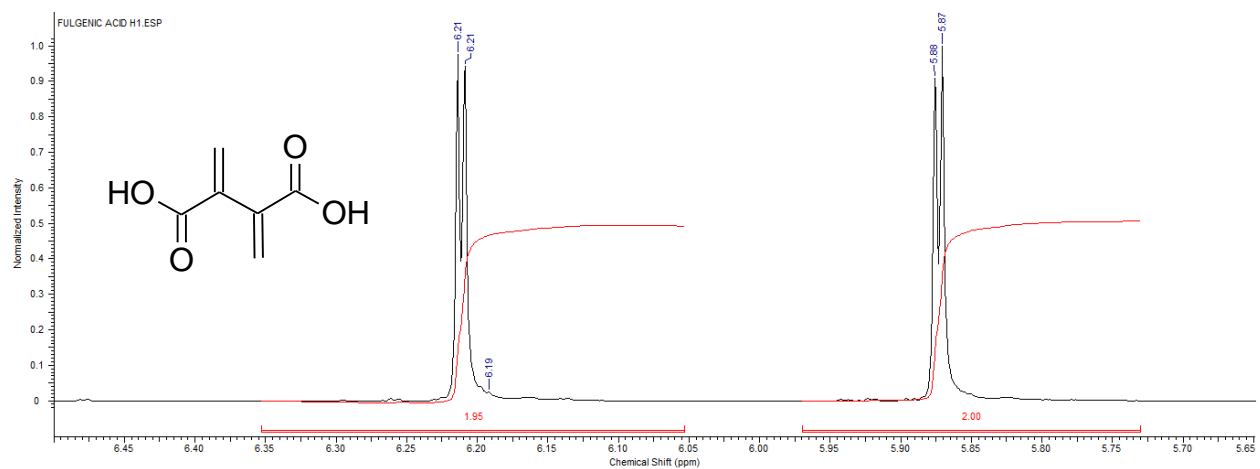


Figure 4.16 ^1H -NMR of fulgenic acid zoomed in

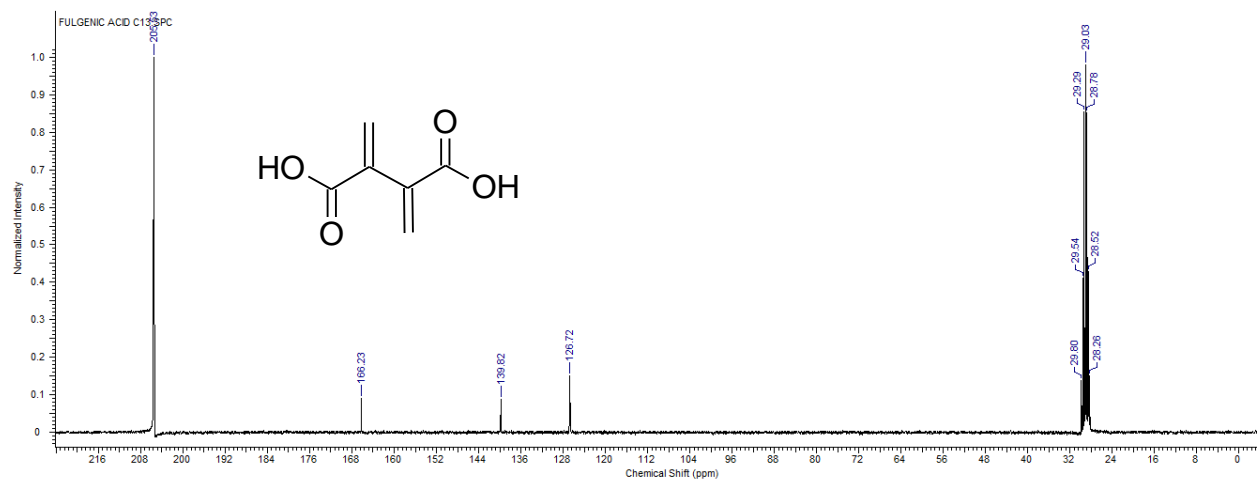


Figure 4.17 ^{13}C -NMR of fulgenic acid

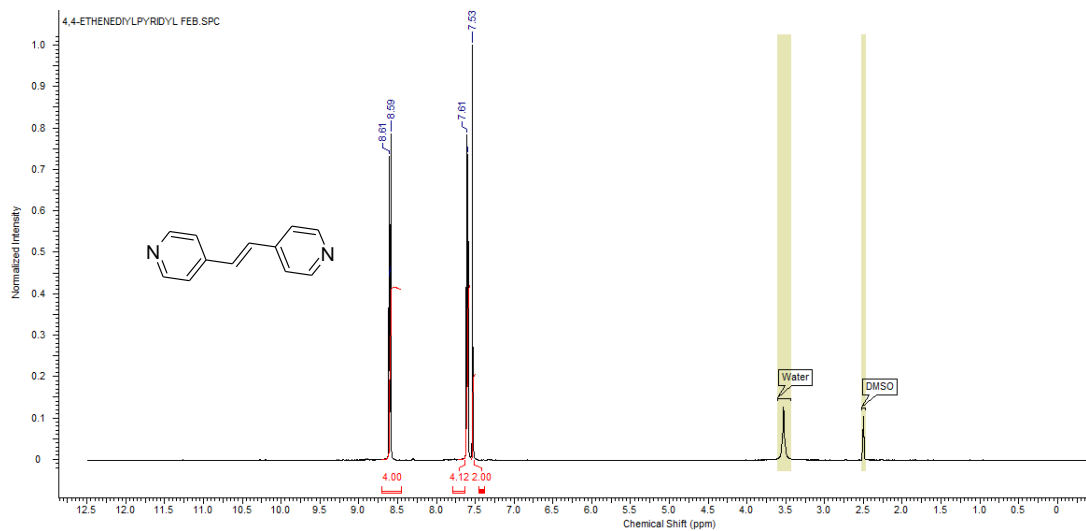


Figure 4.18 $^1\text{H-NMR}$ of 4-4'ethene-1,2-diylpyridine

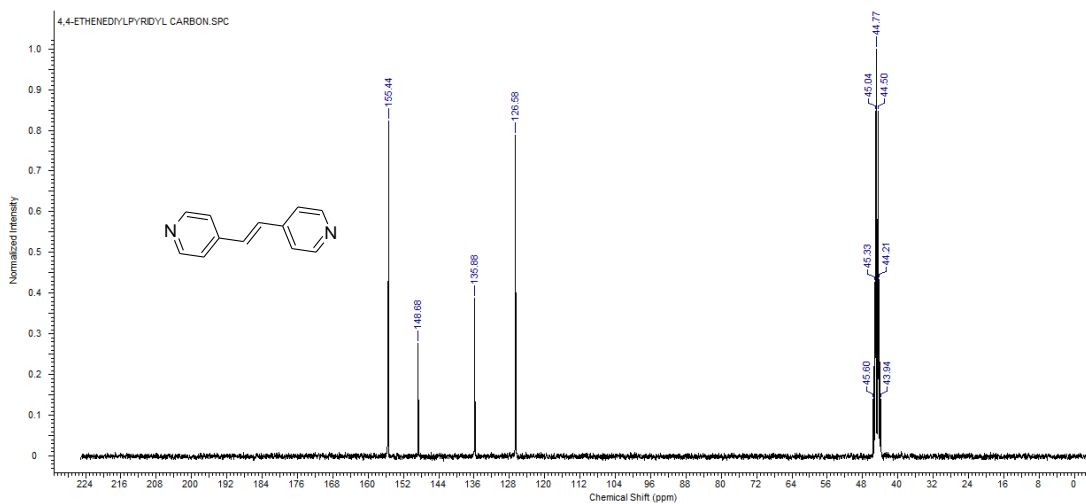


Figure 4.19 $^{13}\text{C-NMR}$ of 4-4'ethene-1,2-diylpyridine

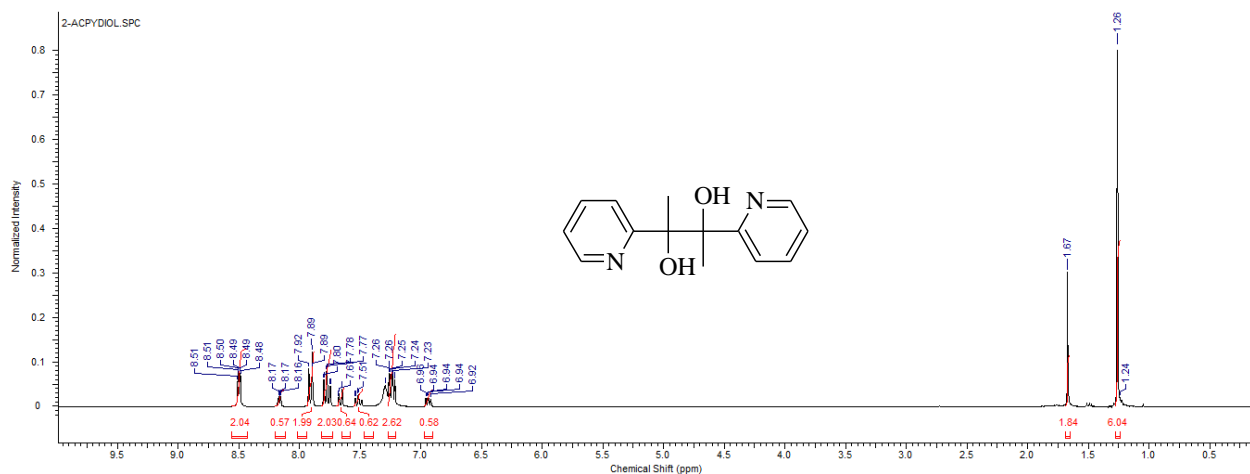


Figure 4.20 ¹H-NMR of 2,3-pyridin-2-ylbutane-2,3-diol

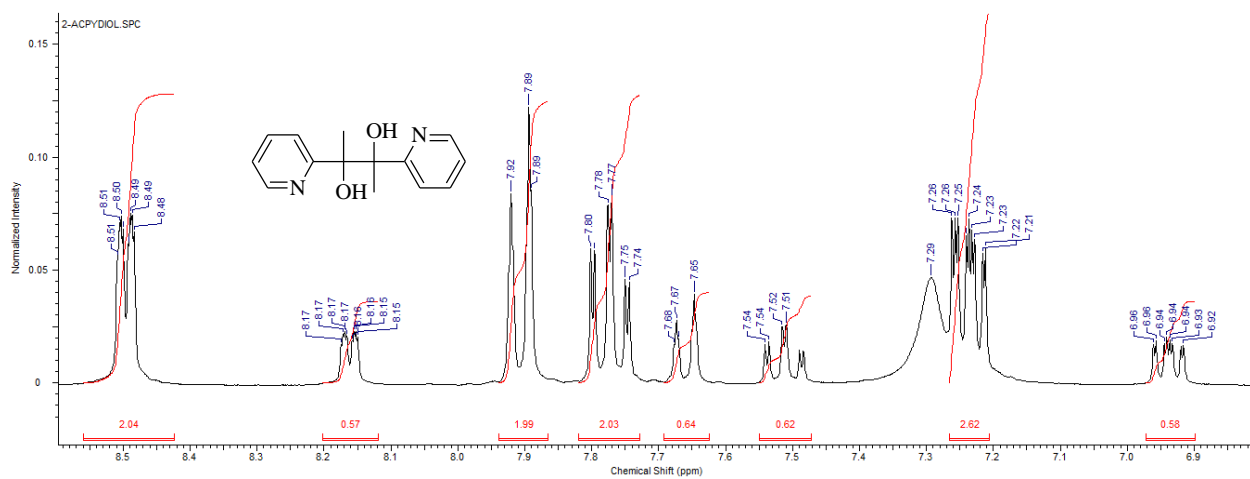


Figure 4.21 ¹H-NMR of 2,3-pyridin-2-ylbutane-2,3-diol zoomed in at the aromatic region

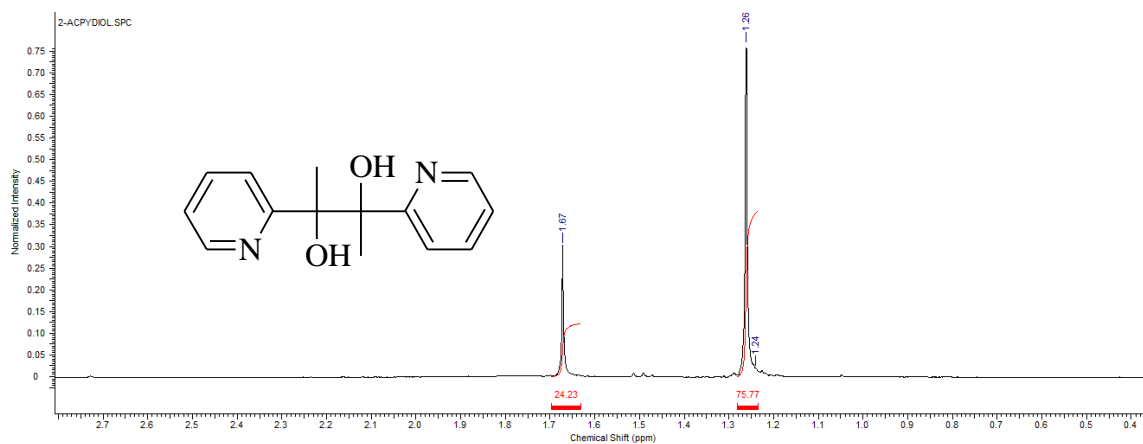


Figure 4.22 ¹H-NMR of 2,3-pyridin-2-ylbutane-2,3-diol showing the isomeric ratio of 24:76

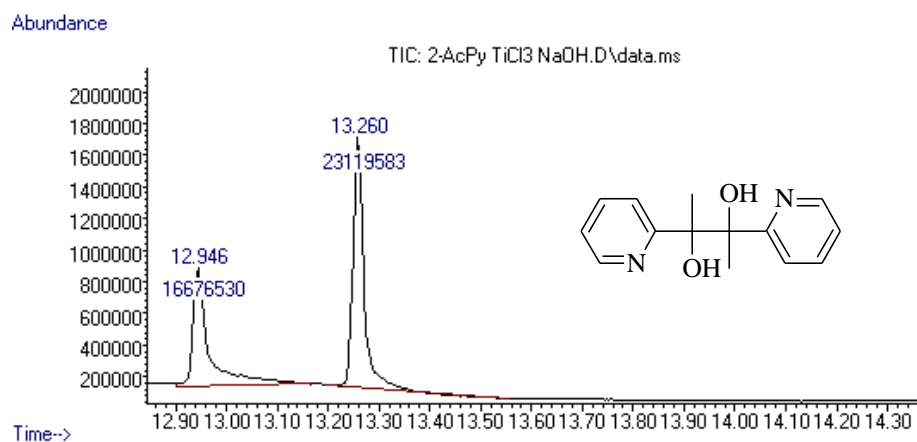


Figure 4.23 Gas chromatogram of 2,3-pyridin-2-ylbutane-2,3-diol showing an isomeric ratio of 43:58

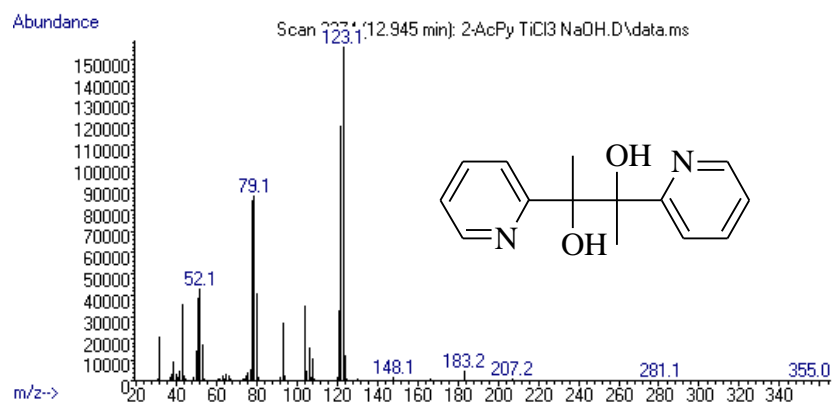


Figure 4.24 Mass spectrum of meso isomer of 2,3-pyridin-2-ylbutane-2,3-diol eluting at 12.945min

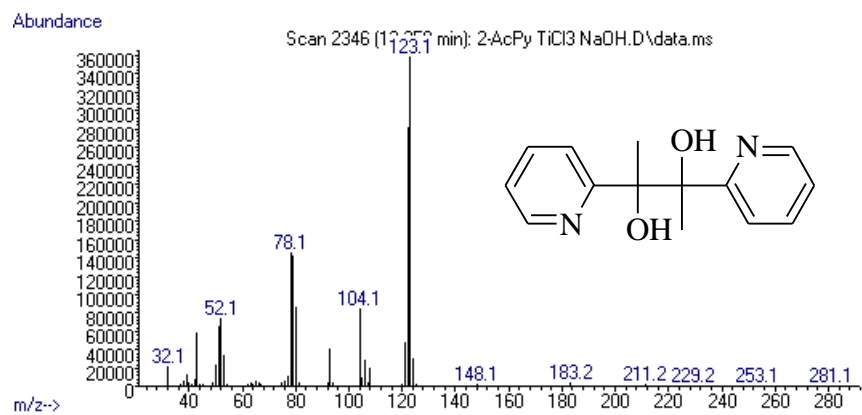


Figure 4.25 Mass spectrum of d and l isomers of 2,3-pyridin-2-ylbutane-2,3-diol eluting at 13.260min

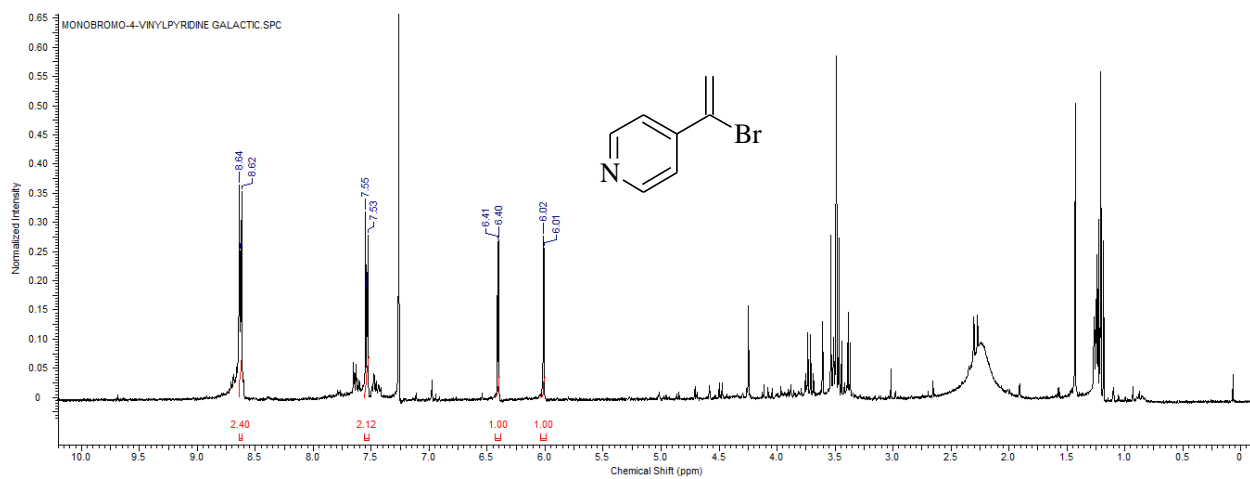


Figure 4.26 $^1\text{H-NMR}$ of crude monobromo-4-vinylpyridine

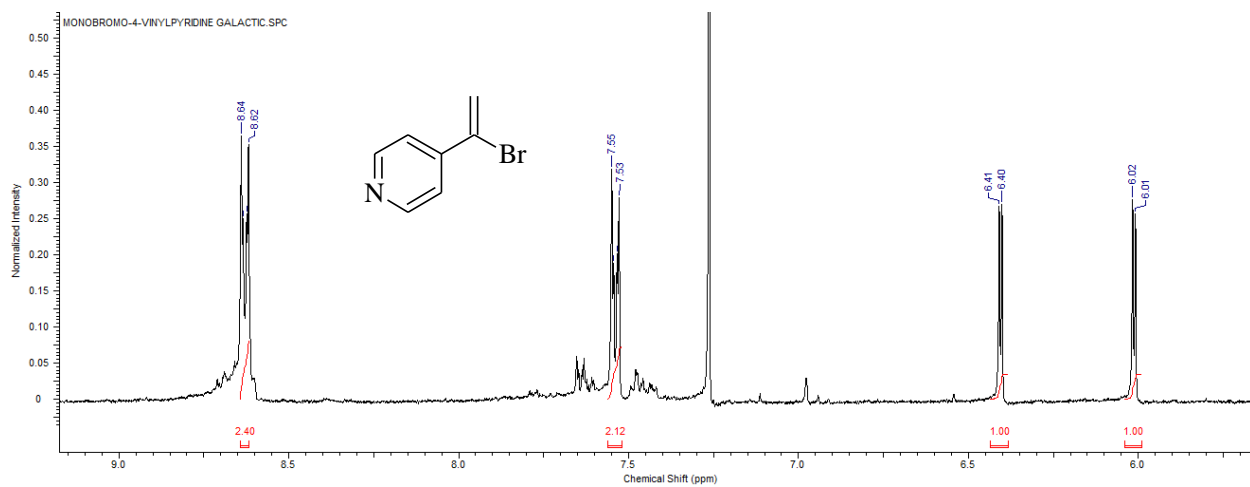


Figure 4.27 $^1\text{H-NMR}$ of crude monobromo-4-vinylpyridine zoomed in

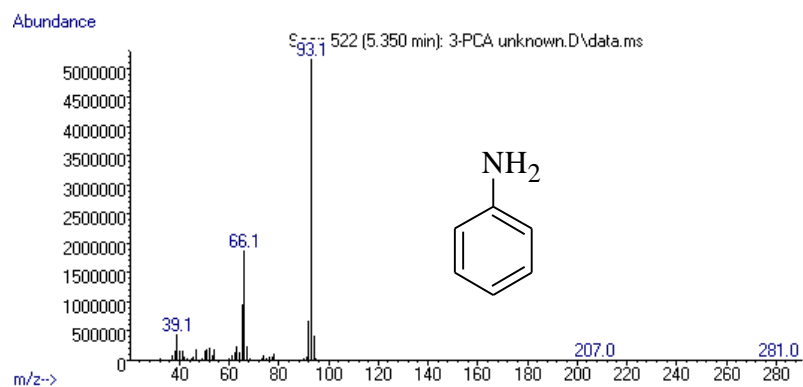


Figure 4.28 Mass spectrum of aniline eluting at 5.350min

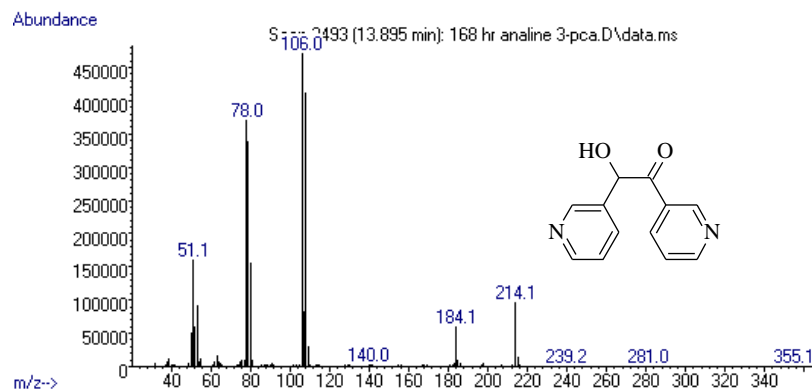


Figure 4.29 Mass spectrum of 2-hydroxy-1,2-di(pyridin-3-yl)ethanone eluting at 13.895min

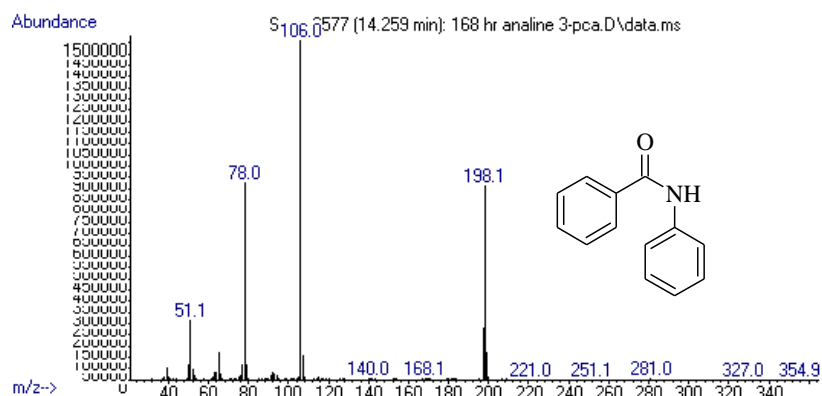


Figure 4.30 Mass spectrum of N-phenyl-3-pyridinecarboxamide eluting at 14.259min

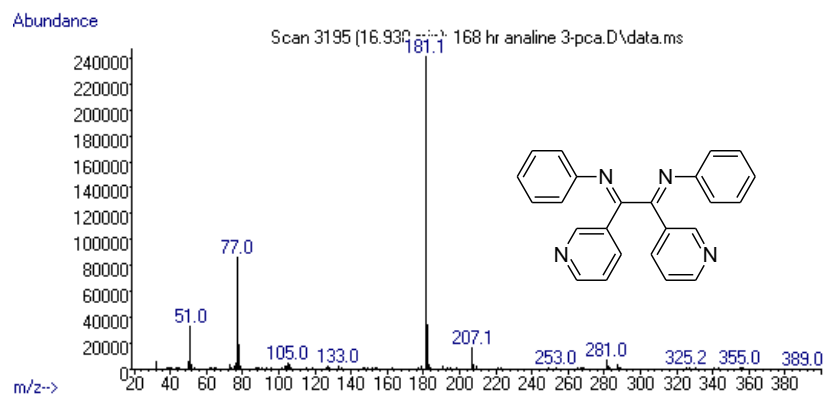


Figure 4.31 Mass spectrum of N,N'[-1,2-di(pyridin-3-yl)ethane-1,2-diylidene]dianiline eluting at 16.930min

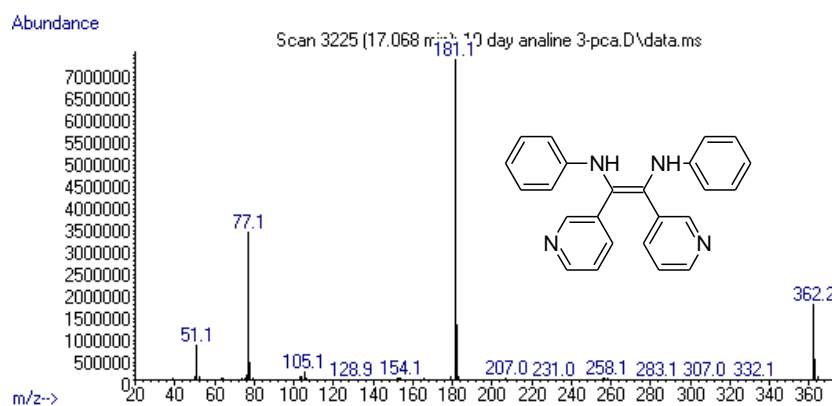


Figure 4.32 Mass spectrum of N,N'-diphenyl-1,2-di(pyridin-3-yl)ethene-1,2-diamine eluting at 17.068min

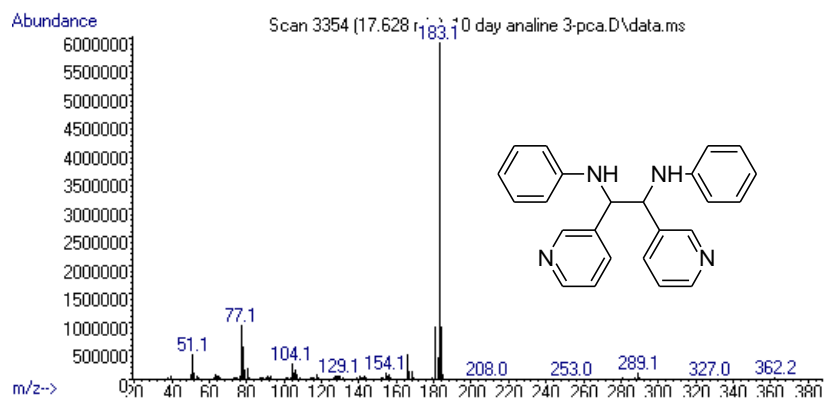


Figure 4.33 Mass spectrum of N,N'-diphenyl-1,2-di(pyridin-3-yl)ethane-1,2-diamine eluting at 17.628min

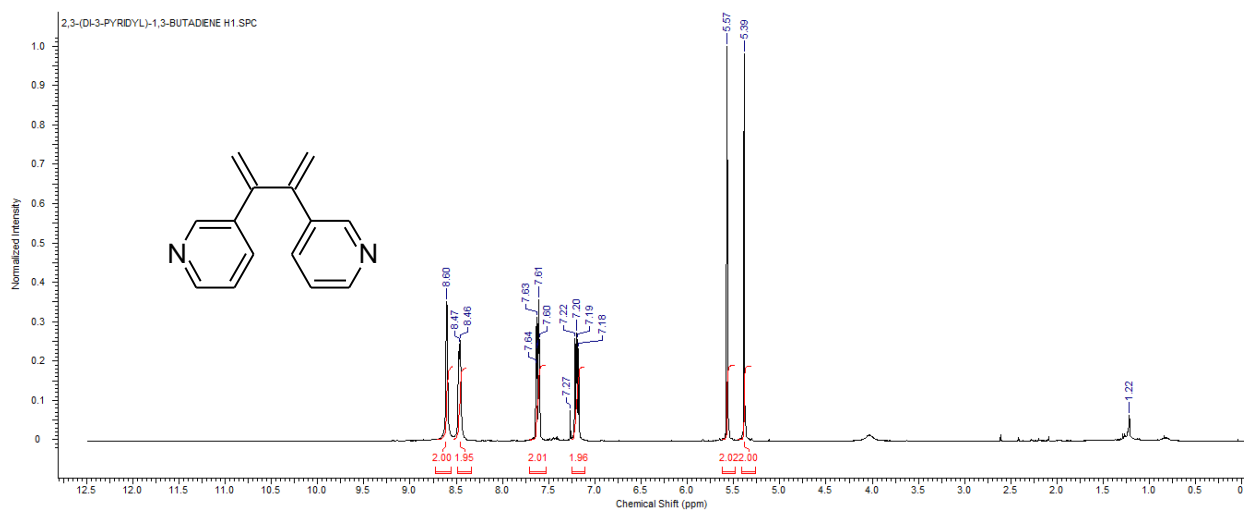


Figure 4.34 $^1\text{H-NMR}$ of 2,3-di(3-pyridyl)-1,3-butadiene

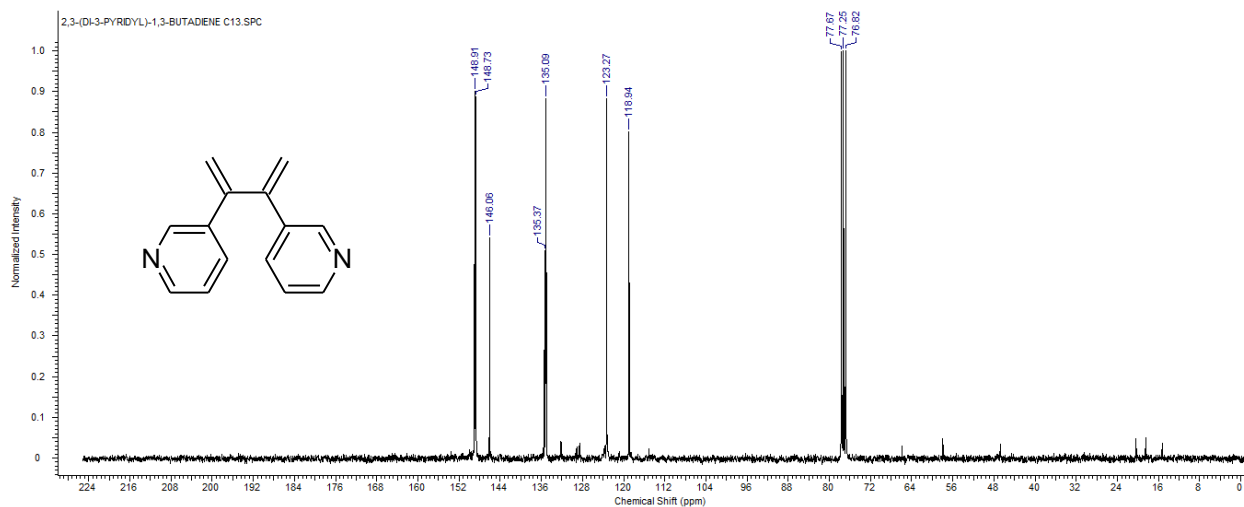


Figure 4.35 $^{13}\text{C-NMR}$ of 2,3-di(3-pyridyl)-1,3-butadiene

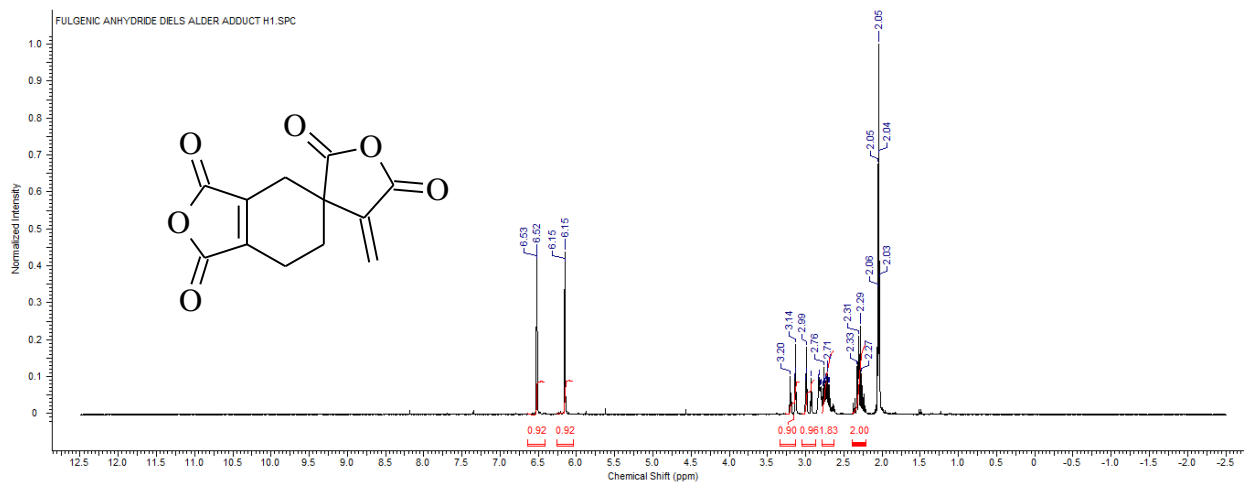


Figure 4.36 $^1\text{H-NMR}$ of fulgenic dimer

APPENDIX A

GAS CHROMATOGRAPH/MASS SPECTROMETER PARAMETERS

INLET PARAMETERS:

Sample Inlet:	GC
Injection Source:	GCALS
Inlet Location:	Front
MS Connected to:	Front Inlet

Heater:	250°C
Pressure:	11.681psi
Total Flow:	28.2 mL/min
Septum Purge Flow:	3mL/min
Mode:	Split
Split Ratio:	20:1

OVEN PARAMETERS:

Oven Temp On:	True
Equilibration Time:	1min
Maximum Oven Temperature:	325 °C
Override Column Max: 325 °C:	False

OVEN RAMP:

	Rate (°C/min)	Value (°C)	Hold Time (min)	Run Time (min)
Initial		80	3	3
Ramp 1	15	300	1	18.667

MS INSTRUMENT PARAMETERS

Solvent Delay	3.00min
EMV Mode	Gain Factor
Gain Factor	1.00 = 1235 V
Acq. Mode	Scan
Scan Speed	Normal

APPENDIX B

Crystallographic data for BMHA-Cu MOF

Table B1 Crystal data and structure refinement.

Empirical formula	C ₁₆ H ₂₅ Cu ₃ O ₁₄	
Temperature/K	150(2)	
Crystal system	triclinic	
Space group	P-1	
a/Å	a = 9.9660(3) Å	α = 95.522(2) °
b/Å	b = 11.9416(3) Å	β = 112.718(2) °
c/Å	c = 12.8417(4) Å	γ = 112.190(2) °
Volume/Å ³	1251.78(7)	
Z	2	
ρ _{calc} /cm ³	1.677	
μ/mm ⁻¹	3.534	
Crystal size/mm ³	0.296 × 0.122 × 0.092	
Radiation	CuKα (λ = 1.54178)	
2θ range for data collection/°	7.782 to 121.154	
Index ranges	-10 ≤ h ≤ 8, -13 ≤ k ≤ 13, -14 ≤ l ≤ 14	
Reflections collected	14852	
Independent reflections	3573 [R _{int} = 0.0618, R _{sigma} = 0.0535]	
Data/restraints/parameters	3573/226/341	
Goodness-of-fit on F ²	1.125	
Final R indexes [I >= 2σ (I)]	R ₁ = 0.0574, wR ₂ = 0.1577	
Final R indexes [all data]	R ₁ = 0.0669, wR ₂ = 0.1714	
Largest diff. peak/hole / e Å ⁻³	1.64/-0.80	

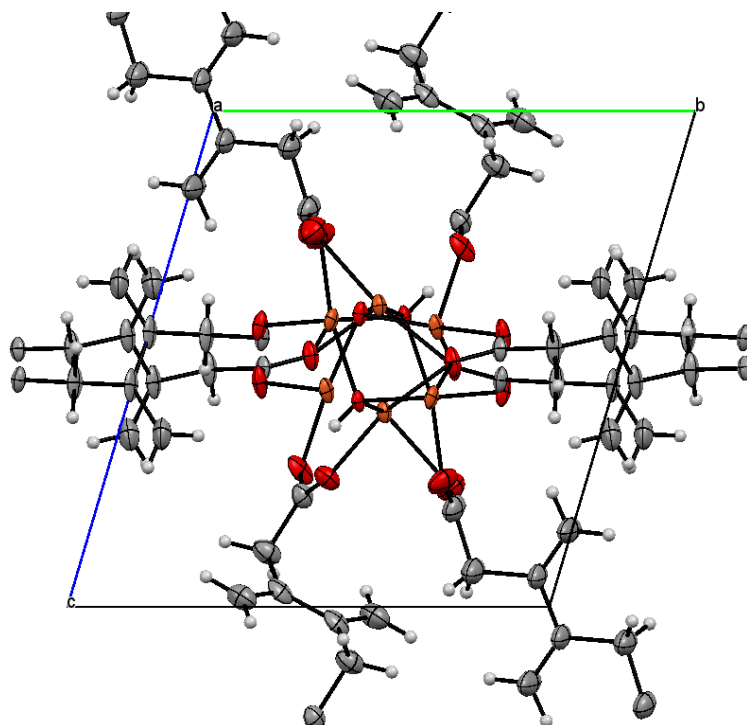


Table B2 Fractional Atomic Coordinates ($\times 10^4$) and Equivalent Isotropic Displacement Parameters ($\text{\AA}^2 \times 10^3$). U_{eq} is defined as $1/3$ of the trace of the orthogonalized U_{ij} tensor.

Atom	<i>x</i>	<i>y</i>	<i>z</i>	$U(\text{eq})$
Cu1	10613.7(10)	6278.8(7)	5779.7(8)	18.9(2)
Cu2	6825.9(9)	4621.9(7)	3925.9(7)	17.1(2)
Cu3	5102.8(10)	4055.7(8)	5640.9(8)	20.8(2)
O1	9026(5)	5221(3)	4148(4)	17.5(8)
O2	4891(5)	4283(3)	4096(4)	19.1(9)
O3	11900(7)	7020(5)	7470(5)	44.4(13)
O4	14232(7)	7218(5)	7582(5)	49.3(14)
O5	10212(5)	7731(4)	5664(4)	25.4(10)
O6	7604(5)	6566(4)	5166(4)	21.5(9)
O7	7448(5)	3509(4)	4937(4)	26(1)
O8	5521(5)	2618(4)	5471(4)	29.8(10)
O9	5538(6)	3999(5)	7240(4)	36.3(11)
O10	3745(5)	4603(4)	7403(4)	28.7(10)
C1	13413(10)	7420(7)	8016(7)	42.3(17)

C2	14228(11)	8202(7)	9280(7)	50(2)
C3	14514(10)	9570(7)	9389(7)	41.4(19)

Table B2 (Cont'd)

Atom	x	y	z	U(eq)
C4	13916(14)	9945(8)	8457(8)	67(3)
C5	8807(7)	7602(5)	5421(6)	21.3(13)
C6	8564(8)	8779(6)	5482(7)	32.3(16)
C7	9900(8)	9966(6)	5535(7)	30.1(14)
C8	10805(10)	10904(7)	6518(7)	42.6(18)
C9	6584(7)	2603(5)	5189(6)	20.3(12)
C10	6946(8)	1490(6)	5219(7)	32.1(15)
C11	5831(8)	411(6)	5468(7)	30.7(14)
C12	6387(10)	216(7)	6524(7)	43.4(18)
C13	4749(8)	4195(6)	7762(6)	28.7(14)
C14	5074(10)	3803(8)	8896(7)	39.4(16)
C15	4533(8)	4324(7)	9690(6)	32.2(15)
C16	3253(9)	3563(8)	9809(7)	42.8(18)
O11	9476(7)	6237(6)	2470(5)	50.2(14)
O12	2415(11)	2379(10)	2230(8)	124(4)
O13	11202(18)	5690(20)	1423(11)	292(8)
O14A	9966(19)	3070(20)	1350(13)	169(12)
O14B	9320(60)	3370(50)	1690(50)	810(180)

Table B3 Anisotropic Displacement Parameters ($\text{\AA}^2 \times 10^3$). The Anisotropic displacement factor exponent takes the form: $-2\pi^2[h^2a^*^2U_{11}+2hka^*b^*U_{12}+\dots]$.

Atom	U ₁₁	U ₂₂	U ₃₃	U ₂₃	U ₁₃	U ₁₂
Cu1	17.3(4)	10.9(4)	30.0(5)	3.7(3)	9.6(4)	9.6(3)
Cu2	16.7(4)	15.1(4)	27.1(5)	9.5(3)	12.6(3)	11.1(3)
Cu3	27.0(5)	17.9(4)	35.2(5)	14.9(4)	21.4(4)	18.3(3)
O1	21.1(19)	13.2(19)	27(2)	10.1(16)	15.0(16)	11.7(15)
O2	17.9(19)	13.5(19)	33(2)	7.2(17)	14.7(16)	11.0(15)
O3	49(3)	39(3)	38(3)	-5(2)	8(2)	29(2)
O4	45(3)	42(3)	45(3)	4(2)	11(2)	18(2)
O5	17.9(19)	12.9(19)	49(3)	6.6(18)	17.7(18)	8.8(15)
O6	19.5(19)	13.1(18)	41(2)	11.6(17)	18.9(17)	10.4(15)
O7	23(2)	21(2)	49(3)	18.6(19)	23.5(19)	14.8(16)
O8	35(2)	21(2)	60(3)	23.8(19)	36(2)	20.2(17)
O9	52(3)	49(3)	45(3)	32(2)	31(2)	46(2)
O10	32(2)	41(3)	31(2)	19(2)	20.0(18)	25.4(19)
C1	50(4)	27(3)	41(4)	4(3)	10(3)	23(3)
C2	67(5)	29(4)	38(4)	5(3)	7(3)	25(3)
C3	57(5)	21(3)	35(4)	5(3)	7(3)	21(3)
C4	110(8)	30(4)	36(4)	4(3)	3(4)	40(4)
C5	21(3)	13(3)	36(3)	7(2)	17(2)	9(2)
C6	28(3)	17(3)	67(5)	17(3)	29(3)	17(2)
C7	28(3)	14(3)	61(4)	15(3)	24(3)	17(2)
C8	49(4)	22(3)	57(4)	16(3)	24(3)	15(3)
C9	16(3)	16(3)	33(3)	10(2)	13(2)	8(2)
C10	30(3)	20(3)	65(4)	20(3)	32(3)	18(2)
C11	33(3)	20(3)	62(4)	21(3)	32(3)	21(2)
C12	44(4)	30(4)	60(4)	22(3)	25(3)	17(3)
C13	32(3)	30(3)	34(3)	13(3)	17(2)	21(3)
C14	50(4)	50(4)	36(3)	21(3)	23(3)	34(3)
C15	36(3)	45(3)	36(3)	26(3)	18(3)	32(3)

C16	43(4)	53(5)	37(4)	21(3)	20(3)	23(3)
O11	39(3)	74(4)	50(3)	33(3)	24(2)	31(3)

Table 3 (Cont'd)

Atom	U₁₁	U₂₂	U₃₃	U₂₃	U₁₃	U₁₂
O12	90(6)	95(7)	77(6)	-17(5)	13(5)	-29(5)
O13	244(8)	770(20)	161(9)	260(11)	162(7)	412(11)
O14A	80(10)	310(30)	81(11)	-45(13)	20(7)	91(13)
O14B	130(40)	190(50)	1700(400)	-230(120)	110(110)	100(40)

Table B4 Bond Lengths.

Atom	Atom	Length/Å	Atom	Atom	Length/Å
Cu1	O5	1.928(4)	O5	C5	1.254(8)
Cu1	O3	1.940(5)	O6	C5	1.255(7)
Cu1	O1¹	1.959(4)	O6	Cu3²	2.254(4)
Cu1	O1	1.977(4)	O7	C9	1.263(7)
Cu1	O7¹	2.385(4)	O7	Cu1¹	2.385(4)
Cu1	Cu1¹	2.9905(16)	O8	C9	1.250(8)
Cu1	Cu2¹	3.0359(11)	O9	C13	1.280(8)
Cu2	O2	1.919(4)	O10	C13	1.227(8)
Cu2	O1	1.922(4)	O10	Cu2²	2.011(4)
Cu2	O10²	2.011(4)	C1	C2	1.512(11)
Cu2	O7	2.042(4)	C2	C3	1.530(10)
Cu2	O6	2.346(4)	C3	C4	1.320(11)
Cu2	O4¹	2.354(6)	C3	C3³	1.490(15)
Cu2	Cu1¹	3.0359(11)	C5	C6	1.514(8)
Cu3	O8	1.925(4)	C6	C7	1.507(9)
Cu3	O9	1.941(5)	C7	C8	1.322(11)
Cu3	O2	1.969(4)	C7	C7⁴	1.469(15)
Cu3	O2²	1.978(4)	C9	C10	1.503(8)
Cu3	O6²	2.254(4)	C10	C11	1.507(9)
Cu3	Cu3²	2.9396(16)	C11	C12	1.333(11)

O1	Cu1¹	1.959(4)	C11	C11⁵	1.469(14)
O2	Cu3²	1.978(4)	C13	C14	1.526(10)

Table B4 (cont'd).

Atom	Atom	Length/Å	Atom	Atom	Length/Å
O3	C1	1.253(10)	C14	C15	1.507(10)
O4	C1	1.228(10)	C15	C16	1.334(11)
O4	Cu2¹	2.354(6)	C15	C15⁶	1.466(15)

¹2-X,1-Y,1-Z; ²1-X,1-Y,1-Z; ³3-X,2-Y,2-Z; ⁴2-X,2-Y,1-Z; ⁵1-X,-Y,1-Z; ⁶1-X,1-Y,2-Z

Table B5 Bond Angles.

Atom	Atom	Atom	Angle/°	Atom	Atom	Atom	Angle/°
O5	Cu1	O3	89.2(2)	O8	Cu3	Cu3²	135.87(15)
O5	Cu1	O1¹	178.39(18)	O9	Cu3	Cu3²	134.69(15)
O3	Cu1	O1¹	92.39(19)	O2	Cu3	Cu3²	41.98(11)
O5	Cu1	O1	97.28(18)	O2²	Cu3	Cu3²	41.76(12)
O3	Cu1	O1	167.7(2)	O6²	Cu3	Cu3²	80.14(10)
O1¹	Cu1	O1	81.11(18)	Cu2	O1	Cu1¹	102.93(18)
O5	Cu1	O7¹	106.39(16)	Cu2	O1	Cu1	111.15(19)
O3	Cu1	O7¹	105.1(2)	Cu1¹	O1	Cu1	98.89(17)
O1¹	Cu1	O7¹	73.55(15)	Cu2	O2	Cu3	113.6(2)
O1	Cu1	O7¹	83.14(16)	Cu2	O2	Cu3²	104.15(18)
O5	Cu1	Cu1¹	137.62(14)	Cu3	O2	Cu3²	96.27(17)
O3	Cu1	Cu1¹	132.32(16)	C1	O3	Cu1	124.3(6)
O1¹	Cu1	Cu1¹	40.78(12)	C1	O4	Cu2¹	122.4(5)
O1	Cu1	Cu1¹	40.34(11)	C5	O5	Cu1	118.6(4)
O7¹	Cu1	Cu1¹	74.66(11)	C5	O6	Cu3²	133.0(4)
O5	Cu1	Cu2¹	142.60(13)	C5	O6	Cu2	128.0(4)
O3	Cu1	Cu2¹	83.45(16)	Cu3²	O6	Cu2	83.83(14)
O1¹	Cu1	Cu2¹	38.09(11)	C9	O7	Cu2	130.5(4)
O1	Cu1	Cu2¹	97.40(12)	C9	O7	Cu1¹	132.0(4)
O7¹	Cu1	Cu2¹	42.16(10)	Cu2	O7	Cu1¹	86.23(16)

Cu1¹	Cu1	Cu2¹	64.50(3)	C9	O8	Cu3	123.5(4)
O2	Cu2	O1	165.80(17)	C13	O9	Cu3	125.2(4)
O2	Cu2	O10²	95.53(18)	C13	O10	Cu2²	131.1(4)

Table B5 (cont'd).

Atom	Atom	Atom	Angle/°	Atom	Atom	Atom	Angle/°
O1	Cu2	O10²	91.27(17)	O4	C1	O3	124.0(7)
O2	Cu2	O7	93.73(17)	O4	C1	C2	120.1(8)
O1	Cu2	O7	82.79(16)	O3	C1	C2	115.9(8)
O10²	Cu2	O7	163.64(19)	C1	C2	C3	112.7(7)
O2	Cu2	O6	79.04(15)	C4	C3	C3³	122.9(8)
O1	Cu2	O6	89.02(15)	C4	C3	C2	121.6(7)
O10²	Cu2	O6	86.15(17)	C3³	C3	C2	115.5(8)
O7	Cu2	O6	108.87(17)	O5	C5	O6	124.2(5)
O2	Cu2	O4¹	98.20(19)	O5	C5	C6	117.8(5)
O1	Cu2	O4¹	94.85(19)	O6	C5	C6	118.0(5)
O10²	Cu2	O4¹	84.4(2)	C7	C6	C5	117.2(5)
O7	Cu2	O4¹	80.93(19)	C8	C7	C7⁴	122.9(8)
O6	Cu2	O4¹	169.89(17)	C8	C7	C6	119.4(7)
O2	Cu2	Cu1¹	143.64(12)	C7⁴	C7	C6	117.7(8)
O1	Cu2	Cu1¹	38.97(11)	O8	C9	O7	123.6(5)
O10²	Cu2	Cu1¹	115.84(13)	O8	C9	C10	119.2(5)
O7	Cu2	Cu1¹	51.61(12)	O7	C9	C10	117.2(5)
O6	Cu2	Cu1¹	118.89(10)	C9	C10	C11	115.1(5)
O4¹	Cu2	Cu1¹	68.91(14)	C12	C11	C11⁵	121.9(8)
O8	Cu3	O9	87.19(19)	C12	C11	C10	119.2(7)
O8	Cu3	O2	94.83(18)	C11⁵	C11	C10	118.9(8)
O9	Cu3	O2	173.7(2)	O10	C13	O9	126.0(6)
O8	Cu3	O2²	169.35(18)	O10	C13	C14	119.7(6)
O9	Cu3	O2²	93.18(18)	O9	C13	C14	114.3(6)
O2	Cu3	O2²	83.73(17)	C15	C14	C13	115.3(6)
O8	Cu3	O6²	110.26(17)	C16	C15	C15⁶	122.5(9)

O9	Cu3	O6²	99.76(19)	C16	C15	C14	120.0(7)
O2	Cu3	O6²	85.16(16)	C15 ⁶	C15	C14	117.4(8)
O2²	Cu3	O6²	80.18(15)				

¹2-X,1-Y,1-Z; ²1-X,1-Y,1-Z; ³3-X,2-Y,2-Z; ⁴2-X,2-Y,1-Z; ⁵1-X,-Y,1-Z; ⁶1-X,1-Y,2-Z

Table B6 Hydrogen Atom Coordinates ($\text{\AA}\times 10^4$) and Isotropic Displacement Parameters ($\text{\AA}^2\times 10^3$).

Atom	x	y	z	U(eq)
H1	9130(80)	5560(50)	3650(40)	21
H2A	15289	8193	9708	60
H2B	13539	7815	9658	60
H4A	14099	10797	8549	80
H4B	13303	9362	7694	80
H6A	7540	8597	4783	39
H6B	8406	8950	6185	39
H8A	11629	11665	6553	51
H8B	10632	10817	7190	51
H10A	8081	1779	5828	39
H10B	6880	1174	4450	39
H12A	5703	-470	6689	52
H12B	7468	763	7113	52
H14A	4514	2871	8688	47
H14B	6259	4076	9343	47
H16A	2915	3892	10311	51
H16B	2680	2692	9392	51
H11W	8540(40)	5920(50)	1920(40)	60
H11X	9550(70)	6850(40)	2880(40)	60
H12W	2360(90)	1880(60)	1710(50)	149
H12X	3390(40)	2830(60)	2650(50)	149
H13W	12130(40)	5780(70)	1600(120)	350
H13X	10660(60)	4930(40)	1300(130)	350
H14W	10910(40)	3200(110)	1740(60)	203
H14X	9570(40)	2950(180)	1810(30)	203

H14Y	9810(60)	3210(100)	1360(30)	969
H14Z	9300(80)	2930(80)	2140(40)	969

APPENDIX C

Crystallographic Data for Zinc Formic Acid crystal.

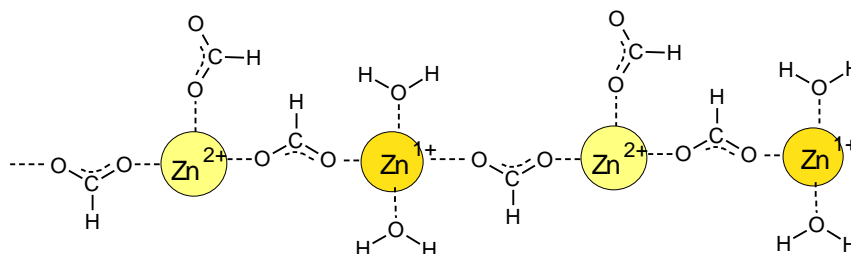


Table C1 Crystal data and structure refinement.

Empirical formula	C ₂ H ₆ O ₆ Zn	
Temperature/K	100(2)	
Crystal system	monoclinic	
Space group	P2₁/c	
	a = 8.66650(10) Å	α = 90 °
	b = 7.08900(10) Å	β = 97.7140(10) °
	c = 9.32180(10) Å	γ = 90 °
Volume/Å ³	567.519(12)	
Z	4	
$\rho_{\text{calc}}/\text{cm}^3$	2.241	
μ/mm^{-1}	5.848	
Crystal size/mm ³	0.514 × 0.187 × 0.175	
Radiation	CuK α (λ = 1.54178)	
2 Θ range for data collection/°	10.3 to 133.65	
Index ranges	-9 ≤ h ≤ 10, -8 ≤ k ≤ 8, -9 ≤ l ≤ 11	
Reflections collected	6059	
Independent reflections	974 [R _{int} = 0.0338, R _{sigma} = 0.0201]	
Data/restraints/parameters	974/6/98	
Goodness-of-fit on F ²	1.127	
Final R indexes [I ≥ 2σ (I)]	R ₁ = 0.0229, wR ₂ = 0.0901	

Final R indexes [all data] $R_1 = 0.0234$, $wR_2 = 0.0911$

Largest diff. peak/hole / $e \text{ \AA}^{-3}$ 0.28/-0.72

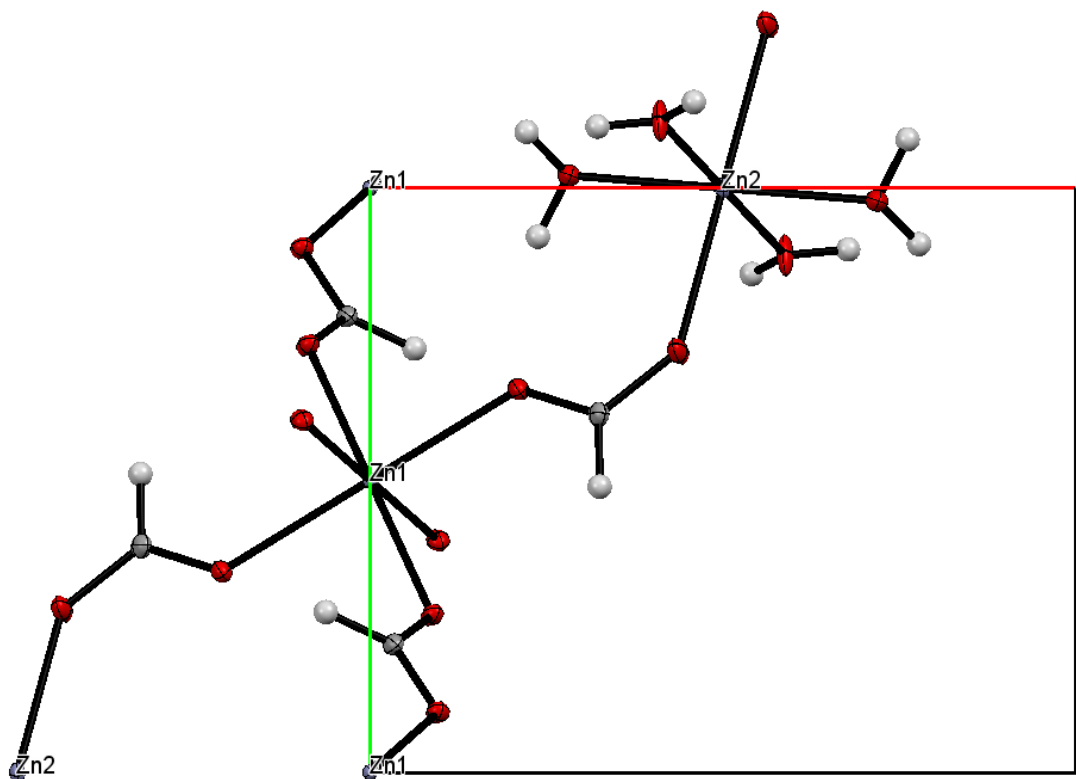


Table C2 Fractional Atomic Coordinates ($\times 10^4$) and Equivalent Isotropic Displacement Parameters ($\text{\AA}^2 \times 10^3$). U_{eq} is defined as $1/3$ of the trace of the orthogonalized U_{ij} tensor.

Atom	x	y	z	U(eq)
Zn1	0	5000	5000	3.8(2)
Zn2	5000	0	5000	5.8(2)
O1	2106.6(13)	3440.7(17)	4993.2(13)	8.1(3)
O2	4367.1(14)	2796.2(18)	4193.1(14)	10.8(4)
O3	881.1(14)	7309.1(17)	4034.4(13)	7.8(3)
O4	963.1(14)	8970.7(18)	2032.1(14)	7.7(4)
O5	5888.3(16)	1151(2)	6950.9(15)	13.8(4)
O6	7180.7(15)	218.1(18)	4275.1(15)	9.3(4)
C1	3241(2)	3873(3)	4353(2)	8.8(4)
C2	331(2)	7803(2)	2777(2)	8.3(4)

Table C3 Anisotropic Displacement Parameters ($\text{\AA}^2 \times 10^3$). The Anisotropic displacement factor exponent takes the form: $-2\pi^2[h^2a^2U_{11}+2hka*b*U_{12}+\dots]$.

Atom	U ₁₁	U ₂₂	U ₃₃	U ₂₃	U ₁₃	U ₁₂
Zn1	3.3(4)	3.3(4)	4.7(4)	-0.03(10)	-0.1(3)	-0.19(10)
Zn2	3.4(4)	6.4(4)	7.4(4)	-0.35(10)	0.3(3)	0.27(10)
O1	6.6(6)	7.6(6)	10.0(7)	-0.7(4)	0.7(5)	1.1(4)
O2	6.9(7)	10.6(7)	15.5(7)	3.0(5)	4.1(5)	2.2(5)
O3	7.6(6)	7.2(6)	8.0(7)	1.7(4)	-0.8(5)	-1.3(4)
O4	7.9(7)	7.2(7)	7.9(7)	1.7(5)	0.4(5)	-0.5(5)
O5	4.0(7)	26.1(8)	11.3(8)	-8.0(6)	1.1(6)	1.2(5)
O6	7.4(7)	6.6(7)	13.3(8)	-0.1(5)	0.0(6)	0.3(5)
C1	7.2(8)	8.9(8)	9.5(9)	0.0(6)	-1.3(7)	-0.4(6)
C2	7.0(8)	6.5(8)	10.9(9)	-0.7(7)	-0.8(7)	-0.5(6)

Table C4 Bond Lengths.

Atom	Atom	Length/ \AA	Atom	Atom	Length/ \AA
Zn1	O3	2.0633(12)	Zn2	O6	2.0965(13)
Zn1	O3¹	2.0633(12)	Zn2	O2⁴	2.1645(12)
Zn1	O4²	2.0959(13)	Zn2	O2	2.1645(12)
Zn1	O4³	2.0959(13)	O1	C1	1.255(2)
Zn1	O1¹	2.1350(12)	O2	C1	1.263(2)
Zn1	O1	2.1350(12)	O3	C2	1.254(2)
Zn2	O5⁴	2.0468(13)	O4	C2	1.253(2)
Zn2	O5	2.0468(13)	O4	Zn1⁵	2.0959(12)
Zn2	O6⁴	2.0965(13)			

¹-X,1-Y,1-Z; ²+X,3/2-Y,1/2+Z; ³-X,-1/2+Y,1/2-Z; ⁴1-X,-Y,1-Z; ⁵-X,1/2+Y,1/2-Z

Table C5 Bond Angles.

Atom	Atom	Atom	Angle/°	Atom	Atom	Atom	Angle/°
O3	Zn1	O3 ¹	180.00(6)	O5 ⁴	Zn2	O6	89.47(6)
O3	Zn1	O4 ²	89.56(5)	O5	Zn2	O6	90.53(6)
O3 ¹	Zn1	O4 ²	90.44(5)	O6 ⁴	Zn2	O6	180.0
O3	Zn1	O4 ³	90.44(5)	O5 ⁴	Zn2	O2 ⁴	89.50(6)
O3 ¹	Zn1	O4 ³	89.56(5)	O5	Zn2	O2 ⁴	90.50(6)
O4 ²	Zn1	O4 ³	180.0	O6 ⁴	Zn2	O2 ⁴	91.02(5)
O3	Zn1	O1 ¹	87.55(5)	O6	Zn2	O2 ⁴	88.98(5)
O3 ¹	Zn1	O1 ¹	92.45(5)	O5 ⁴	Zn2	O2	90.50(6)
O4 ²	Zn1	O1 ¹	93.10(5)	O5	Zn2	O2	89.50(6)
O4 ³	Zn1	O1 ¹	86.90(5)	O6 ⁴	Zn2	O2	88.98(5)
O3	Zn1	O1	92.45(5)	O6	Zn2	O2	91.02(5)
O3 ¹	Zn1	O1	87.55(5)	O2 ⁴	Zn2	O2	180.00(6)
O4 ²	Zn1	O1	86.90(5)	C1	O1	Zn1	126.86(11)
O4 ³	Zn1	O1	93.10(5)	C1	O2	Zn2	132.55(12)
O1 ¹	Zn1	O1	180.0	C2	O3	Zn1	120.83(11)
O5 ⁴	Zn2	O5	180.0	C2	O4	Zn1 ⁵	125.48(12)
O5 ⁴	Zn2	O6 ⁴	90.53(6)	O1	C1	O2	125.11(17)
O5	Zn2	O6 ⁴	89.47(6)	O4	C2	O3	124.26(17)

¹-X,1-Y,1-Z; ²+X,3/2-Y,1/2+Z; ³-X,-1/2+Y,1/2-Z; ⁴1-X,-Y,1-Z; ⁵-X,1/2+Y,1/2-Z

Table C6 Hydrogen Atom Coordinates ($\text{\AA}\times 10^4$) and Isotropic Displacement Parameters ($\text{\AA}^2\times 10^3$).

Atom	x	y	z	U(eq)
H5B	6778(18)	1050(30)	7260(20)	17
H5A	5410(20)	1470(30)	7600(20)	17
H6B	7620(20)	-830(20)	4470(20)	11
H6A	7780(20)	960(20)	4770(20)	11
H1	3255	5108	3958	11
H2	-626	7255	2363	10

APPENDIX D

Crystallographic Data for BMHA: Benzylamine Cocystal

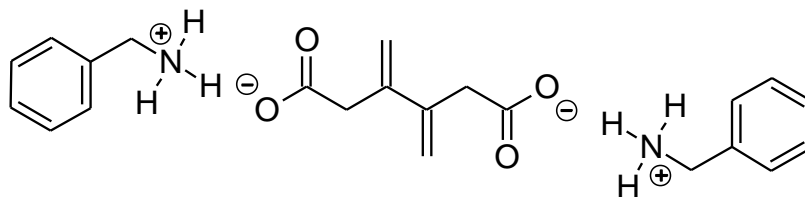


Table D1 Crystal data and structure refinement.

Empirical formula	C ₂₂ H ₂₈ N ₂ O ₄	
Temperature/K	296.15	
Crystal system	monoclinic	
Space group	P2 ₁ /n	
	a = 10.525(6) Å	α = 90 °
	b = 8.435(4) Å	β = 102.145(14) °
	c = 11.826(6) Å	γ = 90 °
Volume/Å ³	1026.3(10)	
Z	2	
ρ _{calc} /cm ³	1.2440	
μ/mm ⁻¹	0.086	
Crystal size/mm ³	N/A × N/A × N/A	
Radiation	Mo Kα (λ = 0.71073)	
2θ range for data collection/°	4.72 to 78.9	
Index ranges	-18 ≤ h ≤ 18, -15 ≤ k ≤ 15, -21 ≤ l ≤ 21	
Reflections collected	48453	
Independent reflections	6111 [R _{int} = 0.0484, R _{sigma} = 0.0290]	
Data/restraints/parameters	6111/0/136	
Goodness-of-fit on F ²	1.206	
Final R indexes [I ≥ 2σ (I)]	R ₁ = 0.0573, wR ₂ = 0.1583	

Final R indexes [all data]

$R_1 = 0.0814$, $wR_2 = 0.1746$

Largest diff. peak/hole / $e \text{ \AA}^{-3}$

0.74/-0.54

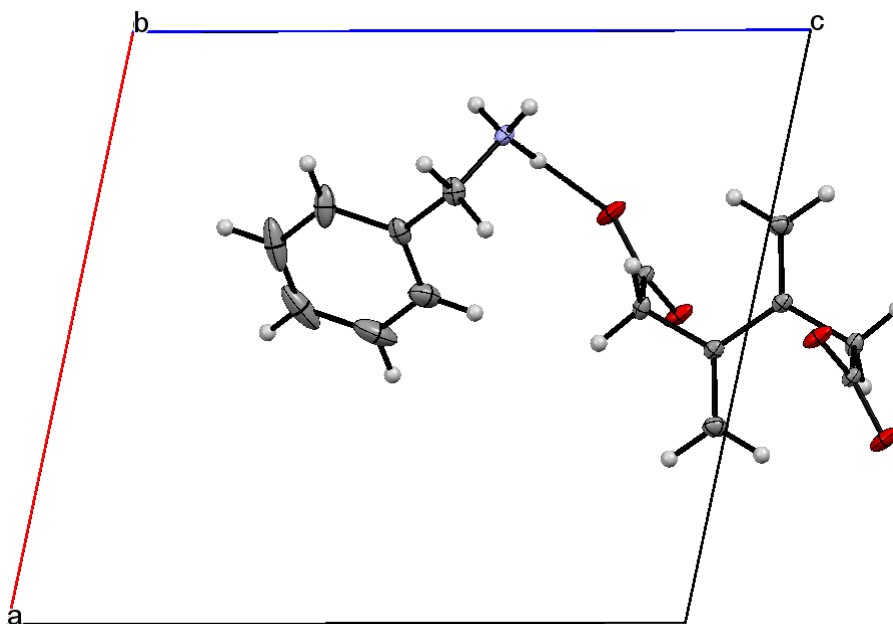


Table D2 Fractional Atomic Coordinates ($\times 10^4$) and Equivalent Isotropic Displacement Parameters ($\text{\AA}^2 \times 10^3$). U_{eq} is defined as 1/3 of of the trace of the orthogonalised U_{ij} tensor.

Atom	x	y	z	U(eq)
O001	3082.0(6)	7695.9(7)	7628.9(5)	20.21(14)
O002	4814.8(5)	8433.8(7)	8937.9(5)	18.31(13)
N003	1767.3(6)	5939.8(8)	5807.9(5)	12.76(11)
C004	4138.3(6)	7396.6(8)	8311.8(6)	11.52(12)
C005	5391.9(6)	5199.5(8)	9568.1(6)	11.57(12)
C006	4684.7(7)	5699.1(9)	8371.7(6)	13.41(13)
C007	3387.8(8)	6225.2(10)	4561.8(7)	18.08(15)
C008	6697.9(7)	5147.2(10)	9832.4(7)	17.27(14)
C009	2710.8(8)	5106.9(9)	5235.2(7)	17.84(14)
C00A	4464.3(9)	7097.2(13)	5129.1(10)	26.65(19)
C00B	2953.6(13)	6408.2(11)	3375.3(8)	29.9(2)
C00C	5091.5(11)	8132.1(15)	4515.5(14)	39.5(3)

C00D	3599.3(17)	7448.5(13)	2764.2(11)	43.4(3)
C00E	4663.1(14)	8309.1(14)	3332.4(14)	44.7(4)

Table D3 Anisotropic Displacement Parameters ($\text{\AA}^2 \times 10^3$). The Anisotropic displacement factor exponent takes the form: $-2\pi^2[h^2a^2U_{11}+2hka*b*U_{12}+\dots]$.

Atom	U₁₁	U₂₂	U₃₃	U₁₂	U₁₃	U₂₃
O001	17.8(2)	16.2(3)	20.6(3)	5.28(19)	-9.6(2)	-6.0(2)
O002	16.9(2)	11.3(2)	21.3(3)	2.09(18)	-8.11(19)	-3.99(19)
N003	13.2(2)	11.2(2)	12.2(2)	-1.34(18)	-1.12(18)	0.41(19)
C004	12.5(2)	10.8(3)	10.0(2)	1.71(19)	-0.59(19)	-1.5(2)
C005	12.4(2)	9.4(2)	12.1(3)	2.56(19)	0.96(19)	-0.5(2)
C006	17.4(3)	11.2(3)	10.6(3)	3.5(2)	0.7(2)	-1.2(2)
C007	23.8(3)	14.2(3)	18.6(3)	5.2(3)	9.7(3)	2.0(2)
C008	12.7(3)	18.3(3)	20.4(3)	3.1(2)	2.7(2)	3.5(3)
C009	24.6(3)	12.3(3)	17.4(3)	1.8(2)	6.4(3)	-0.2(2)
C00A	18.2(3)	27.2(4)	35.5(5)	3.2(3)	7.8(3)	7.0(4)
C00B	58.2(7)	16.0(4)	17.4(4)	5.5(4)	12.3(4)	0.1(3)
C00C	23.9(4)	32.6(5)	68.3(9)	3.2(4)	24.4(5)	13.2(6)
C00D	91.3(11)	21.1(4)	27.6(5)	16.8(6)	35.0(6)	8.1(4)
C00E	62.1(8)	25.4(5)	63.2(9)	13.5(5)	51.0(7)	15.1(5)

Table D4 Bond Lengths.

Atom	Atom	Length/\AA	Atom	Atom	Length/\AA
O001	C004	1.2546(10)	C007	C009	1.5068(13)
O002	C004	1.2644(9)	C007	C00A	1.3981(14)
N003	C009	1.4905(12)	C007	C00B	1.3899(15)
C004	C006	1.5390(12)	C00A	C00C	1.3878(16)
C005	C005¹	1.4805(15)	C00B	C00D	1.4001(17)
C005	C006	1.5134(12)	C00C	C00E	1.385(2)
C005	C008	1.3447(12)	C00D	C00E	1.384(2)

¹1-X,1-Y,2-Z

Table D5 Bond Angles.

Atom	Atom	Atom	Angle/°	Atom	Atom	Atom	Angle/°
O002	C004	O001	123.45(7)	C00B	C007	C00A	119.16(9)
C006	C004	O001	119.26(6)	C007	C009	N003	112.30(6)
C006	C004	O002	117.25(6)	C00C	C00A	C007	120.43(11)
C008	C005	C006	120.27(7)	C00D	C00B	C007	119.89(12)
C005	C006	C004	114.06(6)	C00E	C00C	C00A	120.43(12)
C00A	C007	C009	120.08(8)	C00E	C00D	C00B	120.60(11)
C00B	C007	C009	120.76(9)	C00D	C00E	C00C	119.48(10)

Table D6 Hydrogen Atom Coordinates ($\text{\AA}\times 10^4$) and Isotropic Displacement Parameters ($\text{\AA}^2\times 10^3$).

Atom	x	y	z	U(eq)
H00d	3355.5(8)	4574.8(9)	5818.7(7)	21.41(17)
H00e	2254.6(8)	4305.1(9)	4715.9(7)	21.41(17)
H00g	2235.3(13)	5840.6(11)	2987.8(8)	35.9(3)
H00i	3310.7(17)	7562.1(13)	1969.4(11)	52.0(4)
H00j	5086.9(14)	9000.9(14)	2922.9(14)	53.6(4)
H00h	5804.3(11)	8710.5(15)	4901.3(14)	47.4(4)
H00f	4761.9(9)	6982.9(13)	5922.8(10)	32.0(2)
H00k	3973.5(7)	4967.9(9)	8104.8(6)	16.10(15)
H00l	5277.8(7)	5617.2(9)	7847.9(6)	16.10(15)
H00a	1250(5)	6551(7)	5294.3(16)	15.31(14)
H00b	1291(5)	5228.3(8)	6089(6)	15.31(14)
H00c	2197.8(6)	6537(7)	6383(4)	15.31(14)
H00m	7171(13)	4913(17)	10604(12)	26(3)
H00n	7234(14)	5388(17)	9252(13)	27(3)

APPENDIX E

Crystallographic Data for Fulgenic Acid:2-Aminomethylnaphthylene Cocrystal

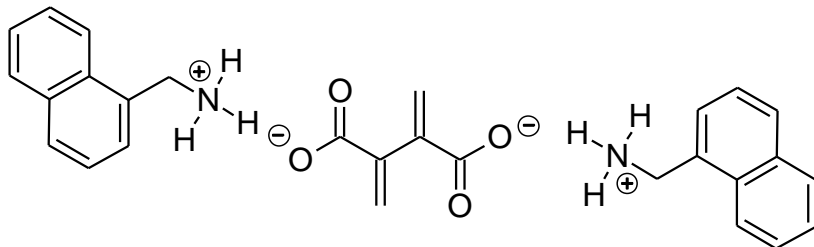


Table E1 Crystal data and structure refinement.

Empirical formula	C ₃₀ H ₃₂ N ₂ O ₄	
Temperature/K	296(2)	
Crystal system	monoclinic	
Space group	P2 ₁ /c	
	a = 10.7662(4) Å	α = 90 °
	b = 13.0275(4) Å	β = 100.195(2) °
	c = 8.3714(3) Å	γ = 90 °
	Volume/Å³ = 1155.61(7)	
	Z = 2	
	$\rho_{\text{calc}}/\text{cm}^3$ = 1.393	
μ/mm^{-1}	0.092	
F(000)	516.0	
Radiation	MoK α (λ = 0.71073)	
2 Θ range for data collection/°	3.844 to 76.018	
Index ranges	-18 ≤ h ≤ 17, -22 ≤ k ≤ 22, -14 ≤ l ≤ 14	
Reflections collected	46048	
Independent reflections	6291 [R _{int} = 0.0515, R _{sigma} = 0.0361]	
Data/restraints/parameters	6291/0/210	
Goodness-of-fit on F ²	1.284	
Final R indexes [I ≥ 2σ (I)]	R ₁ = 0.0743, wR ₂ = 0.1790	
Final R indexes [all data]	R ₁ = 0.1094, wR ₂ = 0.1989	

Largest diff. peak/hole / e Å⁻³

0.71/-0.37

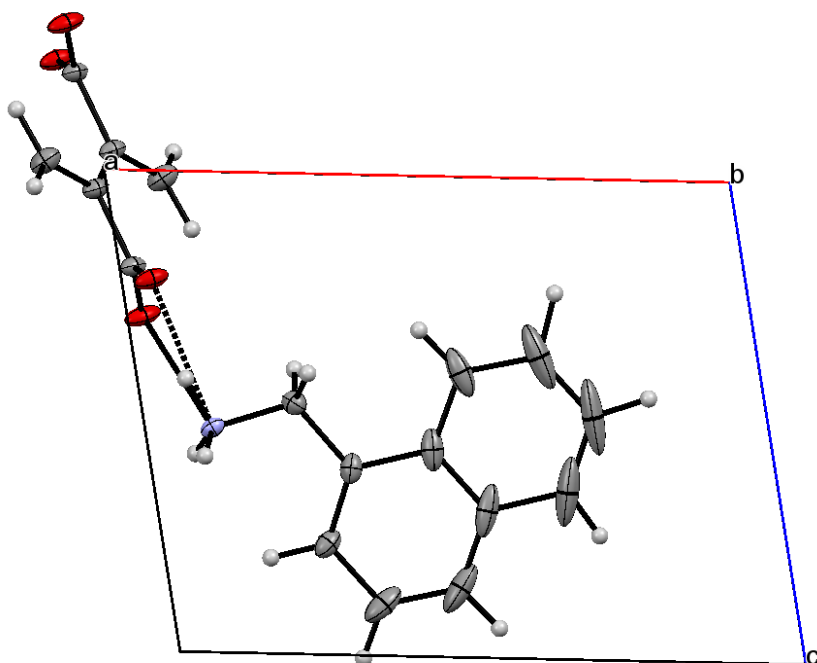


Table E2 Fractional Atomic Coordinates ($\times 10^4$) and Equivalent Isotropic Displacement Parameters ($\text{\AA}^2 \times 10^3$). U_{eq} is defined as 1/3 of of the trace of the orthogonalised U_{ij} tensor.

Atom	<i>x</i>	<i>y</i>	<i>z</i>	U_{eq}
C1	7541.6(10)	3571.4(8)	4779.3(12)	18.51(18)
N1	8912.2(8)	3409.7(6)	5329.9(10)	14.49(15)
O1	9752.9(8)	4952.7(6)	3030.1(8)	24.53(19)
C2	6794.1(9)	3709.2(7)	6119.0(13)	17.93(18)
O2	9517.1(8)	3323.9(5)	2261.5(8)	21.36(17)
C4	6631.4(15)	4023.2(9)	8934.9(17)	34.8(3)
C3	7360.6(11)	3870.3(8)	7697.9(13)	21.3(2)
C5	5348.5(15)	4000.3(10)	8567(2)	42.9(4)
C9	3503.1(15)	3577.6(11)	3713(3)	60.8(6)
C8	2787.4(14)	3710.5(12)	4938(4)	74.3(8)
C7	3380.3(15)	3835.0(11)	6508(4)	62.5(7)
C6	4721.4(12)	3845.3(9)	6939(2)	39.7(4)
C10	4804.0(13)	3569.8(9)	4070(2)	39.5(4)
C11	5444.5(10)	3702.5(8)	5692.6(17)	27.3(2)
C12	9779.5(9)	4253.3(7)	2009.3(10)	16.10(17)

C13	10184.8(9)	4504.7(7)	404(1)	16.28(17)
C14	10917.5(11)	3806.2(8)	-150.6(13)	23.2(2)

Table E3 Anisotropic Displacement Parameters ($\text{\AA}^2 \times 10^3$). The Anisotropic displacement factor exponent takes the form: $-2\pi^2[h^2a^*^2U_{11}+2hka^*b^*U_{12}+\dots]$.

Atom	U₁₁	U₂₂	U₃₃	U₂₃	U₁₃	U₁₂
C1	19.2(4)	17.9(4)	17.5(4)	-1.1(3)	0.7(3)	1.6(3)
N1	18.0(4)	12.8(3)	13.6(3)	0.8(2)	5.6(3)	-0.3(3)
O1	43.0(5)	18.7(3)	14.5(3)	-5.9(2)	12.1(3)	-11.7(3)
C2	15.4(4)	11.8(3)	27.4(4)	-1.3(3)	6.0(3)	-0.2(3)
O2	37.0(4)	14.1(3)	15.0(3)	-1.8(2)	10.1(3)	-7.2(3)
C4	49.8(8)	23.2(5)	39.7(7)	-8.1(5)	30.9(6)	-6.1(5)
C3	24.8(5)	17.6(4)	24.2(4)	-3.6(3)	11.8(4)	-3.0(3)
C5	47.4(8)	21.6(5)	72.8(10)	-4.7(6)	46.6(8)	-2.7(5)
C9	23.7(7)	21.2(6)	123.6(18)	8.5(8)	-25.2(9)	-1.0(5)
C8	13.6(6)	25.0(7)	178(3)	23.5(10)	0.3(10)	-0.5(5)
C7	24.6(7)	23.0(6)	149(2)	18.0(9)	39.2(10)	4.7(5)
C6	24.0(6)	13.9(4)	88.2(12)	2.7(5)	28.9(7)	0.4(4)
C10	21.5(6)	17.7(5)	71.5(10)	2.0(5)	-13.1(6)	1.2(4)
C11	15.1(4)	11.3(4)	55.3(7)	0.1(4)	6.1(4)	-0.4(3)
C12	21.8(4)	15.7(4)	11.2(3)	-1.1(3)	4.3(3)	-5.7(3)
C13	22.8(4)	14.9(4)	12.1(3)	-1.7(3)	5.8(3)	-4.6(3)
C14	30.0(5)	20.7(5)	21.5(4)	0.5(3)	11.6(4)	0.8(4)

Table E4 Bond Lengths.

Atom	Atom	Length/\AA	Atom	Atom	Length/\AA
C1	N1	1.4810(14)	C9	C10	1.379(2)
C1	C2	1.5024(14)	C9	C8	1.398(4)
O1	C12	1.2529(11)	C8	C7	1.366(4)
C2	C3	1.3703(15)	C7	C6	1.425(2)
C2	C11	1.4336(15)	C6	C11	1.4200(19)
O2	C12	1.2695(11)	C10	C11	1.421(2)
C4	C5	1.361(2)	C12	C13	1.5203(12)
C4	C3	1.4199(15)	C13	C14	1.3400(14)

C5 C6 1.425(3)

C13 C13¹ 1.4785(19)

¹2-X,1-Y,-Z

Table E5 Bond Angles.

Atom	Atom	Atom	Angle/°	Atom	Atom	Atom	Angle/°
N1	C1	C2	114.87(8)	C5	C6	C7	122.05(16)
C3	C2	C11	119.97(10)	C9	C10	C11	120.61(19)
C3	C2	C1	122.18(9)	C6	C11	C10	118.79(12)
C11	C2	C1	117.81(10)	C6	C11	C2	118.66(12)
C5	C4	C3	120.13(14)	C10	C11	C2	122.54(12)
C2	C3	C4	121.05(11)	O1	C12	O2	123.20(8)
C4	C5	C6	120.63(11)	O1	C12	C13	119.41(8)
C10	C9	C8	120.8(2)	O2	C12	C13	117.36(8)
C7	C8	C9	119.77(14)	C14	C13	C13 ¹	124.16(10)
C8	C7	C6	121.6(2)	C14	C13	C12	116.02(9)
C11	C6	C5	119.54(12)	C13 ¹	C13	C12	119.75(10)
C11	C6	C7	118.42(18)				

¹2-X,1-Y,-Z

Table E6 Hydrogen Atom Coordinates ($\text{\AA}\times 10^4$) and Isotropic Displacement Parameters ($\text{\AA}^2\times 10^3$).

Atom	x	y	z	U(eq)
H4	9107(14)	2859(12)	5921(19)	29(4)
H3	9253(14)	3933(11)	5873(17)	19(3)
H5	9222(17)	3337(13)	4320(20)	37(4)
H9	7075(17)	4142(13)	10060(20)	37(4)
H8	8307(17)	3897(13)	8010(20)	38(4)
H7	7250(14)	2984(11)	4159(18)	23(3)
H6	7455(14)	4173(12)	4077(18)	26(4)
H10	4820(20)	4119(18)	9380(30)	73(7)
H11	2980(30)	3957(19)	7410(30)	80(8)
H12	3090(20)	3460(19)	2390(30)	76(7)
H13	5359(18)	3449(13)	3210(20)	39(4)

H15	11253(16)	3903(12)	-1210(20)	34(4)
H16	1850(30)	3730(20)	4540(40)	105(10)
H14	11158(14)	3184(12)	387(18)	23(3)

APPENDIX F

Crystallographic Data for Fulgenic Acid

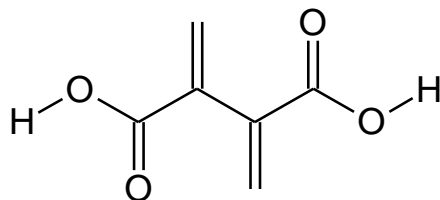


Table F1 Crystal data and structure refinement.

Empirical formula	C ₆ H ₆ O ₄	
Temperature/K	100.15	
Crystal system	monoclinic	
Space group	C2/c	
a/Å	a = 10.26935(16) Å	α = 90°
b/Å	b = 5.49754(9) Å	β = 102.2985(7)°
c/Å	c = 11.18398(18) Å	γ = 90°
Volume/Å ³	616.915(17)	
Z	4	
ρ _{calc} /cm ³	1.5300	
μ/mm ⁻¹	1.141	
F(000)	297.3	
Crystal size/mm ³	0.301 × 0.254 × 0.104	
Radiation	Cu Kα (λ = 1.54178)	
2θ range for data collection/°	16.22 to 133.62	
Index ranges	-12 ≤ h ≤ 12, -6 ≤ k ≤ 6, -13 ≤ l ≤ 12	
Reflections collected	3374	
Independent reflections	535 [R _{int} = 0.0348, R _{sigma} = 0.0203]	
Data/restraints/parameters	535/0/59	
Goodness-of-fit on F ²	1.177	
Final R indexes [I ≥ 2σ (I)]	R ₁ = 0.0271, wR ₂ = 0.0652	

Final R indexes [all data] $R_1 = 0.0275$, $wR_2 = 0.0654$

Largest diff. peak/hole / e \AA^{-3} 0.23/-0.15

Table F2 Fractional Atomic Coordinates ($\times 10^4$) and Equivalent Isotropic Displacement Parameters ($\text{\AA}^2 \times 10^3$). U_{eq} is defined as 1/3 of the trace of the orthogonalised U_{ij} tensor.

Atom	x	y	z	U(eq)
O1	3781.9(8)	2564.9(16)	4458.6(8)	16.1(3)
O2	5670.7(8)	3784.5(15)	3937.0(7)	14.8(3)
C1	4716.8(11)	2398(2)	3818.6(10)	11.4(3)
C2	4548.0(11)	327(2)	2938.8(10)	10.8(3)
C3	3689.0(11)	-1454(2)	2985.9(11)	14.3(3)

Table F3 Anisotropic Displacement Parameters ($\text{\AA}^2 \times 10^3$). The Anisotropic displacement factor exponent takes the form: $-2\pi^2[h^2a^{*2}U_{11}+2hka^*b^*U_{12}+\dots]$.

Atom	U_{11}	U_{22}	U_{33}	U_{12}	U_{13}	U_{23}
O1	16.9(5)	21.5(5)	11.7(5)	-3.3(4)	7.0(3)	-5.6(4)
O2	17.3(5)	16.6(5)	11.2(5)	-3.6(4)	4.9(3)	-2.6(3)
C1	12.7(6)	15.0(6)	5.6(6)	2.0(5)	0.3(4)	3.2(4)
C2	12.2(6)	13.6(6)	5.6(6)	2.6(5)	-0.7(4)	1.6(4)
C3	14.2(6)	16.8(6)	11.5(6)	1.3(5)	2.3(5)	0.9(5)

Table F4 Bond Length.

Atom	Atom	Length/ \AA	Atom	Atom	Length/ \AA
O1	C1	1.3173(14)	C2	C2 ¹	1.488(2)
O2	C1	1.2261(14)	C2	C3	1.3264(17)
C1	C2	1.4903(16)			

¹1-X,+Y,1/2-Z

Table F5 Bond Angles.

Atom	Atom	Atom	Angle/ $^\circ$	Atom	Atom	Atom	Angle/ $^\circ$
O2	C1	O1	123.78(11)	C2 ¹	C2	C1	115.75(8)
C2	C1	O1	114.60(10)	C3	C2	C1	121.49(11)
C2	C1	O2	121.61(10)				

¹1-X,+Y,1/2-Z

Table F6 Hydrogen Bonds for C2onc.

D	H	A	d(D-H)/Å	d(H-A)/Å	d(D-A)/Å	D-H-A/°
O1	H1	O2¹	0.89(2)	1.78(2)	2.6709(12)	178.2(19)

¹1-X,1-Y,1-Z

Table F7 Hydrogen Atom Coordinates ($\text{Å} \times 10^4$) and Isotropic Displacement Parameters ($\text{Å}^2 \times 10^3$) for C2onc.

Atom	x	y	z	U(eq)
H1	3981(19)	3790(40)	4990(20)	49(6)
H3a	3118(14)	-1440(30)	3572(13)	17(3)
H3b	3602(13)	-2840(30)	2421(13)	15(3)

REFERENCES

-
- ¹ Tranchemontagne, D. J.; Hunt, J. R.; Yaghi, O. M. Room Temperature Synthesis of Metal-Organic Frameworks: MOF-5, MOF-74, MOF-177, MOF-199, and IRMOF-0. *Tetrahedron*. 2008, 64, 8553–8557.
- ² Michaelides, A.; Aravia, M.; Siskos, M. G.; Skoulika, S. Photochemical reactivity of a lamellar lanthanum MOF. *CrystEngComm* 2015, 17(1), 124-131.
- ³ Ling Qin, Ze-Min Ju, Zhong-Jie Wang, Fan-Dian Meng, He-Gen Zheng, and Jin-Xi Chen. Interpenetrated Metal–Organic Framework. *Cryst. Growth Des.*, 2014, 14 (6), pp 2742–2746.
- ⁴ Batten, SR; Champness, NR; Chen, X-M; Garcia-Martinez, J; Kitagawa, S; Öhrström, L; O'Keeffe, M; Suh, MP; Reedijk, J, Terminology Of Metal-Organic Frameworks and Coordination Polymers. *Chemistry International -- Newsmagazine for IUPAC*. 2013, 35.
- ⁵ Rowsell, J. L. C.; Millward, A. R.; Park, K. S.; Yaghi, O. M. Hydrogen Sorption in Functionalized Metal–Organic Frameworks. *Journal of the American Chemical Society* 2004, 5666–5667.
- ⁶ Rosyid, O.; Jablonski, D.; Hauptmanns, U. Risk Analysis for the Infrastructure of a Hydrogen Economy. *International Journal of Hydrogen Energy* 2007, 32 (15), 3194–3200.
- ⁷ Ma, L., Abney, C., and Lin, W. (2009) Enantioselective catalysis with homochiral metal–organic frameworks. *Chemical Society Reviews* 38, 1248.
- ⁸ Xamena, F. X., Corma, A., & Garcia, H. (2007). Applications for Metal–Organic Frameworks (MOFs) as Quantum Dot Semiconductors. *J. Phys. Chem. C The Journal of Physical Chemistry C*, 111(1), 80-85.
- ⁹ Diels, O.; Alder, K. Synthesen In Der Hydroaromatischen Reihe. *Justus Liebigs Ann. Chem.* Justus Liebig's Annalen der Chemie. 1928, 460, 98–122.
- ¹⁰ Cohen, S. M. ChemInform Abstract: Postsynthetic Methods for the Functionalization of Metal-Organic Frameworks. *ChemInform* 2012, 43 (16).
- ¹¹ Srikrishna, A.; Nagaraju, S.; Kondaiah, P. Application of Microwave Heating Techniques for Rapid Synthesis of γ , δ -Unsaturated Esters. *Tetrahedron* 1995, 51 (6), 1809–1816.
- ¹² Beard, K. D., Crystal Engineering: Solid State Reactivity of Butadiene Monomers in Crystals. MS Thesis, Western Carolina University, Cullowhee, NC, 2008.
- ¹³ Lee, S. Y.; Kulkarni, Y. S.; Burbaum, B. W.; Johnston, M. I.; Snider, B. B. Type I Intramolecular Cycloadditions of Vinylketenes. *The Journal of Organic Chemistry* 1988, 53 (9), 1848–1855.

-
- ¹⁴ Deshpande, S. G. A Facile Synthesis of Fulgenic Acid via Base Induced 1,4-Dehydrobromination of (Bromomethyl)Methylmaleic Anhydride. *Synthesis* 1999, (08), 1306–1308.
- ¹⁵ Tazoe, K.; Uchikawa, Y.; Feng, X.; Yamato, T. Synthesis and Structure of 2,3-Bis(5- Tert -Butyl-2-Methoxyphenyl)Buta-1,3-Diene by Bromine Elimination of (Z)-1,4-Dibromo-2,3-Bis(5- Tert -Butyl-2-Methoxyphenyl)-2-Butene. *Synthetic Communications* 2012, 42 (21), 3128–3139.
- ¹⁶ Bailey, William J., Robert L. Hudson, and Edwin T. Yates. "Pyrolysis of Esters. XXIV. 2, 3-Dicarboxy-1, 3-butadiene1, 2." *The Journal of Organic Chemistry* 1963, 28 (3), 828-831.
- ¹⁷ Clerici, A.; Porta, O. Reduction of Aromatic Carbonyl Compounds Promoted by Titanium Trichloride in Basic Media. Stereochemistry Studies. *The Journal of Organic Chemistry* 1985, 50 (1), 76–81.
- ¹⁸ Garrison, C., 1, 4-Topochemical Polymerization of a Butadiene. MS Thesis, Western Carolina University, Cullowhee, NC, 2006.
- ¹⁹ Hiyama, T.; Nozaki, H. A Facile, Stereospecific Preparation of Olefins from Pinacols. *Bulletin of the Chemical Society of Japan BCSJ* 1973, 46 (7), 2248–2249.
- ²⁰ Corey, E.; Hopkins, B. A Mild Procedure for the Conversion of 1,2-diols to Olefins. *Tetrahedron Letters* 1982, 23 (19), 1979–1982
- ²¹ Corey, E. J.; Winter, R. A. E. A New, Stereospecific Olefin Synthesis from 1,2-Diols. *Journal of the American Chemical Society* 1963, 85 (17), 2677–2678.
- ²² Gonzalez-De-Castro, A.; Xiao, J. Green and Efficient: Iron-Catalyzed Selective Oxidation of Olefins to Carbonyls with O₂. *J. Am. Chem. Soc. Journal of the American Chemical Society* 2015, 137 (25), 8206–8218.
- ²³ Zhang, Y.; Li, J.; Li, X.; He, J. Regio-Specific Polyacetylenes Synthesized from Anionic Polymerizations of Template Monomers. *Macromolecules* 2014, 47 (18), 6260–6269.
- ²⁴ Piou, T.; Rovis, T. Rh(III)-Catalyzed Cyclopropanation Initiated by C–H Activation: Ligand Development Enables a Diastereoselective [2 + 1] Annulation of N-Enoxyphthalimides and Alkenes. *J. Am. Chem. Soc. Journal of the American Chemical Society* 2014, 136 (32), 11292–11295.
- ²⁵ Champness, N. R.; Khlobystov, A. N.; Majuga, A. G.; Schröder, M.; Zyk, N. V. An Improved Preparation of 4-Ethynylpyridine and Its Application to the Synthesis of Linear Bipyridyl Ligands. *Tetrahedron Letters* 1999, 40 (29), 5413–5416.
- ²⁶ Alunni, S.; Laureti, V.; Ottavi, L.; Ruzziconi, R. Catalysis of the β -Elimination of HF from Isomeric 2-Fluoroethylpyridines and 1-Methyl-2-Fluoroethylpyridinium Salts. Proton-Activating Factors and Methyl-Activating Factors as a Mechanistic Test To Distinguish between Concerted

E2 and E1cb Irreversible Mechanisms. *The Journal of Organic Chemistry* 2003, 68 (3), 718–725.

²⁷ Pine, S. H.; Pettit, R. J.; Geib, G. D.; Cruz, S. G.; Gallego, C. H.; Tijerina, T.; Pine, R. D. ChemInform Abstract: Carbonyl Methylenation Using A Titanium-Aluminum (Tebbe) Complex. *Chemischer Informationsdienst* 1985, 16 (35). 1212-1216

²⁸ Andersson, M.; Österlund, L.; Ljungström, S.; Palmqvist, A. Preparation of Nanosize Anatase and Rutile TiO₂ by Hydrothermal Treatment of Microemulsions and Their Activity for Photocatalytic Wet Oxidation of Phenol. *The Journal of Physical Chemistry B J. Phys. Chem. B* 2002, 106 (41), 10674–10679.

²⁹ Xie, R.-C.; Shang, J. K. Morphological Control in Solvothermal Synthesis of Titanium Oxide. *Journal of Materials Science* 2007, 42 (16), 6583–6589.

³⁰ Hopf, H., Dendralenes, The Breakthrough, *Angewante Chemie International Edition*, 2001, 40 (4), 705-707.